COMPUTATIONAL STUDIES OF REACTIVE OXYGEN AND SULFUR SPECIES

By

Álvaro Castillo Aguilar

A dissertation submitted to the Graduate Faculty in Chemistry in partial fulfillment of the requirements for the degree of Doctor of Philosophy, The City University of New York

2011

This manuscript has been read and accepted for the
Graduate Faculty in Chemistry in satisfaction of the
Dissertation requirement for the degree of Doctor of Philosophy.

PROFESSOR Dr. ALEXANDER GREER

Date

Chair of Examining Committee

PROFESSOR Dr. MARÍA TAMARGO

Date

Executive Officer

PROFESSOR Dr. STEPHEN P. FEARNLEY

PROFESSOR Dr. JOSEPH J. DANNENBERG

PROFESSOR Dr. ROBERTO A. SÁNCHEZ DELGADO

Supervisory Committee

THE CITY UNIVERSITY OF NEW YORK

2011

ABSTRACT

COMPUTATIONAL STUDIES OF REACTIVE OXYGEN AND SULFUR SPECIES

By

Álvaro Castillo Aguilar

Advisor: Professor Dr. Alexander Greer

In this thesis, we summarized the use of computational chemistry methods to provide insight into the chemistry of reactive intermediates species like singlet oxygen, thiozone, radical and diradicals of mercapto-quinones, and benzyl alkynyl sulfides anions. The theoretical methods used included Density Functional Theory, and hybrid [Molecular Orbital:Molecular Orbital] methods and the Conductor-like Polarizable Continuum Model for condensed phase calculations.

The first chapter deals with carbon nanotubes as a class of host cavities to encapsulate the unstable molecule thiozone (S_3). We computed single-walled carbon nanotube (SWNT)−thiozone pairs. Nanotube diameter selectivity for isomerization of the C_{2v} form of S_3 to the D_{3h} form proved to be elusive. 1,2,3-Thiozonide formation took place on the convex side of nanotubes of low tube radii, such as the armchair (4,4) and (5,5) SWNTs. The second chapter focused on singlet oxygen release from a naphthalene endoperoxide which bears a flexible $(CH_2)_{22}$ polymethylene "lid". Monte Carlo and ONIOM calculations that incorporated semiempirical and density functional theory were used in the study. Interestingly, the polymethylene chain appears to function as a gatekeeper for the oxygen, where, instead of coming full circle, a semi-circle rotation of the polymethylene bridge

protected the peroxide group, limiting the dissociation of $^1O_2$ from the naphthalene site. The third chapter deals with condensed-phase calculations of the reaction of aryl substituted benzyl 1-alkynyl sulfides with potassium *t*-methoxide in acetonitrile. This reaction produces 2-aryl 2,3-dihydrothiophene products. Experimental evidence (from our collaborators) indicates that there is a rapid exchange of protons and tautomerism of the alkynyl unit prior to cyclization to the dihydro-thiophenes. The fourth and last chapter is devoted to DFT calculations of quinones, radicals and diradicals. Calculations on these reactive species arising from mercapto- and bismercaptocatechols were conducted seeking to provide insight into their relative stability.

ACKNOWLEDGMENTS

The author wishes to express his gratitude to Professor Dr. Alexander Greer, whose dedicated assistance allowed for the completion of this graduate research. Professor Greer's cunning insight and broad understanding of the scientific method to solve problems has been, and surely will continue to be, a source of inspiration. Professor Greer also taught him the importance of attention to scientific rigor and detail, showing the reach a chemist's mind within the framework of a modern approach. Professor Greer's patience and advice were fundamental for the completion of this work. (The author will be always in debt). The author is also grateful to Professors Drs. Stephen P. Fearnley, Joseph J. Dannenberg and Roberto A. Sanchez-Delgado, members of the dissertation committee. Their time spent reading the annual committee reports is highly appreciated, as is as their comments and guidance during the annual meetings. Special thanks are given to the collaborators, whose work inspired part of the work presented in this dissertation. It is thanks to them that the completion of part of this work was possible, undoubtedly due to the generous share of their expertise, time and devotion to the problems at hand. Drs. Joel F. Liebman and Adrian L. Schwan deserve a place of honor for their chemical awareness. The work presented in this dissertation would not have been possible without the assistance of Dr. Florian Lengyel, former Assistant Director for Research Computing at The CUNY Graduate Center. In a similar manner, gratitude is extended to the staff at the City University of New York (CUNY) High Performance Computing Center (HPCC). Appreciation is extended to all the members of the Chemistry Department at Brooklyn College, especially to group members, for their support and friendship.

The author is indebted to his friends and family.

A mis padres,

Dr. Álvaro Castillo Suárez,
Doña Belcy Aguilar de Castillo

y mis hermanas,

Dra. María Carolina Castillo Aguilar
Mónica Andrea Castillo Aguilar

CONTENTS

LIST OF FIGURES

CHAPTER 1

CHAPTER 2

CHAPTER 3

LIST OF SCHEMES

CHAPTER 1

CHAPTER 2

CHAPTER 3

LIST OF TABLES

CHAPTER 1

CHAPTER 2

CHAPTER 3

CHAPTER 4

"*Every attempt to employ mathematical methods in the study of chemical questions must be considered profoundly irrational and contrary to the spirit of chemistry. If mathematical analysis should ever hold a prominent place in chemistry - an aberration which is happily almost impossible - it would occasion a rapid and widespread degeneration of that science.*"

Augustus Compte, French philosopher, 1798-1857; in *Philosophie Positive*, 1830.

List of Abbreviations and Terms

The list of abbreviations and terms is made of terminology that appears in this thesis. A better description of most of the computational methods can be found in the literature or in the Gaussian 09 User's Reference, which is available online (link provided below).

http://www.gaussian.com/g_tech/g_ur/g09help.htm

S^2	Spin expectation value; it should have a value of 0 for singlets, 0.75 for radicals and 2.0 for triplet diradicals, providing that no spin contamination is present.
6,6 site	In a [60]fullerene, the bond common to two 6 membered rings.
a,b site	In a [70]fullerene, the bond common to two 6 membered rings that does not lie along the C_5 axis.
c,c site	In a [70] fullerene, the bond common to two 6 membered rings that lies along the C_5 axis.
AM1	Austin model 1, a semiempirical quantum mechanical model.
ANO	Atomic natural orbital basis sets.
B3LYP	Becke three-parameter and, Lee-Yang-Parr exchange-correlation functional.
B3P86	Becke three-parameter, with the gradient corrections of Perdew, along with his 1986 non-local correlation functional functional.
BSSE	Basis set superposition error.
CAM-B3LYP	Handy and coworkers' long range corrected version of B3LYP using the Coulomb-attenuating method.
CASPT2	Complete active space with second-order perturbation theory.
cc-pV*n*Z	Dunning's correlation consistent basis sets.

CCSD(T)	Coupled-cluster with single and double and perturbative triple excitations.
CI	Configuration interaction. A post-Hartree Fock method.
CPCM	Conductor-like polarizable continuum model, a solvation model.
D95V	Dunning/Huzinaga valence double-zeta basis set.
DDQ	2,3-dichloro-5,6-dicyano-1,4-benzoquinone.
deg.	Degrees.
DFT	Density functional theory.
DNP	Double-numerical with polarization functions basis set.
DZ+P	Double zeta-polarization contracted Gaussians basis set
eq.	Equivalent.
FT-microwave	Fourier transform microwave.
G*n*	Gaussian-*n* composite methods for high accuracy molecular energies.
GGA	Generalized gradient approximation
IEFPCM	Integral equation formalism polarizable continuum model, a solvation model.
IR	Infrared.
IRC	Intrinsic reaction coordinate.
LanL2DZG(d)	A basis set consisting of D95V basis set for the 1st row, and Los Alamos effective core potential plus double zeta on Na-La, Hf-Bi.
M0*n*-2X	Truhlar and Zhao's hybrid meta DFT methods.
MM+	Extension of the MM2 molecular mechanics force field.
MP*n*	Møller–Plesset perturbation theory method of n^{th} order.
MR-ccCA	Multireference correlation consistent composite approach
MRCI+Q	Multireference configuration interaction with quasi-degenerate Davidson corrections.

ONIOM	Our own n-layered integrated molecular orbital and molecular mechanics
PBE	Perdue-Burke-Ernzerhof functional.
PCM	Short for IEFPCM.
PES	Potential energy surface
PW91	Exchange component of the Perdew-Wang DFT functional.
RHF	Restricted Hartree Fock.
s	Seconds.
SCF	Self-consistent field.
SVWN	Local Spin Density Approximation. Also known as LSDA.
SWNT	Single walled carbon nanotube
TS	Transition State.
TZ	Triple zeta basis set.
TZVP	Triple zeta valence plus polarization basis set.
UV	Ultraviolet.
zpe	Zero-point energy.

Chapter 1. Encapsulation and Convex-Face Thiozonolysis Chemistry of Thiozone (S_3) with Carbon Nanotubes

1.1. Introduction

In this chapter, the goal was to compute various carbon nanotube−thiozone combinations for the inclusion of thiozone (S_3) into a hollow nanotube space, to rationalize when 1,2,3-thiozonide formation can take place, and to examine the thiozonolysis mechanism. S_3 has two possible isomeric forms, C_{2v} symmetric S_3 (**1**) is the sulfur analog of O_3. C_{2v} S_3 has been detected by UV-visible, microwave, and FT-IR spectroscopy,[1] additionally it has been observed in the atmospheres of Venus and Io due to volcanic activity.[2] The D_{3h} form of S_3 (**2**) has eluded experimental observation. In organic synthesis, there is rather sparse use of S_3,[3] due to its tendency to form heavier allotropes, such as cyclic S_8,[4] even though the generation of S_3 is seemingly straightforward in the disproportionation of S_2O.[5] Another source of S_3 has been suggested in the decomposition of natural product benzopentasulfanes.[6]

1, C_{2v} **2**, D_{3h}

Scheme 1-1. C_{2v} and D_{3h} isomeric forms of thiozone.

Carbon nanotubes have not yet been used to encapsulate sulfur allotropes such as thiozone.[7] The literature on nanotube calculations include convex-surface diameter-dependent reactions in which higher reactivity for the lower radii nanotubes is predicted.[8,9] For example, DFT calculations on singlet oxygen with (*n,0*) zigzag singlet-walled carbon nanotubes (SWNT) have shown an increased exothermicity with nanotubes of reduced diameters, and also that type (metallic, chiral, non-metallic) did not play a role in this diameter-reactivity relationship.[10] Recent DFT calculations using GGA-PW91/DNP to model the addition of methylamine to C_{60}, C_{50}, (5,5) SWNT and (10,10) SWNT revealed a similar curvature dependence,[11] although the addition of benzenediazonium salts to SWNTs was controlled by the optical band gap of the tube rather than the pyramidalization of the carbon atoms.[12] In a similar manner, DFT-ONIOM methods have shown that the 1,3-dipolar cycloadditions of formoazomethine ylide and fulminic acid takes place only on the smallest diameter SWNTs.[9b]

Using CNTs as host for S_3 requires that the CNT does not react with the S_3. It also requires that dimerization and oligomerization can be prevented. We selected to study the smallest CNTs that could accommodate S_3. Armchair, zigzag, and chiral SWNT of diameter 5.4 – 9.5 Å were considered. SWNT nomenclature is based on viewing the CNTs as rolled graphene sheets; Scheme 2 illustrates how this nomenclature is related to an unfolded graphene sheet, in which armchair nanotubes result when the *m* and *n* integers are equal, zigzag nanotubes take the form (*n,0*), and chiral nanotubes result when $m \neq n \neq 0$).[13] Reactions of S_3 in the interior and the exterior of the SWNTs were considered (Figure 1). The study was divided into: (i) free gaseous S_3 (ii) SWNT encapsulated S_3, and (iii) S_3 sulfuration of convex aromatic surfaces (producing 1,2,3-thiozonide structures reminiscent of organic trisulfanes[14] and molozonides).[8] For simplicity, our study neglected

possible S_3 reactions at nanotube end-caps, regions around the rim[15] (such as the COOH functionality introduced onto SWNTs) or defect sites.[16]

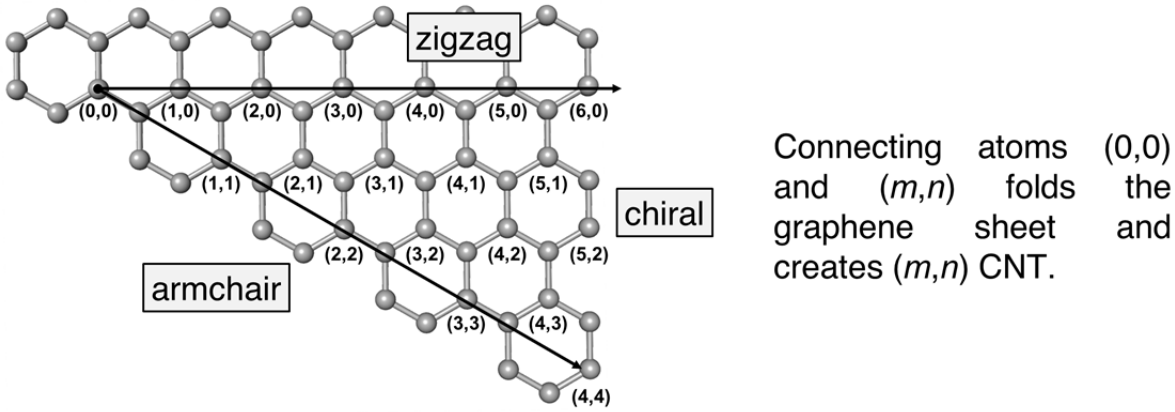

Scheme 1-2. Nomenclature of SWNTS derived from a graphene segment with indexed lattice points (*m*,*n*). (adapted from ref. 16).

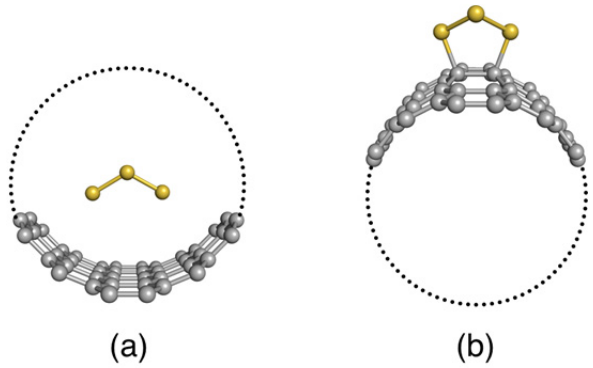

Figure 1-1. Schematic of (a) **1** encapsulated inside a SWNT, and (b) a SWNT 1,2,3-thiozonide.

1.2. Computational Methods

Geometry optimizations were performed with the Gaussian-09 program package[17] using standard protocols[18,19] and the M06-2X,[20] B3P86,[21] or SVWN[22] functionals with either basis sets 6-

31G(d), 6-311+G(2d), or STO-3G. Calculations were also conducted with ONIOM(B3P86/6-31G(d) for geometry optimizations and ONIOM(B3P86/6-311+G(2d):SVWN/STO-3G) for single point energies.[23] Geometries were optimized to minima or saddle points on the potential energy surface and the IRC calculations were performed on the transition state structures. All calculated values included thermal corrections for enthalpy. Sulfuration calculations were carried out where the ONIOM treatment separated the dinaphtho(2,1,8,7-*hijk*:2',1',8',7'-*stuv*)ovalene and the S_3 unit from the rest of the nanotube (Figure 1-2). The junction between B3P86 and SVWN was at the remaining carbon atoms around the perimeter of the ovalene unit; for example, the 78 carbon atoms for the armchair (4,4) SWNT, the 198 carbon atoms for armchair (8,8) SWNT, and the 150 carbon atoms for graphene. Calculations of encapsulated S_3 were carried out with B3P86/6-311+G(2d) only for the S_3 unit. W1U calculations were used to assess the nature of the ground state of S_3. The length of the CNTs was set to 2 nm.

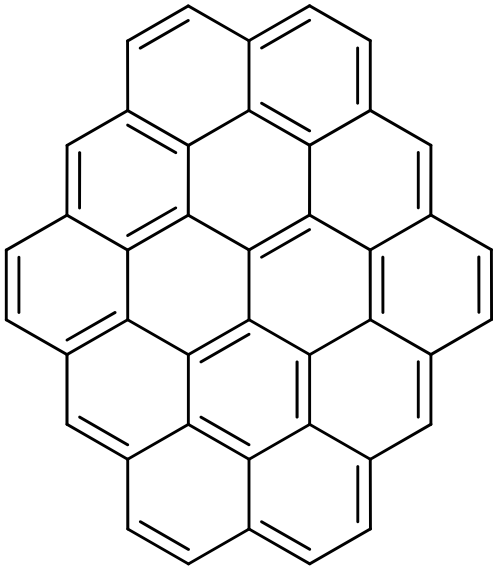

Figure 1-2. The dinaphtho[2,1,8,7-*hijk*:2',1',8',7'-*stuv*]ovalene unit used in the B3P86 portion of the ONIOM calculations.

1.3. Results and Discussion

1.3.1. Calculated Structures of Thiozone.

We summarized data on thiozone in Table 1-1; the geometries and energetics of S_3 obtained from various theoretical methods and its experimental geometry are also tabulated. Except for SCF/DZ+P[24b] and M06-2X, all calculations employed in Table 1-1 favor the C_{2v} form of S_3 to the D_{3h} form by 4.8 to 7.9 kcal/mol.[24] Reaching **2** from **1** is a high barrier process (26.4 to 36.9 kcal/mol) as reported before,[25] this cyclization is a symmetry forbidden process attributed to the gain of a σ bond in **2** and the loss of a π bond in **1**. The interconversion of **1** and **2** has been studied by Ruedenberg *et al.* Their calculations suggested a process that occurs via a C_{2v} transition state, that lies in the vicinity of a conical intersection.[26] Additionally, calculations on the nature of its ground state by Peterson *et al.*[24i] have shown the singlet as the lowest lying electronic state. Our W1U calculations put the triplet state 30.3 kcal above the singlet.

To our surprise, the M06-2X method was not reliable. First, the near isoenergetic o-S_3 vs c-S_3 values predicted made it difficult to justify the use of this method, and secondly, the singlet-triplet gap (ΔE_{ST}) was calculated to be only 18.1 kcal/mol. Even the inclusion of tight *d* polarization basis set functions on the M06-2X calculations did not produce relative energies similar to the coupled-cluster and CI calculations or bond lengths similar to the FT-microwave structure. On the other hand, the B3P86/6-311+G(2d) calculations provide reasonable energetics, a good geometry and an acceptable ΔE_{ST} of 26.0 kcal/mol. For example, the B3P86/6-311+G(2d) computed S1-S2 bond length had a 0.01 Å discrepancy, and S1-S2-S3 bond angle 0.7° discrepancy to the experimental structure.[24a]

Table 1-1. Calculated Properties and Energetics of the Open C_{2v} and Cyclic D_{3h} Forms of S_3 [a-c]

method	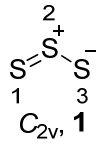 C_{2v}, **1** S1-S2, Å	S1-S2-S3, deg.	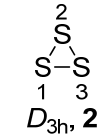 D_{3h}, **2** S1-S2, Å	Isomerization barrier [a]	rel. E of D_{3h}–C_{2v} [a]	ref.
experiment	(1.917)	(117.4)	-	-	-	*d*
SCF/DZ+P	1.907	117.2	2.083	-	-9.3	*e*
B3LYP/cc-pVTZ	1.960	117.5	2.127	-	7.4	*f*
B3LYP/LanL2DZG(d)	1.956	117.5	2.130	24.8	7.9	*g*
B3P86/6-311+G(2d)	1.927	118.1	2.097	26.4	6.6	*g*
M06-2X/6-311+G(2d)	1.936	118.0	2.102	28.9	-2.8	this work
M06-2X/cc-pV5Z	1.900	117.6	2.063	-	-1.3	this work
M06-2X/cc-pV(Q+d)Z	1.896	117.7	2.062	29.4	-0.9	this work
M06-2X/cc-pV(5+d)Z	1.896	117.7	2.062	30.1	-0.9	this work
MRCI+Q/ANO6532	1.937	117.8	2.094	36.9	6.8	*h*
CCSD(T)/ANO6532	1.932	117.3	2.093	-	5.6	*h*
CCSD(T)/cc-pV5Z	1.918	117.3	2.077	-	4.8	*i*
CASPT2/ANO-QZP	1.924	117.3	2.083		6.7	*j*
MR-ccCA-AQCC(S_DT)	-	-	-	-	5.3	*k*

[a] Energies in kcal/mol and reported from the calculated global minimum. [b] Experimental values in parentheses. [c] The computed S1-S2-S3 angle in D_{3h} S_3 was 60.0 º in all cases. [d] Ref. 24a. [e] Ref. 24b. [f] Ref. 24c. [g] Ref. 24d. [h] Ref. 24e. [i] Ref. 24f. [j] Ref. 24g. [k] Ref. 24h.

1.3.2. Nanotube-Encapsulated Thiozone.

The ONIOM ground state structures and energetics of encapsulated **1** and **2** are listed in Table 1-2. Our calculations show that **1** is more stable than **2** within the SWNTs. The opposite was never found. Expected polarization effects of nanotubes [27] to stabilize confined dipolar **1** had essentially no detectable effect. The smallest diameter nanotube analyzed was the (4,4), with a diameter of 5.4 Å, taking into account the C and S atomic radii[28] this CNT was judged to be too

small to encapsulate **2**. The S1-S2-S3 bond angle was more linear for **1**@(4,4) SWNT compared to free **1**. For **1**@(5,5) SWNT, the C_{2v} S_3 molecule was aligned parallel to the tube along the *z*-axis, not perpendicular to it in the *x*- or *y*-axes (Figure 1-3). The S_3 molecule can adopt different orientations in the (5,5), (6,6), (7,7), and (8,8) SWNTs.

Table 1-2. Calculated Properties and Energetics of **1** and **2** Encapsulated in Nanotubes [a-c]

	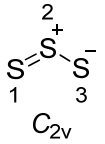 C_{2v}		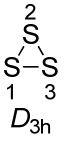 D_{3h}			
SWNT	S1-S2, Å	S1-S2-S3, °	S1-S2, Å	S1-S2-S3, °	rel. energy S_3 (D_{3h} - C_{2v})	nanotube diameter, Å[e]
(4,4)[c]	1.933	121.2	-	-	-	5.4
(5,5)	1.934	116.6	2.056	59.5	13.2	6.8
(6,4)	1.932	116.9	2.060	59.7	8.9	6.8
(9,0)	1.928	117.6	2.064	60.2	9.8	7.1
(8,2)	1.934	117.3	2.067	60.3	10.1	7.2
(7,4)	1.927	117.6	2.073	59.8	7.2	7.6
(6,6)	1.926	117.7	2.089	59.5	7.2	8.2
(7,7)	1.927	118.0	2.091	60.0	7.6	9.5

[a] Energies in kcal/mol; length of the nanotube = 2 nm. [b] Calculated by ONIOM(B3P86/6-311+G(2d):SVWN/STO-3G)//ONIOM(B3P86/6-31G(d):SVWN/STO-3G). [d] D_{3h} S_3: S2-S3 = 1.92 Å; S2-S3-S1 = 67.3°. [e] Nanotube diameters taken from ref. 29.

Because the rotation depended on the space available for the S_3 molecule, C_2 rotation is facile within the (7,7) and (8,8) SWNTs along the *z*- or *x*-axis, in contrast to the (5,5) SWNT (~40-50 kcal/mol) and the (6,6) SWNT (~20 kcal/mol) (Figure 1-4). The computations yielded no addition of S_3 to the inner wall of the nanotubes (even for the larger diameter tubes), undoubtedly because of the acute inverse pyramidalization that would be necessary to produce a thiozonide. Even along the *z*-axis, the thiozone does not react with the flat surface. An open-shell stepwise pathway to a biradical intermediate was also sought, but no structure optimized to a C-S bonded compound or to a three-membered ring SWNT-**1**-persulfide structure with a linear sulfur linkage was found.

Comparably, DFT calculations have also indicated that alkyl radicals do not react with the inner walls of carbon nanotubes due to the high-energy cost to produce a "negative" distortion of the tube geometries.[30]

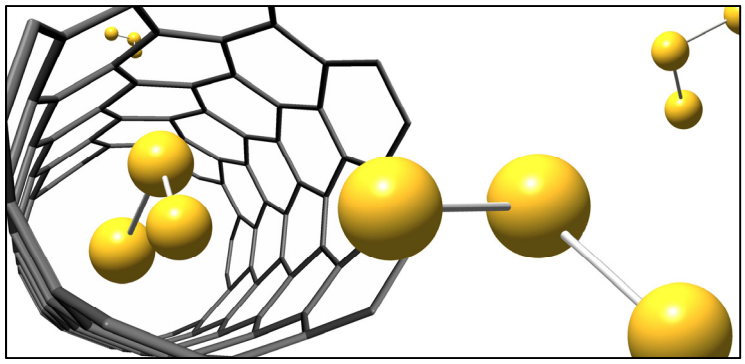

Figure 1-3. The S_3 molecule preferentially lies along the z-axis of the armchair (5,5) SWNT, which is flat. There was a high energy (~40-50 kcal/mol) for the rotation of S_3 within this nanotube.

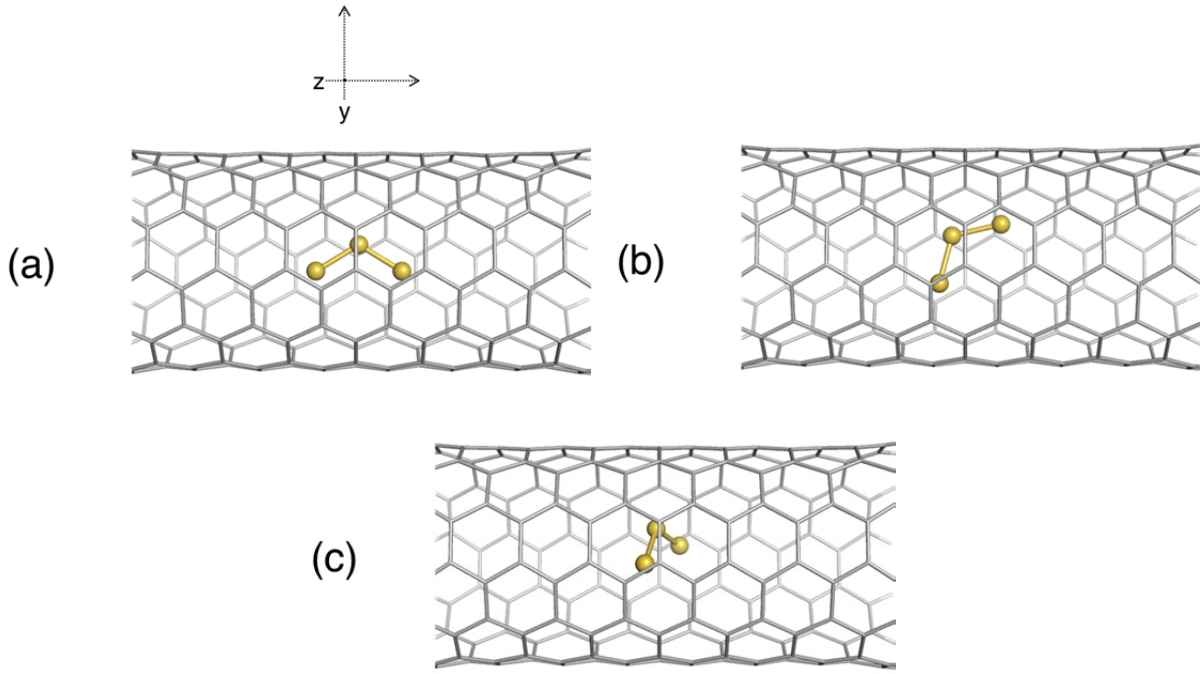

Figure 1-4. Side-on view of rotation **1** within the (6,6) SWNT. Conformer (c) was less stable by ~20 kcal/mol compared to (a) or (b).

Molecular dynamics calculations were not carried out, so we can only provide a qualitative picture based on the above static computed structures. Because of the large radii, undoubtedly many S_3 molecules can reside within the (6,6), (7,7) and (8,8) SWNTs which could oligomerize to other sulfur allotropes or plug the nanotubes. The coupling product cyclic S_6 does not fit within the (5,5) SWNT, however there is sufficient but limited space for cyclic S_8 within the (6,6) SWNT (Figure 5). *Catena*-sulfur could form,[31] and our ONIOM inner tube S_3 dimerization results agree with the previous assessment for a triplet S_6 chain product,[32] whose egress or translational motion would likely be restricted by reptation.[33] Reactions inside nanotubes are possible, as an example, the intercalation of CdI_2 and molten elemental sulfur guests has been reported, leading to a CdS@SWNT composite, but in larger diameter tubes 1-1.4 nm[34] than those studied here.

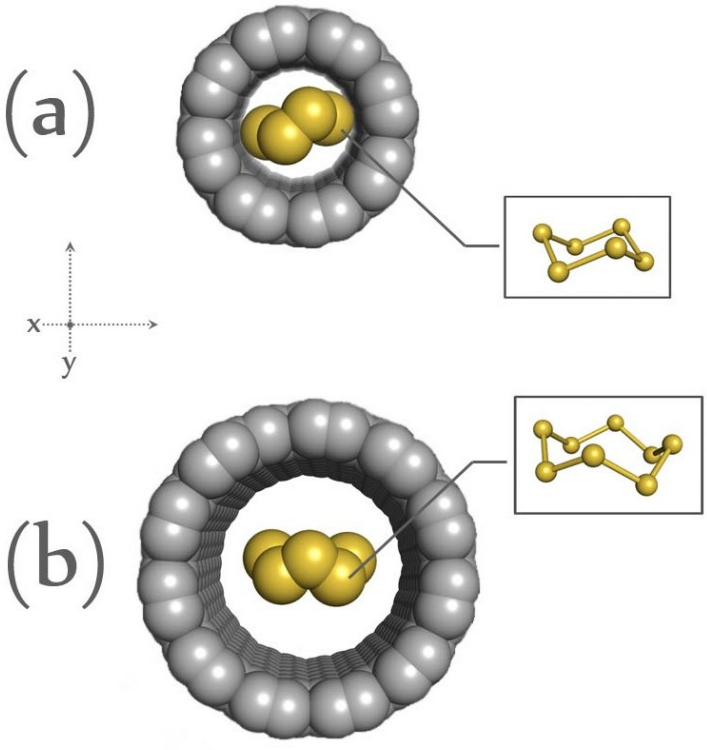

Figure 1-5. End-on view of (a) cyclic S_6@(5,5) SWNT, and (b) cyclic S_8@(6,6) SWNT.

1.3.3. Mode of Attack of Thiozone on the Exterior of Curved Aromatic Compounds.

Three modes for the attack of S_3 were considered. Because C_{60} has greater curvature than any nanotube studied here, it served as a model compound to examine thiozonation paths. Figure 1-6 shows the three routes studied for the addition of **1** to C_{60}, the 1,3-dipolar addition to form 3',4',5'-trithiacyclopenta(1,9)(C_{60})(5,6)fullerene **5** (path A), the (2 + 2) cycloaddition to form the 3',4'-dithiacyclobuta-1-sulfide(1,9)(C_{60})(5,6)fullerene **6** (path B), and the chelotrope addition to form the 3'-thiacyclopropa-1,1-disulfide(1,9)(C_{60})(5,6)fullerene **7** (path C). Path A involves the symmetrical formation of the C1-S1 and C2-S3 bonds in **TS4/5** to give thiozonide **5**. The $C_{60}S_3$ thiozonide **5** has C_s symmetry and C1-S1 and C2-S3 bond lengths of 1.87 Å (Figure 1-7). Path B involves formation of the C1-S1 and C2-S2 bonds in **TS4/6** to give 1,2-dithietane-1-sulfide **6**. Dithietane **6** has a branched S2=S3 bond that is 1.92 Å in length. Path C involves formation of the C1-S2 and C2-S2 bonds in **TS4/7** to give C_{2v} symmetric thiirane-1,1-disulfide **7**. Compound **7** has S1-S2 and S2-S3 bond lengths of 1.94 Å and a structure analogous to a thiirane sulfone.[35]

As expected, the 1,3-dipolar addition of S_3 at the 6,6 site was preferred compared to the [2 + 2] cycloaddition and chelotrope paths. The computed barriers of paths A-C were 5.6 kcal/mol, 28.0 kcal/mol, and 42.6 kcal/mol, respectively. Path A was exothermic by 21.2 kcal/mol. In contrast, path B was endothermic by 1.4 kcal/mol, and path C was endothermic by 29.7 kcal/mol. Unlike the endergonic 1,3-dipolar cycloaddition of azomethine ylide to various nanostructures[36] at 298 K, the ΔG_{rxn} of path A was -5.9 kcal/mol suggesting the trisulfane product may be stable at room temperature. The results are understandable in terms of a 1,3-dipole process (reported by Huisgen about fifty years ago) for species such as ozone.[37] In this regard there is some similarity to the fullerene/ozone system. Previous PBE/TZ calculations have shown the addition of ozone to C_{60} at

the 6,6 site to be exothermic by 31.5 kcal/mol, and to C_{70} at the *a,b* site to be exothermic by 30.6 kcal/mol.[38,39]

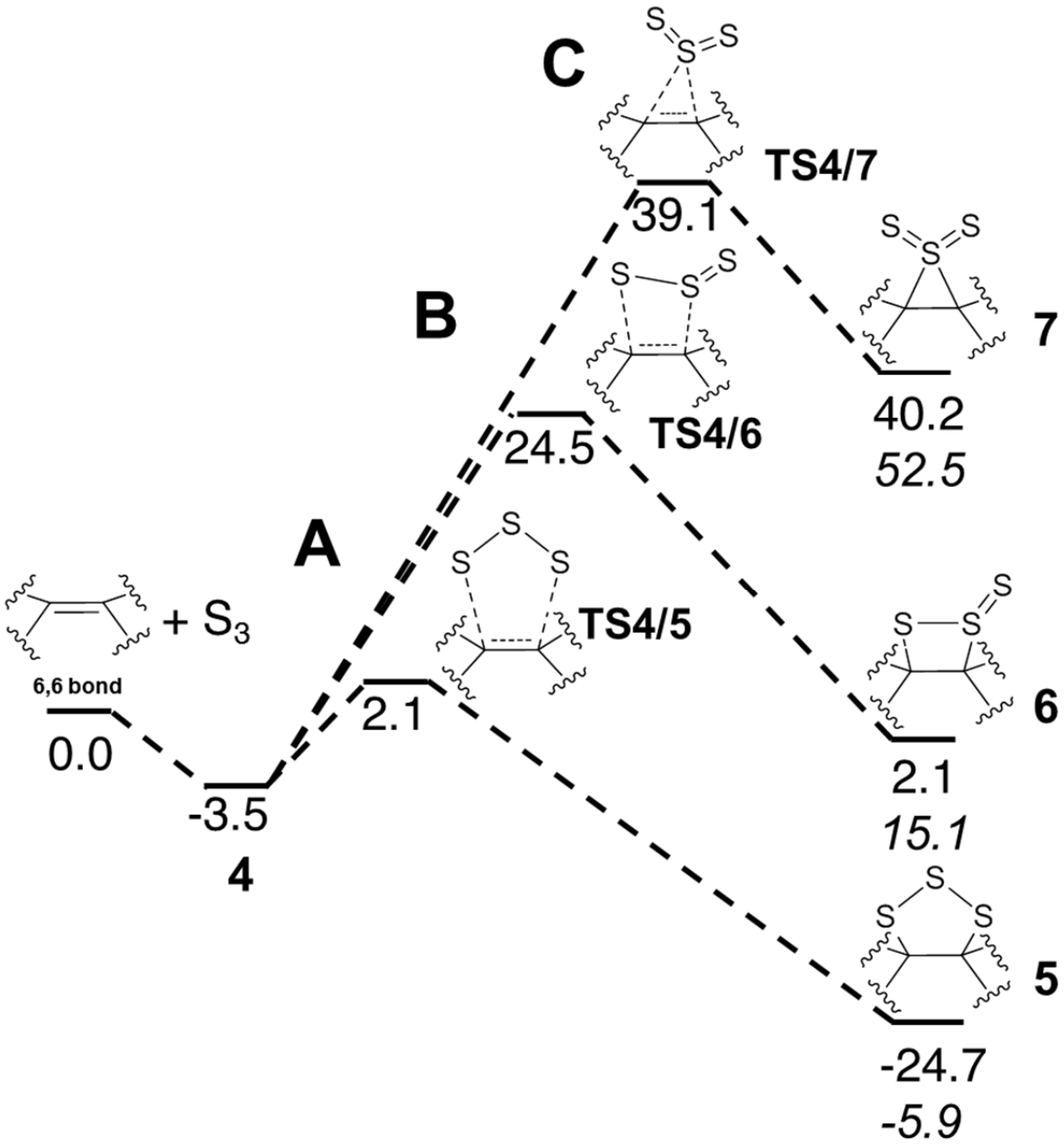

Figure 1-6. ONIOM(B3P86/6-311+G(2d):SVWN/STO-3G)//ONIOM(B3P86/6-31G(d):SVWN/ STO-G3) computed energetics of the S_3 [60]fullerene sulfuration, which includes thermal corrections for enthalpy at 298K (in kcal/mol). The values for free energy are in italics.

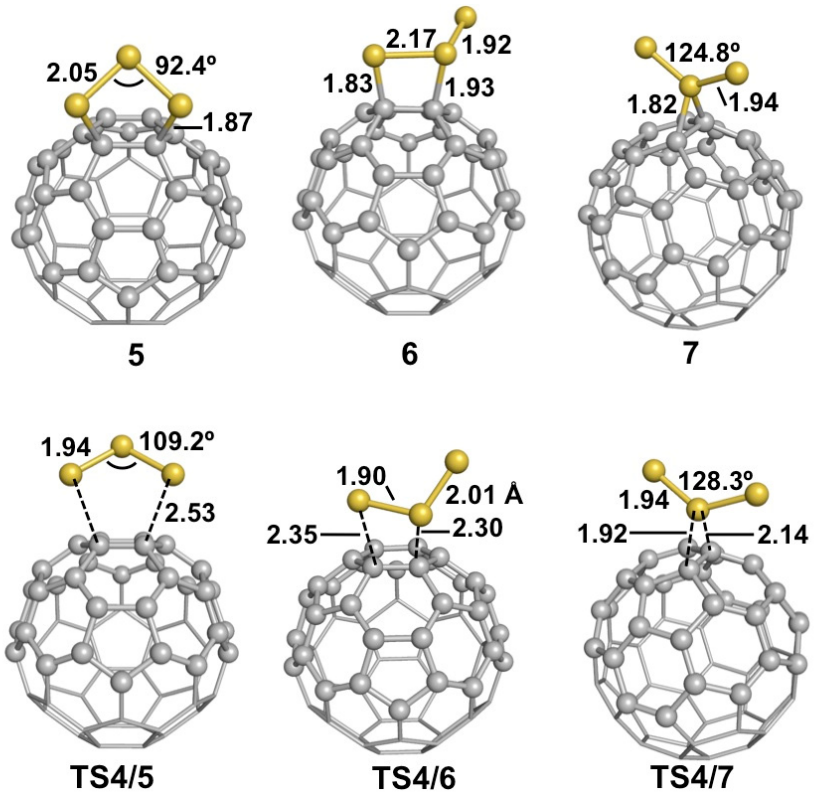

Figure 1-7. ONIOM(B3P86/6-31G(d):SVWN/STO-3G) optimized geometries of minima and transition structures (bond distances are in Å, angles are in deg.). The B3P86 layer is in ball-and-stick model and the SVWN layer is in tube model. The grey atoms are carbon and the yellow atoms are sulfur.

An interesting feature of the 1,2,3-trithiane ring of $C_{60}S_3$ **5**, is that it has an envelope conformation with a pucker angle of 121.0° and a barrier to ring inversion of $\Delta H^{\ddagger}$ = 20.3 kcal/mol at the B3P86/6-31G(d) level (A) in Figure 1-8. 1,2,3-trisulfane arenes, such as trithiolane (6b,12b-epitrithioacenaphtho(1,2-*a*)acenaphthylene have similar but lower barriers to ring inversion ($\Delta H^{\ddagger}$ = 13.9 kcal/mol by dynamic NMR analyses), ((B) in Figure 1-8).[40] This difference in $\Delta H^{\ddagger}$ can be attributes to the lack of flexibility of the C_{60} cage. The structural features of the enveloped-shaped **5** is similar to that of molozonides, and both reactions have large barriers for back dissociation of S_3 or O_3. Harpp and Smith have reported the S-S bond cleaving process of a trisulfide, but this process required phosphorus compounds to lead to sulfur extrusion.[13]

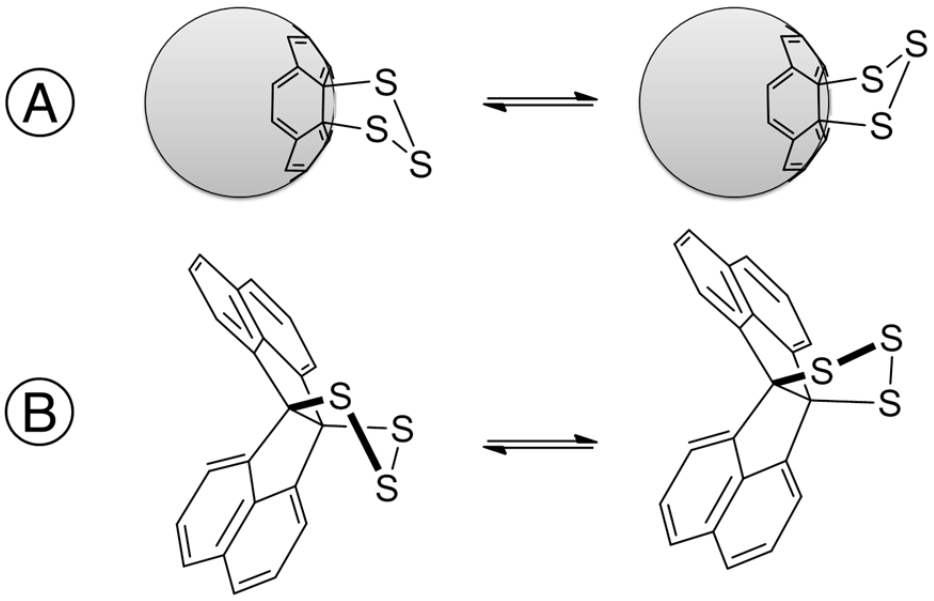

Figure 1-8. Ring flipping inversion of $C_{60}S_3$ and trithiolane (6b,12b-epitrithioacenaphtho[1,2-a]acenaphthylene. The puckering angle is a measure of deviation of the ring from planarity as defined as the angle formed by the center sulfur and the midpoint of the plane made by the flanking two carbon-sulfur bonds.

1.3.4. Thiozonation of the Convex Face of SWNTs.

In this section, ONIOM calculations were employed to examine the exterior thiozonolysis of armchair (*n*,*n*) SWNTs (*n* = 4-8) (Table 1-3 and Figure 1-9). There were multiple reactive sites on the SWNTs; however, we selected a reaction where the orientation of the S1 and S3 atoms of S_3 added at the orthogonal 6,6 site in the middle of the nanotube. For comparison, calculated values were also included for graphene and C_{60}. Only the 1,3-dipolar cycloaddition step was examined since the second step involving S-S bond rearrangement to the four-membered ring dithiacyclobutasulfide should be a high energy process (*vide supra*). The ONIOM geometries of **5** and **9**-**13** were substantially different from **14** and **15**. In the former, the C-S bond distances were less than 2.0 Å, in the latter, they were ~4.0 Å. **The** *abcd* dihedral angle change (defined in Table 1-3), used to gauge the

magnitude of change in sp^3 character of the trisulfane product versus the sp^2 character of the initial all-carbon precursor also showed a curvature-dependent thiozonation. Thiozonides were formed for **5**, **9**-**13**, and S_3 was physisorbed for **14** and **15**. The greater curvature (smaller diameter) of the arene host led to enhanced stability of the thiozonide product. The thiozonation was exothermic for C_{60}, as well as for the SWNTs of diameters less than ~6.8 Å, with reagent *abcd* dihedral angles less than ~157° in the series examined.

Table 1-3. Calculated Structural Parameters of Thiozonides or Thiozone Adducts of (60)Fullerene, SWNTs, and Graphene[a,b]

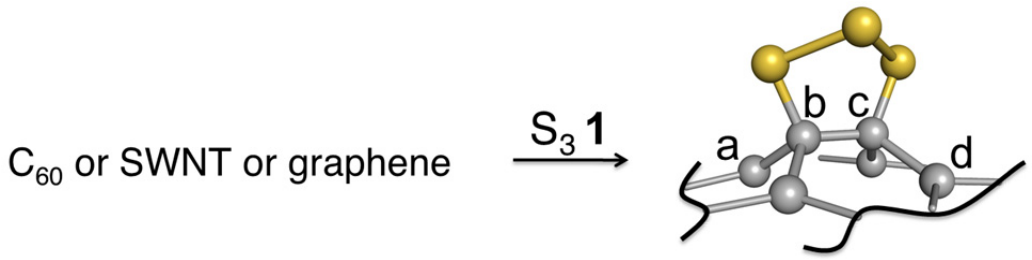

Thiozonide	C1-S1 (Å)	S1-S2-S3 (Å)	*abcd* in reagent (°)	*abcd* in product (°)
$C_{60}S_3$ **9**	1.86	92.5	138.4	115.2
(4,4) SWNT S_3 **10**	1.91	93.0	156.4	130.3
(5,5) SWNT S_3 **11**	1.93	93.0	156.9	132.0
(6,6) SWNT S_3 **12**	1.94	92.9	160.8	133.2
(7,7) SWNT S_3 **13**	1.96	93.0	163.4	134.1
(8,8) SWNT S_3 **14**	3.96	117.6	165.3	-
GrapheneS_3 **15**	4.01	118.4	180.0	-

[a] Optimized at the ONIOM(B3P86/6-31G(d):SVWN/STO-3G) level. The B3P86/6-31G(d) portion of the ONIOM calculation included S_3 and the dinaphthoovalene core, and SVWN/STO-3G was used on the remaining portion of the molecule. [b] Length of the SWNTs = 2 nm.

It can be noted that a low-energy path to cleavage of the S-S and C-S bonds in **5** was not found, **5** did not decompose to Criegee-like intermediates [thione ($R_2C=S$) and thiosulfine ($R_2C=S^+$-S^-)] and $C_{60}S_3$ thiozonide **5** converts to the four-membered ring 1,2-dithietane-1-sulfide **(6**) in a high-energy process (53.6 kcal/mol). By comparison, fullerene molozonides are labile[41] and decompose

by Criegee carbonyl/carbonyl-*O*-oxide pairs.[42] The carbonyl oxygen attacks the carbonyl-*O*-oxide carbon leading to O_2 departure and sp^3 epoxide or sp^2 oxidoannulene formation (such as the *a,b*-isomer and *c,c*-isomer, respectively in C_{70}). SWNT thiozonolysis pathways were not sought.

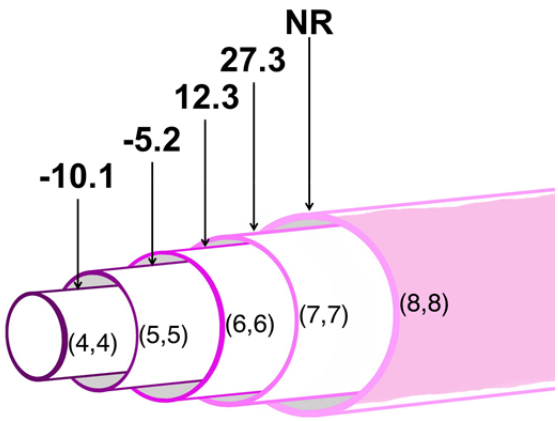

Figure 1-9. Schematic representation of the (*n,n*) SWNTs (n = 4-8) and the ΔH_{rxn} (kcal/mol) for the formation of thiozonides connected orthogonally along the *x*- or *y*-axes. Energetics were computed at the ONIOM(B3P86/6-311+G(2d):SVWN/STO-3G)//ONIOM(B3P86/6-31G(d):SVWN/STO-3G) level. NR= No reaction.

1.4. Conclusion

The calculations of free and nanotube-encapsulated thiozone are in accordance with experimental results and previous calculations, with the open form having greater stability. There was no reactivity of S_3 with the nanotube interior itself. The (5,5) SWNT was unique among the thiozone-trapped CNTs, as **1** was situated parallel to the tube, although the difficulty of translational motion of S_3 (or the reptative motion of S_6 or S_9 chain products) was not computed. Larger diameter SWNTs ((*n,n*) *n* = 6-8)) have larger spaces to trap many S_3 molecules, but there was restricted or insufficient space for cyclic S_6 in the (*5,5*) SWNT and cyclic S_8 in the (6,6) SWNT. Thiozonolysis was

predicted to trisulfurate convex arene surfaces, such as the (4,4) and (5,5) SWNTs, due to greater convexity than the (6,6), (7,7), and (8,8) SWNTs. The 1,3-dipolar addition of S_3 was preferred compared to the [2 + 2] cycloaddition and chelotrope paths.

Chapter 2. Theoretical Studies of a Singlet Oxygen-Releasing Dioxapaddlane (1,4-diicosa naphthalene-1,4-endoperoxide)

2.1. Introduction

1,4-Dimethyl naphthalene (**1**) reversibly binds $^1O_2$; upon heating, the naphthalene endoperoxide (**2**) dissociates $^1O_2$ and a small amount of $^3O_2$ (Scheme 2-1).[1] Modifications of substituents at the 1,4-positions of naphthalene have been made.[2-8] For example, naphthalene **3** has bulky substituents slowing the rate of $^1O_2$ addition at the 1,4-positions so that binding at the 6,9-positions also takes place.[9-11] Singlet oxygen release has also been examined in polymeric endoperoxides,[12-18] such as 1,4-dimethyl-2-poly(vinylnaphthalene-1,4-endoperoxide).[19] However, no studies have yet focused on the $^1O_2$ release from a naphthalene endoperoxide molecule bearing a "lid".

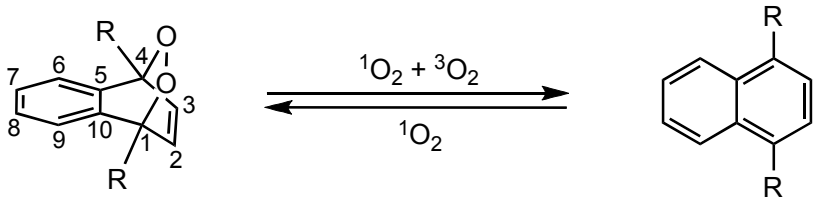

2 (R=CH_3) **1** (R=CH_3)

4 (R=$CH(CONHCH_2CH_2(OH)CH_2OH)_2$) **3** (R=$CH(CONHCH_2CH_2(OH)CH_2OH)_2$)

Scheme 2-1. Reaction of 1,4-disubstituted naphthalenes with singlet oxygen.

Lid bearing compounds are treatable by computational methods; however, such studies remain highly challenging. Owing to its multiconfigurational character, computational studies on $^1O_2$ with compounds containing 10 or more carbon atoms are rather uncommon.[20-30] Encouragingly, Wasserman *et al.*[31] showed that B3LYP/6-311+G(d) calculations can reproduce the experimental energetics of several naphthalene-$^1O_2$/naphthalene endoperoxide pairs—including compounds **1** and **2**. Due to the success of the study of Wasserman *et al.*,[31] one may anticipate that replacing the methyls at the 1,4-positions with a polymethylene-bridge would be amenable to computation [e.g., 1,4-diicosa naphthalene (**5**) and 1,4-diicosa naphthalene-1,4-endoperoxide (**6**)] (Scheme 2-2).

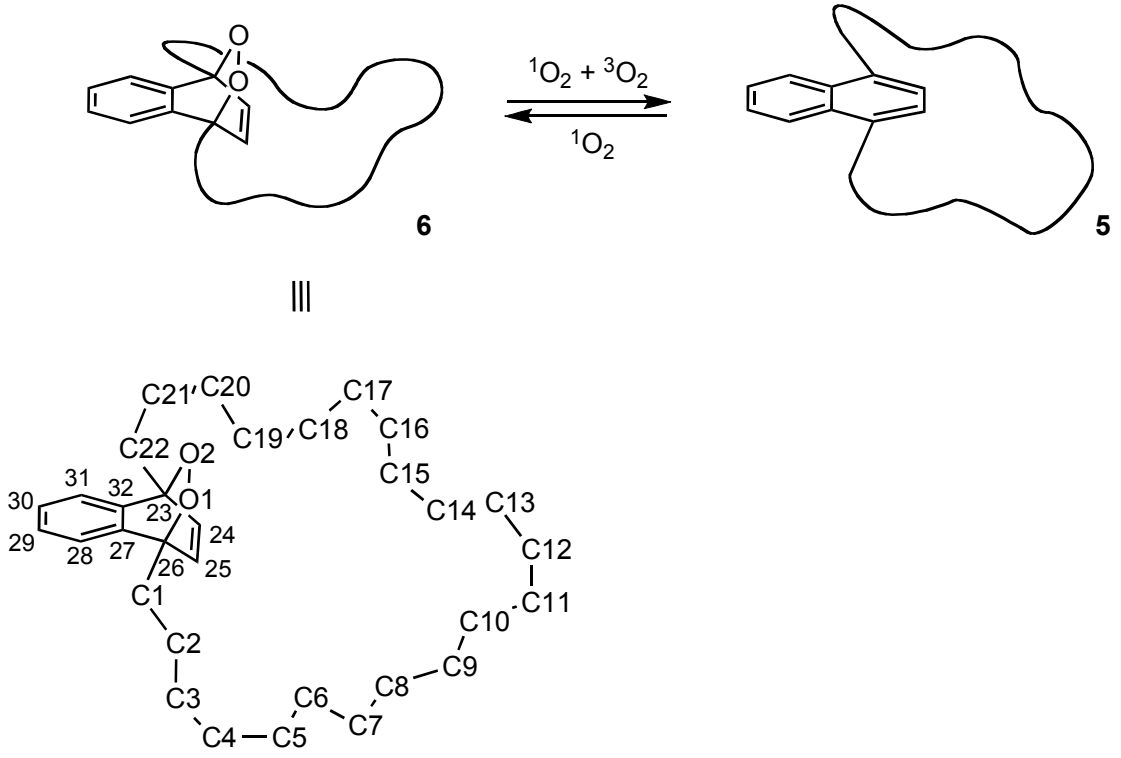

Scheme 2-2. Release of singlet oxygen from 1,4 diicosa naphthalene-1,4-endoperoxide.

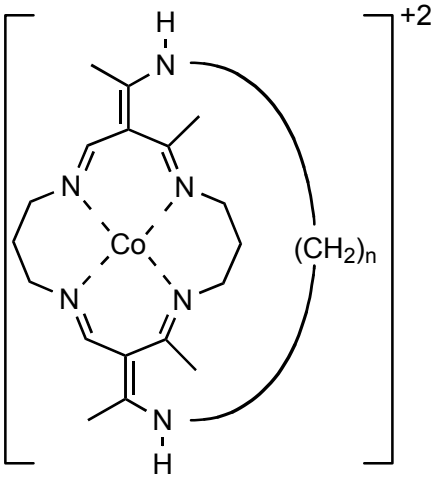

7 axial N-methylimidazole not shown

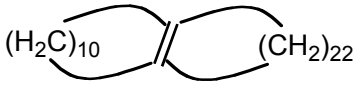

8

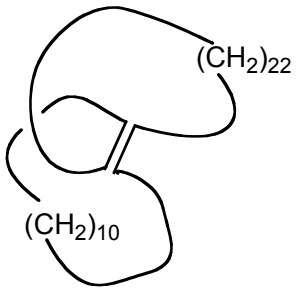

9

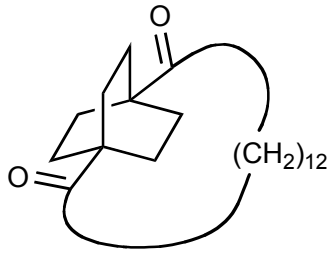

10

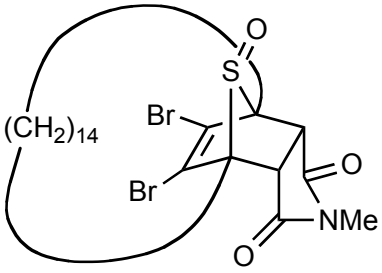

11

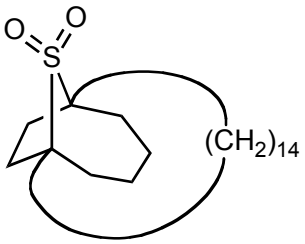

12 synthesis attempted

Scheme 2-3. A selection of compounds which contain polymethylene bridges.

Researchers have examined polymethylene-bridged molecules for many years.[32-43] The length and anchor position of the polymethylene chain can expose or "hide" a reactive site of a compound (Scheme 2-3). In 1980, Busch *et al.*[44,45] showed that the chain of length six (rather than five) methylenes increased the affinity of oxygen in cobalt cyclidene **7**, which formed a CoO_2 adduct. In

1980, Marshall[40] showed that unlike *trans*-fused **9**, *cis*-fused **8** forms a colored charge-transfer complex with tetracyanoethylene (TCNE) due to its less shielded alkene site. Another intriguing class of polymethylene-bridged compounds are paddlanes, such as structures **10**-**12**.[46-56] Theoretical calculations have yielded valuable information on the reactivity and conformational properties of polymethylene-bridged compounds[57-61] and paddlanes.[62-64]

Here, we present results of Monte Carlo and ONIOM calculations that incorporated AM1 and B3LYP to analyze the conformational influence of the polymethylene chain in the cycloreversion of **6**, yielding $^1O_2$ and **5**. The **5/6** pair was selected because the polymethylene chain was sufficiently long that it could undergo rope-skipping conformational changes on the basis of Dreiding models, creating a possible O_2 binding site at the 23,26-positions (atom numbering in Scheme 2-2). Binding or release of $^1O_2$ at the 28,31-positions was not computed. The idea was that chain rotation (full-circle vs semi-circle) might lead to increased endoperoxide stability at higher temperatures based on an increased rate of rotation, which led us inquire into a possible oxygen "gatekeeper" mechanism.

2.2. Computational Details

Semi-empirical and density functional theory (DFT) calculations were conducted with the Gaussian 03 program package.[65] Monte Carlo calculations were conducted with Hyperchem 8.0.[66] Standard computational protocols were used[67] and the structures were viewed with the GaussView program.[68] A previous computational study demonstrated that the 6-311+G(d) basis set adequately described the naphthalene endoperoxide decomposition reaction surface.[31] The transition state structures **TS-AM1** and **TS-B3LYP**, and those connecting the pairs **5**/**6**, **13**/**14**, **15**/**16**, and **17**/**18**

were confirmed to be transition states by frequency calculations and by conducting internal reaction coordinate (IRC) calculations for the reaction path for the transition. IRC calculations were not performed on the ONIOM derived transitions state structures. Conformations of **6** were searched by the Monte Carlo method with the MM+ force field. The MM+ calculations were followed by AM1 optimizations with the Fletcher-Reeves conjugate gradient algorithm and the lowest energy conformations reoptimized by ONIOM(B3LYP/6-311+G(d):AM1). **6TSa/b**, **6TSb/c**, **6TSc/d**, **6TSd/e**, and **6TSe/a** were assumed to be transition state structures, since they cannot be examined by IRC calculations with G03. All energetics obtained were corrected for zero-point energy (ZPE). The ONIOM treatment separated part of the lid from the rest of the molecule, in which the junction between B3LYP/6-311+G(d) and AM1 was at the C2-C3 and C20-C21 bonds (cf. Scheme 2-2 and Scheme 2-4).

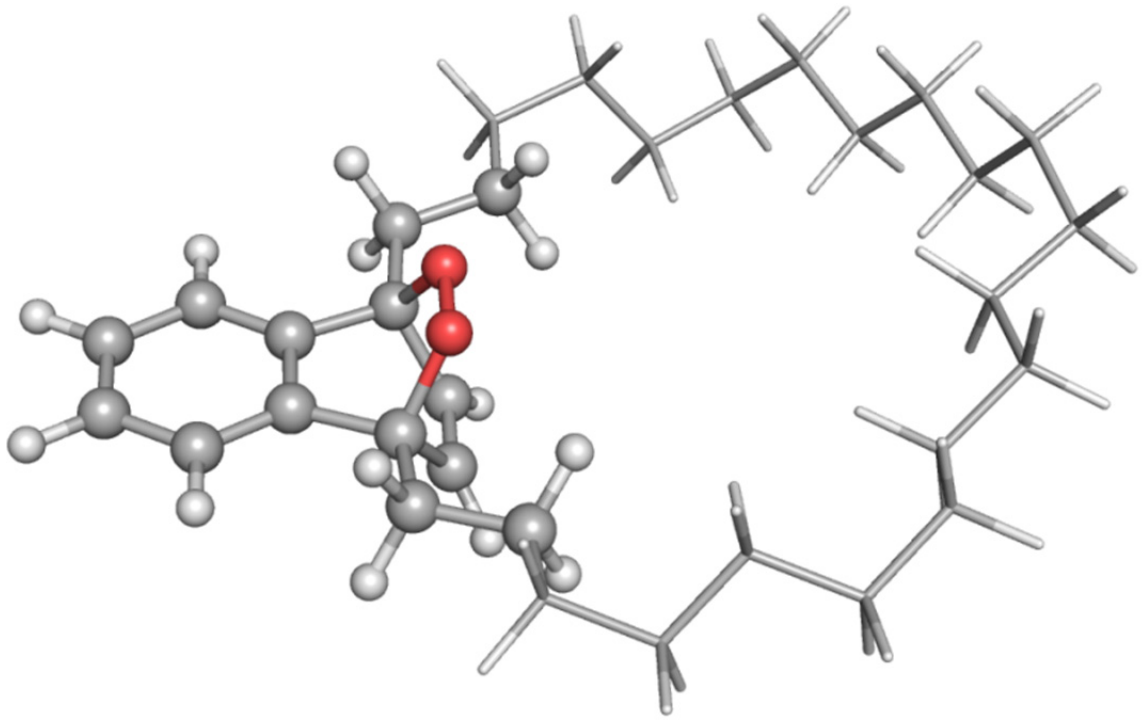

Scheme 2-4. The DFT portion of the ONIOM calculation is shown with a ball-and-stick model, and the AM1 portion is shown with a tube model.

2.3. Results and Discussion

2.3.1. Singlet Oxygen Release from Endoperoxides.

Our first aim was to evaluate whether naphthalene endoperoxide decompositions could be accurately computed with the fairly low-cost computational methods B3LYP/6-311+G(d)//AM1 and ONIOM(B3LYP/6-311+G(d):AM1). Our paper builds on Wasserman's previous DFT study of naphthalene endoperoxides, in which the B3LYP/6-311+G(d) energy of $^1O_2$ was estimated to be -150.30756 Hartrees.[31] AM1 and B3LYP/6-311+G(d) transition state structures (TSs) corresponding to the decomposition of naphthalene endoperoxide **2** to naphthalene **1** and $^1O_2$ are shown in Figure 2-1. **TS-AM1** has a shorter C1-O1 bond (0.24 Å), C4-O2 bond (0.09 Å), and O1-O2 bond (0.12 Å) compared to **TS-B3LYP**, and the O2-O1-C1-C2 torsion angle is 18° larger [cf. 58° (**TS-AM1**) vs 40° (**TS-B3LYP**)]. Similar transition structure geometries were found for $^1O_2$ dissociation from 1,4-diicosa naphthalene-1,4-endoperoxide **6**, naphthalene-1,4-endoperoxide **14**, 1-ethylnaphthalene-1,4-endoperoxide **16**, 1,4,5-trimethylnaphthalene-1,4-endoperoxide **18**.

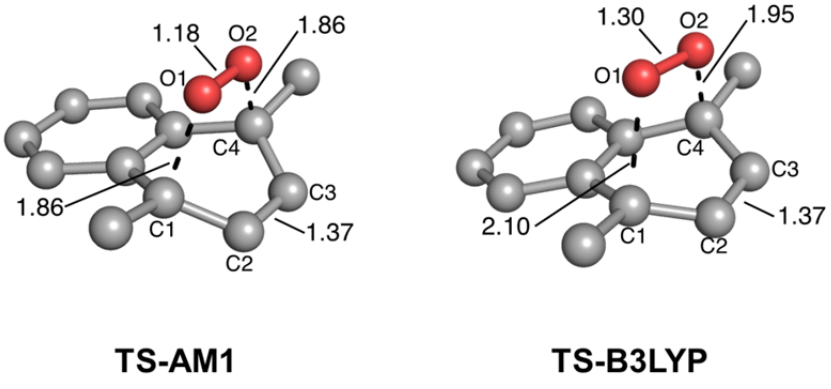

Figure 2-1. AM1 optimized (*left*) and B3LYP/6-311+G(d) optimized (*right*) transition state structures for the decomposition of 1,4-dimethyl-1,4-naphthalene endoperoxide **2** to 1,4-dimethyl-1,4-naphthalene **1** and $^1O_2$. For clarity, the hydrogen atoms are not shown.

The decomposition of naphthalene endoperoxides is reminiscent of retro Diels-Alder reactions of "masked" dienes (Scheme 2-5).[69-72] Masked dienes such as compound **19** are similar to the naphthalene compounds studied here, in which DFT methods often yield results in excellent agreement with experiment;[69-75] however, the B3LYP functional is not devoid of shortcomings especially with larger sized molecules.[76-78] We find the decomposition of endoperoxides **2**, **6**, **14**, **16**, and **18** to be endothermic by 6-17 kcal/mol (Table 2-1). The energy of **2** relative to **1** and $^1O_2$ was similar with B3LYP/6-311+G(d) (11 kcal/mol) and B3LYP/6-311+G(d)//AM1 (13 kcal/mol) calculations. The activation energy barriers for the release of $^1O_2$ from the endoperoxides ranged from 20-28 kcal/mol. The B3LYP/6-311+G(d)//AM1 structure **TS-AM1** (25 kcal/mol) was predicted to be 4 kcal/mol higher in energy than the B3LYP/6-311+G(d) structure **TS-B3LYP** (21 kcal/mol) for the reaction of **2** to **1** and $^1O_2$.

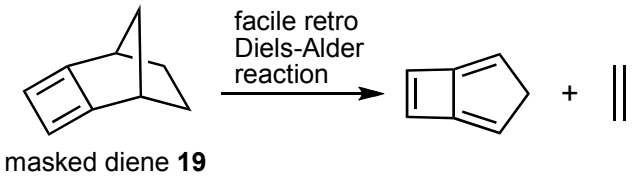

Scheme 2-5. A retro Diels-Alder reaction of a maked diene.

The computed barrier heights are similar to the experimental free energy barriers [cf. experimental value of **2** ($\Delta G^{\ddagger}$=23.6 kcal/mol) with B3LYP/6-311+G(d)//AM1 ($\Delta E^{\ddagger}$=25 kcal/mol), and the experimental value of **17** ($\Delta G^{\ddagger}$=25.9 kcal/mol) with B3LYP/6-311+G(d)//AM1 ($\Delta E^{\ddagger}$=26 kcal/mol)]. ONIOM(B3LYP/6-311+G(d):AM1) produces an activation energy of 22 kcal/mol when the junction between B3LYP and AM1 was situated at the methyl and methylene carbon atoms in the **15**/**16** pair (Reaction C, Table 2-1).

Table 2-1. Calculated and Experimental Energetics for Decomposition Reactions of Endoperoxides.

	Reaction	ΔE‡ (kcal/mol) B3LYP[a,d]	ΔE‡ (kcal/mol) B3LYP //AM1[b,d]	ΔE‡ (kcal/mol) ONIOM[c]	ΔG‡ exptl. (kcal/mol)[g]	ΔE (kcal/mol) B3LYP[a,d]	ΔE (kcal/mol) B3LYP //AM1[b,d]	ΔE (kcal/mol) ONIOM[c]
A	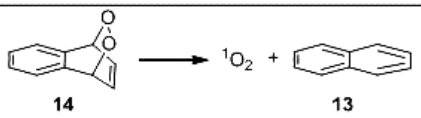 **14** **13**	21	26	-	-	6	6	-
B	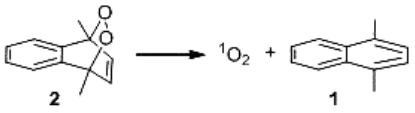 **2** **1**	21	25	-	23.6	11	13	-
C[e]	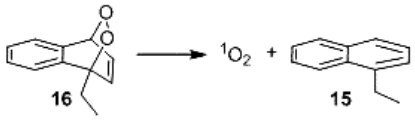 **16** **15**	20	25	22	-	10	9	6
D	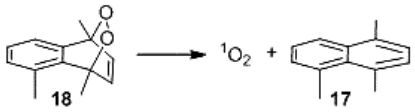 **18** **17**	21	26	-	25.9	14	17	-
E	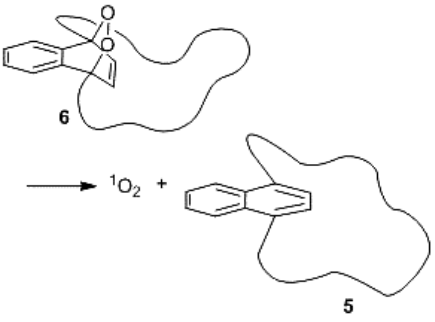 **6** **5**	-	28[f]	22[f]	-	-	10	15

[a] B3LYP/6-311+G(d). [b] B3LYP/6-311+G(d)//AM1. [c] ONIOM(B3LYP/6-311+G(d):AM1). [d] B3LYP/6-311+G(d) values obtained in ref. 31 by using a B3LYP/6-311+G(d) energy for $^1O_2$ of -150.30756 Hartrees. [e] Reaction **C** reports values for the "out" conformer of 1-ethylnaphthalene-1,4-endoperoxide **16**, which is more stable than the "in" conformer by 0.2 kcal/mol (

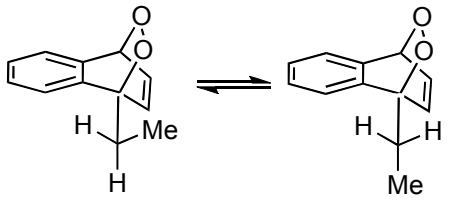

"out" conformer **16** "in" conformer **16**). [f] The global minima for 1,4-diicosa naphthalene **5** and 1,4-diicosa naphthalene-1,4-endoperoxide **6** were found based on a Monte Carlo conformational search of the potential energy surface with the MM+ force field and reoptimization of the lowest energy conformers by ONIOM(B3LYP/6-311+G(d):AM1). [g] Ref. 31.

The qualities of the energetics of the B3LYP/6-311+G(d)//AM1 and ONIOM(B3LYP/6-311+G(d):AM1) calculations were very good compared with those obtained with B3LYP/6-311+G(d) and experimental observations.[31] The data suggested that naphthalene endoperoxide decompositions can be computed to within ±3 kcal/mol with B3LYP/6-311+G(d)//AM1 for **2**, **14**, **16**, and **18**, and ONIOM(B3LYP/6-311+G(d):AM1) for **6** and **16**.

2.3.2. Conformational Analysis of "Jump Rope" Endoperoxide 6.

Our second aim was to compute the lowest energy path for **6** corresponding to a 360° circular rotation of the polymethylene chain around the endoperoxide core. Endoperoxide **6** is an example of a paddlane, where the fused benzene and peroxide groups are rigid and the polymethylene chain is very flexible. Conformations of **6** were searched by the Monte Carlo method with the MM+ force field followed by AM1 optimizations. The dihedral angle θ = C(25)-C(26)-C(1)-C(2) (defined below), was followed in 10° increments and the dihedral angle φ = C(24)-C(23)-C(22)-C(21) was followed in 15° increments, each independently, for the 360° rotation of the rope (i.e., 36 × 24 grid) (Figure 2-2). The dihedral angle θ is positive for a counter clockwise movement from C(2) to C(25) as one looks from C(1) to C(26). The φ dihedral angle is positive for a counter clockwise movement from C(21) to C(24) as one looks from C(23) to C(22). Due to the high flexibility of the polymethylene chain, each of the 864 points on the 36 × 24 grid (not surprisingly) possessed thousands of conformations. For example, **6a** was found from a search of 4456 conformations, which arose from an initial geometry that was chosen to have the polymethylene group facing *anti* to the fused benzene ring. Thus, restrictions were applied to obtain a rough estimation as to the nature of the conformational potential energy surface. Cutoff criteria were used where each of the 864 points on the 36 × 24 grid was limited to 10,000 optimizations and a rejection criteria of 6 kcal/mol.

This cutoff criteria led to the generation of ~200 conformations for each of the 864 points. The resulting lowest energy conformation from these ~200 conformations was optimized by AM1 and then reoptimized by ONIOM(B3LYP/6-311+G(d):AM1). The lowest energy pathway for the 360° rotation of the polymethylene chain in **6** was deduced from the three-dimensional plot in Figure 2-2.

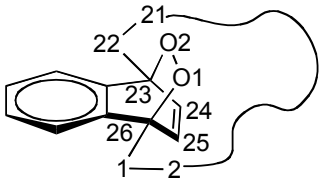

6a

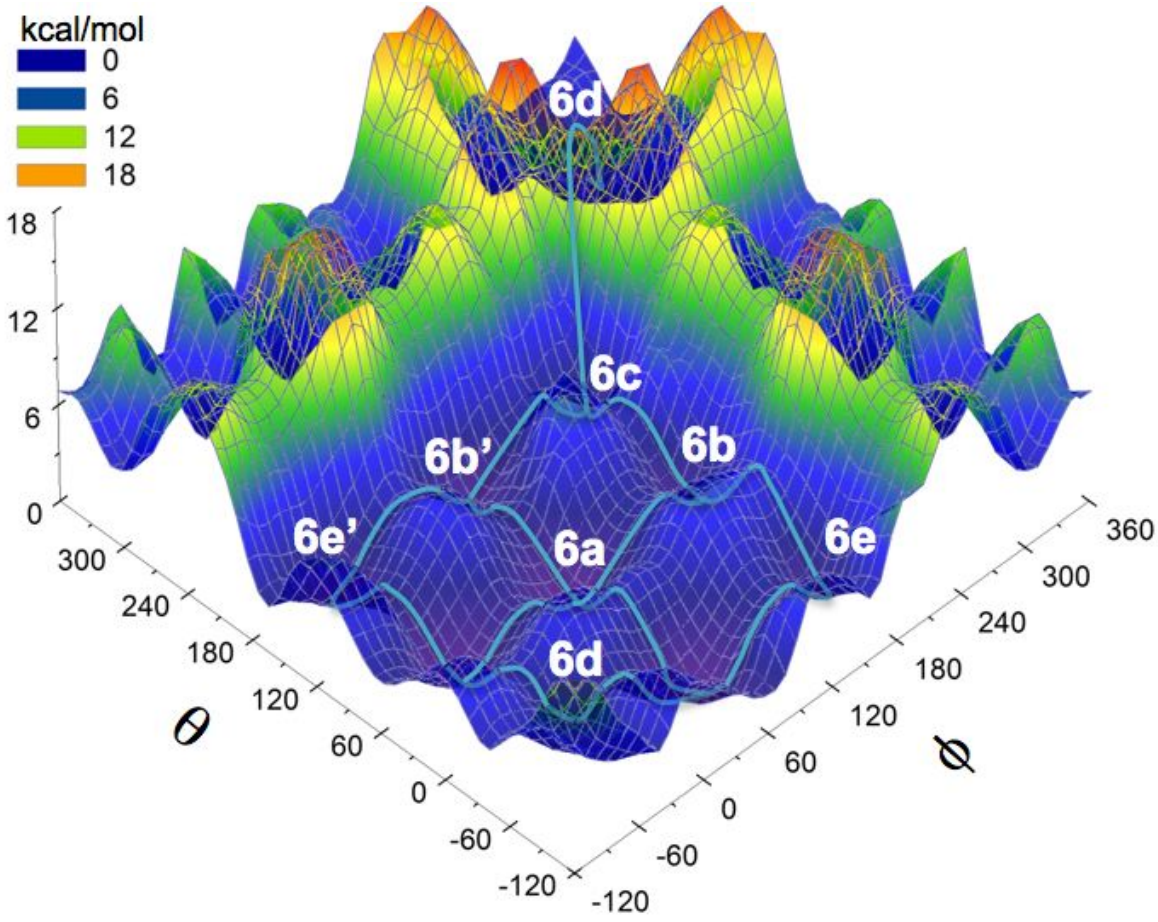

Figure 2-2. 3-Dimensional computed energy plot for the rotation of the polymethylene chain in **6**.

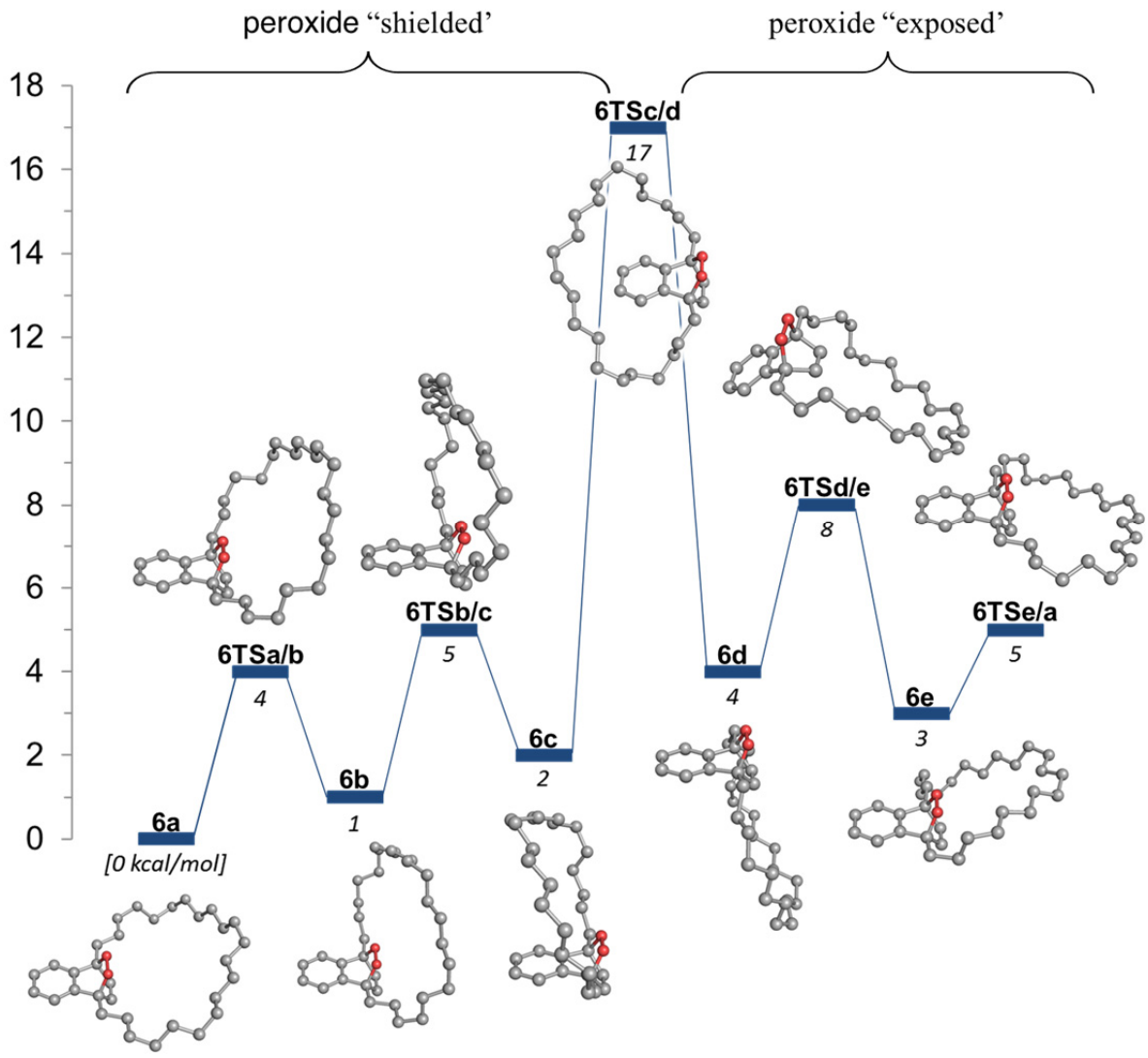

Figure 2-3. Side-on views of geometries and the conformational variations for the lowest energy path for rotation of the polymethylene chain of **6** in a counterclockwise direction. The peroxide group (red) is connected to carbon atoms (gray) where the naphthalene and polymethlyene attach. The hydrogen atoms are not shown. The lowest energy conformations were obtained by HyperChem and reoptimized at the ONIOM(B3LYP/6-311+G(d):AM1) level.

Figure 2-3 shows the most important geometries, in which conformers are displayed in side-on views. The jump rope rotation process is not particularly remarkable. As expected, we find that **6a** is the global minimum, in which the polymethylene chain is *anti* to the largest of the 3 paddles of the paddlane, the fused benzene ring. The torsion angles optimized for **6a** were $\theta = 54°$ and $\varphi = 60°$.

A transition state has been located (**6TSa/b**) connecting **6a** with **6b**, which predicts the C(23)-O(2) bond eclipses the C(21)-C(22) bond, in which with θ = 59° and φ = 120°. The activation barrier of **6TSa/b** is 2 kcal/mol. Rotamer **6b** has the C(22)-C(23) connector bond *gauche* to the peroxide and alkene, the C(1)-C(26) connector bond *gauche* to the fused benzene and alkene. Rotamer **6b'** has the C(1)-C(26) connector bond *gauche* to the peroxide and alkene, and the C(22)-C(23) connector bond *gauche* to the fused benzene and alkene. Rotamers **6b** and **6b'** led to **6c**. Transition state **6TSb/c** predicted that the C(26)-O(1) is eclipsed by the C(1)-C(2) bond, in which θ = 120° and φ = 166°. In minimum **6c**, the polymethylene chain is situated *anti* to the alkene group, where with θ = 160° and φ = 167°. Transition state **6TSc/d** represents the polymethylene chain passing over the fused benzene ring and was the highest point on the PES (17 kcal/mol, Figure 2-3) due to a repulsive steric interaction between the benzene hydrogens and the methylene hydrogens. Rotamer **6d** has the polymethylene chain *anti* to the peroxide group. Transition state **6TSd/e** has the C(1)-C(2) and C(25)-C(26) bonds eclipsed, in which with θ = 0° and φ = 56°. Rotamer **6e** has the C(1)-C(26) connecting point of the chain *gauche* to the peroxide and alkene, the C(22)-C(23) connecting point of the chain *gauche* to the fused benzene and alkene. Rotamer **6e'** has the C(22)-C(23) connecting point of the chain *gauche* to the peroxide and alkene, and the C(1)-C(6) connecting point of the chain *gauche* to the fused benzene and alkene. Transition state **6TSe/a** connects **6e** with **6a**, in which the activation barrier is 5 kcal/mol where θ = 49° and φ = 0°.

The two-layered ONIOM approach using DFT and semiempirical theory often performs well and supports experimental findings.[78-81] Nonetheless, our Monte Carlo and ONIOM approach was further investigated to determine whether it would successfully reproduce the experimental energetics of a test compound, dioxa-1,5-naphthalenophane (**19**), which involved a 180° rotation in a "jump rope" enantiomerization reaction (Figure 2-4).[58,59]

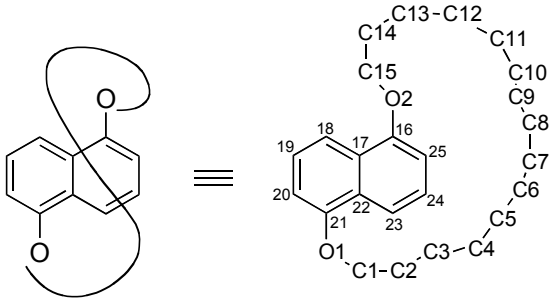

19

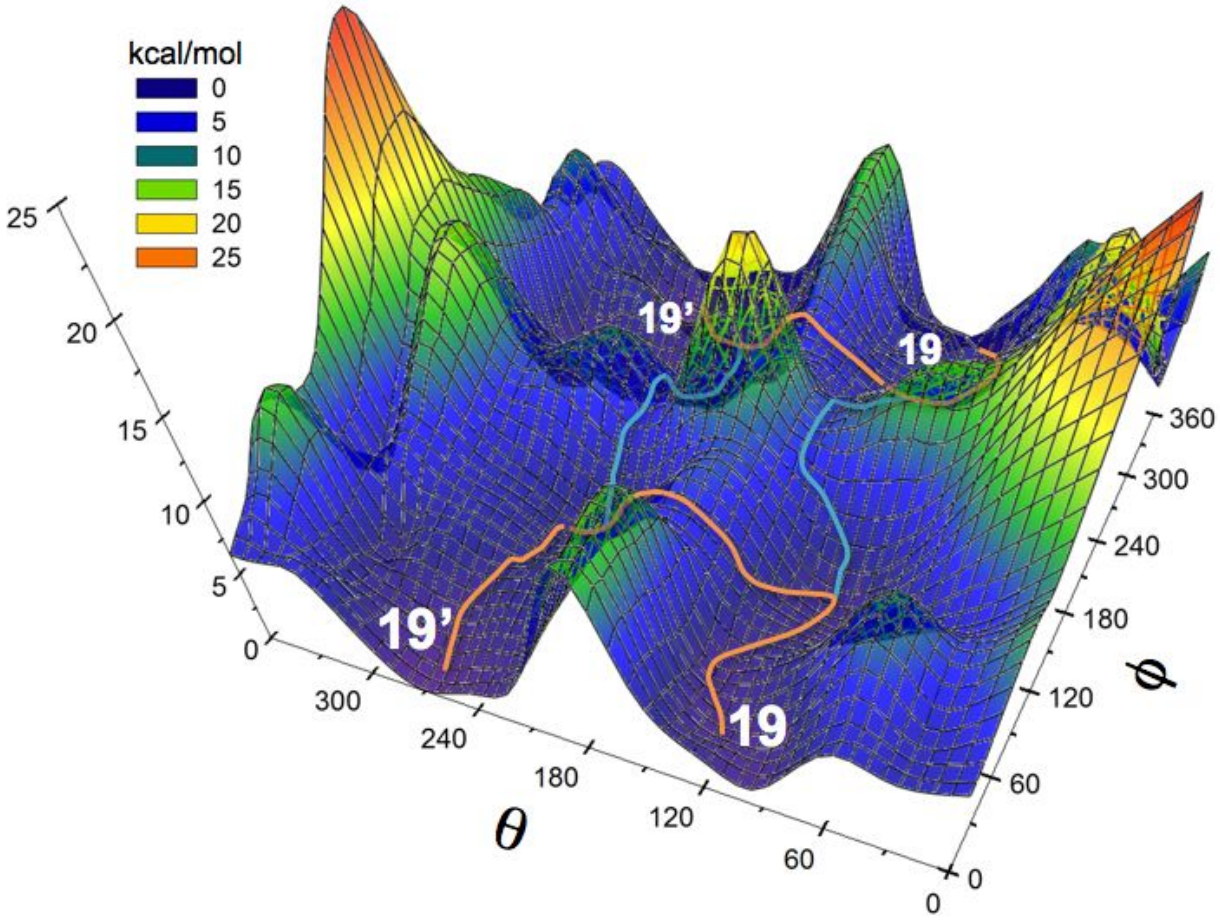

Figure 2-4. 3-Dimensional computed energy plot for the 180° rotation of the polymethylene chain in **19**. Orange lines represent pathways to enantiomerizations. Blue lines represent the full-circle rotation of the polymethylene chain.

The dihedral angles θ = O(2)-C(15)-C(14)-C(13) and φ = C(20)-C(21)-O(1)-C(1) were followed in 20° increments, each independently, for the 360° rotation of the rope (i.e., 19 × 19 grid). Cutoff criteria were used (similar to that for **6**) where each of the 361 points yielded ~200 conformations, in which the lowest in energy was optimized by AM1 and then reoptimized by ONIOM(B3LYP/6-311+G(d):AM1). The dihedral angle θ (defined above) is positive for a clockwise movement from C(20) to C(1) as one looks from C(21) to O(1). The φ dihedral angle is positive for a clockwise movement from O(2) to C(13) as one looks from C(15) to C(14). The transition structure connecting **19** with **19'** on the front portion of the figure contained θ = 162° and φ = 117°. A similar transition structure can be found at the back portion of the figure, which represents an approximate mirror image of the first transition structure. This Monte Carlo and ONIOM treatment resulted in an activation energy ($\Delta E^{\ddagger}$ = 6 kcal/mol) for a 180° rotation of the jump rope in **19**, which was similar with the experimental enantiomerization process measured to be 7.6 ± 0.8 kcal/mol.[50-57]

Even though the reproduction of the experimental enantiomerization barrier in **19** was successful, the conformational search on endoperoxide **6** may miss some details. For example, there was no guarantee that the minima found at each step were accessible in a continuous revolution of the angles on the 36 × 24 grid. The 22 C atoms in the ring have ~60 heavy-atom vibrational modes, in which the hydrogen atoms are assumed not to affect the matter substantially. Thus, 10,000 Monte Carlo steps may be sufficient to find a minimum if the structure is well-behaved; that is, in a simpler system relative to a structure such as **6**, which had a significant number of local minima.

2.3.3. Effect of the Polymethylene Lid on $^1O_2$ Formation.

Our third aim was to examine the influence of chain rotation of **6** with the unimolecular formation of $^1O_2$ and **5**. The calculations determined conformational stability of **6** based on the position of the polymethylene bridge and a trend for dissociation of $^1O_2$ with the "active" forms **6d**, **6e**, **6a** >> **6b**, **6c** appearing in different order compared to conformer stability **6a** > **6b** > **6c** > **6e** > **6d**. ONIOM saddle points connecting **6** with **5** and $^1O_2$ have been located for conformers **6a**, **6d**, and **6e**. Attempts at transition state optimizations for **6b** and **6c** resulted in rotation of the polymethylene bridge away from the dissociating $^1O_2$ site. Only those conformations that did not have the polymethylene lid situated over the peroxide group readily decomposed to $^1O_2$ and **5**. For example, rotamer **6d** had the polymethylene lid *gauche* to the benzene and ethylene groups so the peroxide group is highly exposed. Due to the low rotation energies connecting conformers **6a**-**6e** via **6TSa/b**, **6TSb/c**, **6TSd/e**, and **6TSe/a**, we postulate that the polymethylene chain functions as a gatekeeper for the oxygen, protecting the peroxide moiety, and potentially limiting the dissociation of $^1O_2$ from the naphthalene site.

The B3LYP/6-311+G(d)//AM1 activation energy for the dissociation of $^1O_2$ from **6a** ($\Delta E^{\ddagger}$=28 kcal/mol) was predicted to be higher than for **2** ($\Delta E^{\ddagger}$=25 kcal/mol), but the ONIOM(B3LYP/6-311+G(d):AM1) activation energy for **6a** was found to be lower ($\Delta E^{\ddagger}$=22 kcal/mol), but no trend emerges (Table 2-1). Naphthalene **5** may reversible bind $^1O_2$, and while this process was not modeled, one may expect that the jump-rope substituent at the 23,26-positions of naphthalene would slow the rate of $^1O_2$ addition to **5** so that competitive binding of $^1O_2$ at the 28,31-positions could also take place.[9-11] Reiterating a point made in the Introduction, the bulky

maloamide substituents in **3** are known to exert steric interactions that slowed binding of $^1O_2$ at the 1,4-positions, binding of $^1O_2$ at the 6,9-positions in a ratio of ~1:100 (1,4:6,9).

2.4. Conclusion

Our computational examination of a hypothetical $^1O_2$-carrier **6** was inspired by rope-skipping molecules that have been the subject of study for over 30 years.[40-61] The qualities of the energetics of $^1O_2$ dissociation from naphthalene endoperoxides with B3LYP/6-311+G(d)//AM1 and ONIOM(B3LYP/6-311+G(d):AM1) were very good compared with those obtained with B3LYP/6-311+G(d) and experimental observations.[1-31] The energetics of $^1O_2$ dissociation from the naphthalene site can only be tentatively determined in relation to the position of the $(CH_2)_{22}$ polymethylene lid due to the need for improved models that can compute the dynamics of the lid and the extent of chain clearance required in the singlet oxygen-release process. Conformers **6b**-**6e** were 4 kcal/mol or less above the global minimum **6a**, and the polymethylene chain favored semi-circle rotation where the ability to dissociate $^1O_2$ from conformers **6b** and **6c** was diminished due to shielding. In a similar vein, a large body of literature is available for $^1O_2$ generation, and a growing fraction of it is focusing on the escape of $^1O_2$ from confined and shielded environments.[82-88]

Chapter 3. Computational Chemistry and Mechanism of a Base Induced 5-*endo* Cyclization of Benzyl Alkynyl Sulfides

3.1. Introduction

2,3-Dihydrothiophenes are useful synthetic precursors for many compounds including thiophenes,[1] thionucleoside derivatives[2] and penicillin mimics.[3] Synthetic routes to 2,3-dihydrothiophenes are varied and numerous,[1f,4] with based-induced cyclizations playing an important role. Under basic conditions, starting substrates usually require the presence of electron withdrawing or other functionality to facilitate condensation chemistry or to directly participate in the cyclization.[5] However, some cyclizations that make use of transition metals to target dihydrothiophenes[6] do not require any strong directing functionality.[6a] Radical based cyclizations, free of strong electron withdrawing groups can provide mixtures of 2,3- and 2,5-dihydrothiophenes.[7]

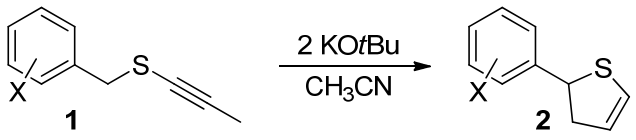

Equation 3-1. Benzyl alkynykl sulfides cyclize to 2,3-dihydrothiophenes in the presence of potassium *t*-butoxide.

A synthetic procedure that created 2,3-dihydrothiophenes (**2**) by way of a *t*-butoxide induced 5-*endo* cyclization of 2-substituted arylmethyl alkynyl sulfides (Equation 3-1), was reported by the Schwan group back in 2000.[8] That reaction was thought to involve benzylic deprotonation and cyclization at the terminal carbon of the propynyl chain, even though the starting material did not possess unsaturation in the terminal carbon, nor held any other skeletal functionality to bring about carbon-carbon bond formation. The experimental results showed that although there was no ostensible need for strong electron withdrawing groups or other reactive functionality in the substrates, there nevertheless was a requirement for an electron withdrawing group on the aryl ring. In the communication, some mechanistic data was offered, but some intriguing uncertainties remained.[8] How was it that the cyclization occurred most efficiently when the starting material did not have unsaturation at the propynyl terminus? Which tautomeric form of the 3-carbon unit is accepting the electron density? This chapter presents computational evidence concerning the mode of cyclization of the substrates.

The present work was done in collaboration with the group of Professor A. Schwan at the University of Guelph. In their 2000 work,[8] many optimized reaction parameters were reported including solvent and substrate concentration. Nevertheless, it was subsequently learned that KO*t*Bu is preferred over sodium or lithium *t*-butoxide. Thus, treating the starting sulfides (**1**) with 2 eq. of KO*t*Bu in acetonitrile at various temperatures for 24 hours affords a dihydrothiophene (**2**) with the aryl group at the 2-position and the double bond at the 4 position, Equation 3-1.[8] The products and yields are outlined in Table 3-1. The initial notion that a 2-substituted aryl group is required for cyclization[8] was found to be invalid, as the results show that electron withdrawing groups at other aryl positions promote the reaction. Additionally, it was observed that the presence of nitro groups prevented the reaction, and starting material was fully recoverable in the 2-nitro case (**1r**),

Table 3-1. KO*t*Bu Promoted Cyclization Products of Benzyl 1-Alkynyl Sulfides.[a]

#	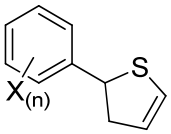	temp. (°C)[b]	Yield[c]
2a	X = 2-H	reflux	28[d,e]
b	X = 2-I	0	75
c	X = 2-Br	0	74
d	X = 2-Cl	0	74
e	X = 2-Me	reflux	0
f	X = 2-Ph	reflux	41[d,e]
g	X = 2-F	reflux	45
h	X = 2-CN	reflux	64
i	X = 3-I	rt	68
j	X = 4-I	rt	45
k	X = 3-CF_3	reflux	59
l	X = 2-SPh	reflux	66
m	X = 2-S(O)Ph	reflux	45[f]
n	X = 2-$S(O)_2$Ph	reflux	68
o	X = 2,5-$(OMe)_2$	reflux	44[d,e]
p	X = 3,5-$(OMe)_2$	reflux	54[c]
q	X = 3-NO_2	reflux	0
r	X = 2-NO_2	reflux	0
s	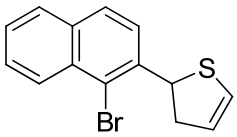	0	72
t	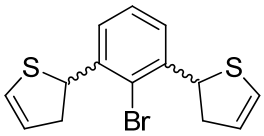	60[f,g]	47
u	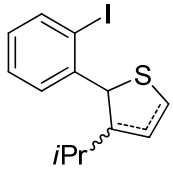 2,3/2,5 = 1/1.7	0	69[b]

[a] Reprinted with permission from reference 9.
[b] Reaction temperature. Compounds **1** were stirred for 24 h. unless otherwise indicated.
[c] Yield is of isolated material unless otherwise indicated.
[d] Yield based on consumed starting material.
[e] Refluxed for 8 h.
[f] 1:1 mixture of diastereomers.
[g] Refluxed for 6 h.
[h] Ratio of isomers based on double bond position: 2,3/2,5 = 1/1.7

whereas full decomposition occurred in the 3-nitro case (**1q**). The experimental results also pointed out that replacing the aryl groups with heteroaryl groups prevented the reaction. Specifically, 2-bromothien-3-ylmethyl 1-propynyl sulfide, 2-furfuryl 1-propynyl sulfide and 2-fluoro-4-iodopyrid-3-yl 1-propynyl sulfide did not cyclize. Also, positioning an iodine group at the peri position did not prompt cyclization of 8-iodonaphthalen-1-ylmethyl 1-propynyl sulfide.

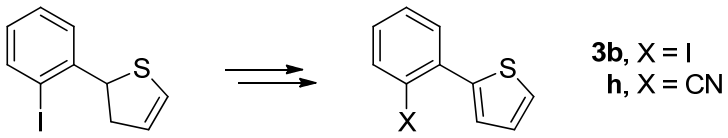

Equation 3-2. Dyhidrothiophenes **2b** and **2h** can be converted to the respective thiophenes.

A selection of dihydrothiophenes has been shown to be oxidizable to thiophenes.[1c,1e-g] Accordingly, our collaborators have achieved the successful conversion of heterocycles **2b** and **2h** into thiophenes **3b** and **3h** in 73 and 81% yields respectively, with DDQ[1e] in $CHCl_3$. (Equation 3-2). Moreover the additional functionality on the aryl unit provides a reactive feature for further adaption toward compounds and polymers with useful electronic properties.[10]

The cyclization represents a rare instance where C-C bond formation occurs without the need for functionality directly participating in condensation or other reactive chemistry. Apparently, after deprotonation, the unsaturation of the 3-carbon substituent on sulfur is sufficient to activate ring closure.

3.2. Computational Methods

Density Functional Theory (DFT) calculations were conducted using the Gaussian 09[11] suite of programs. The CAM-B3LYP method corrected for the long range deficiencies of B3LYP and provided results close to coupled cluster calculations.[12,13] Condensed phase calculations for acetonitrile were carried out with the conductor-like polarizable continuum model (CPCM) of Cossi and coworkers,[12] with the smoothing formalism that Karplus and York developed.[14] The solute molecular cavity was specified using the Bondi radii values.[15] The computed values include thermal (273.15 K) corrections for enthalpy. Transition states were confirmed by examining the negative eigenvalue of the hessian matrix and by intrinsic reaction coordinate (IRC) calculations. GaussView 5 was used for the visualization of the molecules and the vibrational modes.[16]

There are some shortcomings with the B3LYP functional.[17] For example, medium and long-range electron correlation errors are common.[18] The CAM-B3LYP functional was selected because of its good performance in calculations of electronic polarizabilities, as well as long-range exchange interactions by a Coulomb attenuating method, and medium-range interactions with an error fitting function.[19] Table 3-2 shows that the CAM-B3LYP calculation predicts greater stability of propyne vs allene, which is opposite to that found by experimental, and M05-2X and CCSD(T) methods.[20-23] The relative energetics the MP4,[24] CCSD(T), and CAM-B3LYP calculations are quite similar to each other for methyl(prop-1-yn-1-yl)sulfane and methyl(propa-1,2-dien-1-yl)sulfane. However, our CAM-B3LYP calculations are not expected to have greater accuracy than ~4 kcal/mol. The average errors of B3LYP in thermochemistry calculations was ~3.6 kcal/mol (from a database of 177 reactions).[20]

Table 3-2. Relative Energies Of Propyne and Allene, and Of Methyl Prop-1-yn-1-yl Sulfane and Methyl Propa-1,2-dien-1-yl Sulfane.

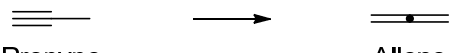

method	E (kcal/mol)	Reference
Experimental	-1.4	21
CCSD(T)/cc-pVQZ/MP2/cc-pVTZ	-1.4	22
M05-2X/6-311+G(2df,2p)	-1.2	23
CAM-B3LYP/6-311+G(d,p)	0.8	this work

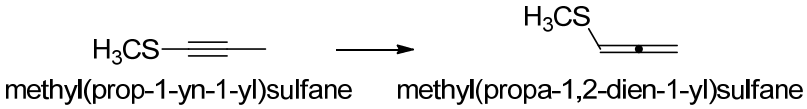

method	E (kcal/mol)	Reference
MP4/6-31+G(d)//RHF/6-31+G(d)	1.3	24
IEFPCM-MP4/6-31+G(d)//PCM-RHF/6-31+G(d)	1.8	24
CAM-B3LYP/6-311+G(d,p)	3.4	this work
CPCM-CAM-B3LYP/6-311+G(d,p)	2.6	this work
CCSD(T)/cc-pVQZ/MP2/cc-pVTZ	1.3	this work
CPCM-CCSD(T)/cc-pVQZ/CPCM-MP2/cc-pVTZ	0.6	this work

3.3. Results and Discussion

3.3.1. Mechanism and Computations

Density Functional Theory calculations were conducted to help rationalize the base induced 5-*endo* cyclization of benzyl 1-alkynyl sulfides, which led us to the mechanistic proposal outlined in Scheme 3-1, slightly modified from that reported in the original communication of 2000.[8] Model system **1a** was used to mimic the core of benzyl alkynyl sulfides bearing substituents on the aryl ring. Because it was impractical to compute the reaction with the potassium *t*-butoxide base, the potential energy surface was calculated for the formation of 2,3-dihydrothiophene **2a** in a reaction of **1a** with

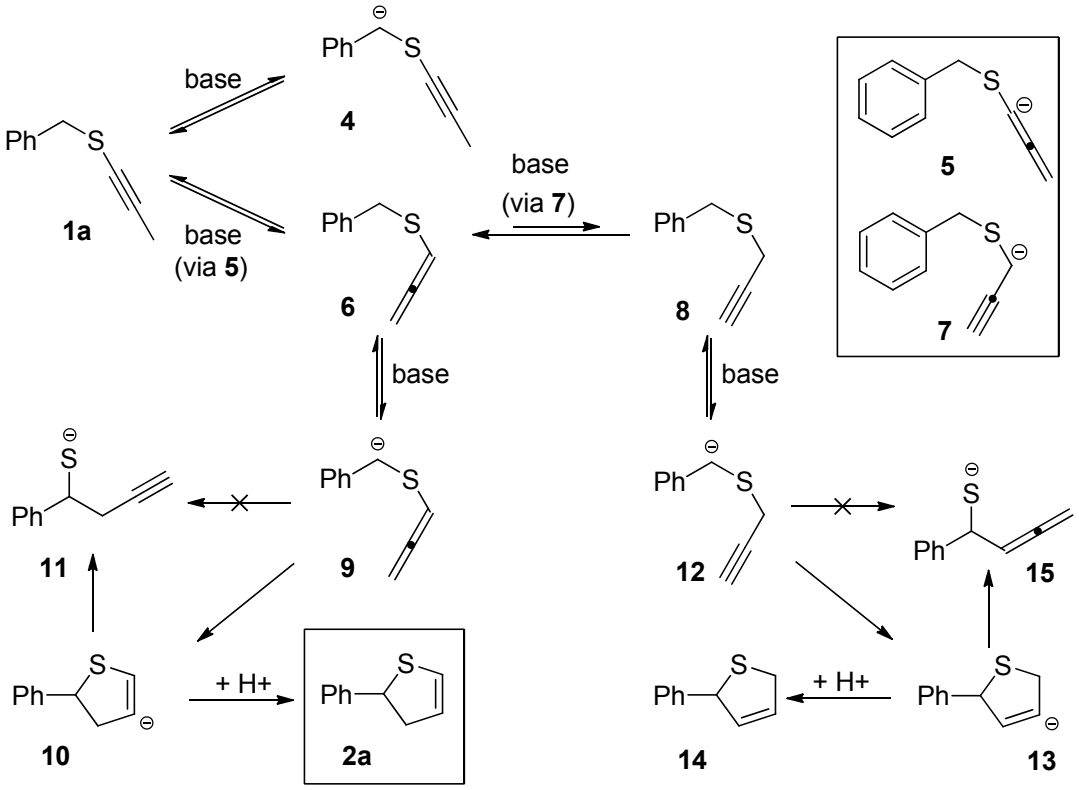

Scheme 3-1. Proposed Mechanism for the base promoted cyclization of benzyl 1-alkynyl sulfides.

potassium methoxide. Geometries were optimized with CAM-B3LYP/6-311+G(d,p)[25] as this basis set is defined for K^+ and provides a good trade off of accuracy and performance. Acetonitrile calculations were carried out with the CPCM solvent model.[12]

The calculated structures are shown in Figure 3-1A-B where K^+-π interactions are found for all structures. It is interesting to note that π-cation interactions are influenced less by inductive effects and more by through-space effects between the metal ion and substituents on the aromatic rings,[26] and that the nitro substituent causes the ring to have a very weak π-cation interaction. Calculation of K^+-π interactions are prone to the basis set superposition error (BSSE), currently

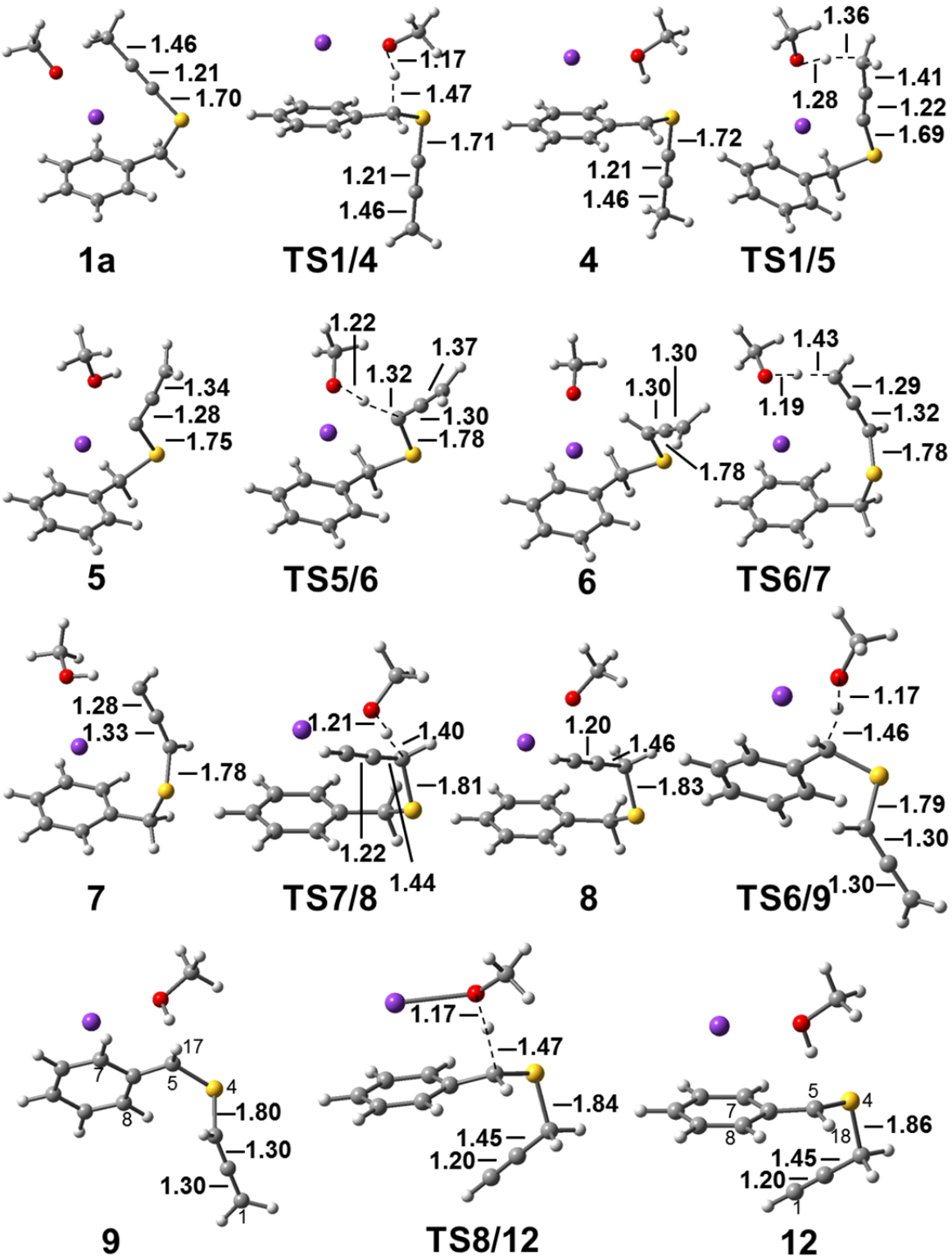

Figure 3-1A. Optimized CPCM-CAM-B3LYP/6-311+G(d,p) geometries for the KOMe induced cyclization of **1a**. Calculations were carried out in acetonitrile. K^+, KOMe, and MeOH molecules were modeled explicitly. Bolded numbers aligned near the structures are bond distances in Å. Non-bolded numbers on some of the structures are the atomic numbers referred to in Table 3-3.

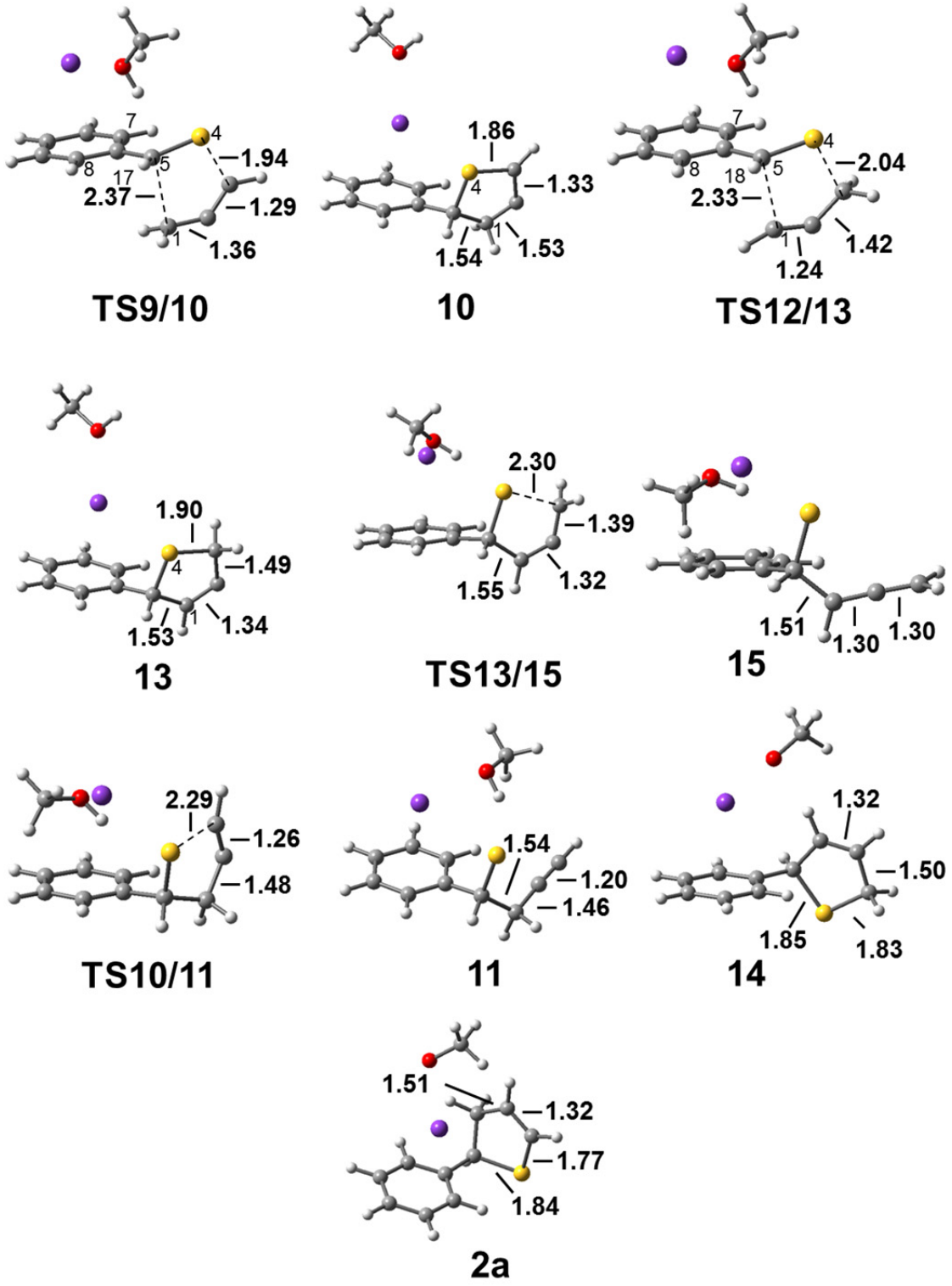

Figure 3-1B. Optimized CPCM-CAM-B3LYP/6-311+G(d,p) geometries for the KOMe induced cyclization of **1a**. Calculations were carried out in acetonitrile. K^+, KOMe, and MeOH molecules were modeled explicitly. Bolded numbers aligned near the structures are bond distances in Å. Non-bolded numbers on some of the structures are the atomic numbers referred to in Table 3-3.

Gaussian09 does not provide for a manner to correct this error in condensed phase calculations, so we studied the $K^+ + C_6H_6 \rightarrow C_6H_6\text{-}K^+$ system in the gas phase and accounted for the BSSE by using the counterpoise method.[27a] Our calculations showed that the magnitude of the BSSE for this reaction is only 0.3 kcal/mol, suggesting that this correction is not necessary in this system. Because of the complexity of the PES for the parent system **1a**, a computational examination of substituent effects was beyond the scope of our study.

The energetic features of the reaction are shown in Figure 3-2A-C. From Figure 3-2A it is clear that allenyl species **6** plays a key role in the cyclization process to 2,3-dihydrothiophene **2a** because it is stabilized compared to **8**. The formation of **4** from **1a** is a "dead end" and did not convert to cyclic products. Allene **6** is formed in a two-step process from **1a** via intermediate **5**. A transition state for the loss of a benzylic proton from **6** has an activation barrier of 7.9 kcal/mol (Figure 3-2B). Upon formation of deprotonated allene **9**, it can undergo a unimolecular 5-*endo*-trig cyclization yielding anion **10**, followed by protonation to form **2a**. While the thia-Wittig rearrangement has been elucidated yielding **11** (Figure 3-2C), the experimental data suggest a rapid protonation of **10** and the formation of **2a**. An alternative mechanism involves the conversion of deprotonated alkyne **12** via a 5-*endo*-dig cyclization to give **13** followed by protonation to form **14**; however, the path to **12** is higher in energy. Our collaborators performed control experiments in order to provide further understanding of the reaction mechanism. When the reaction was performed in CD_3CN, the products possessed essentially full deuteration at the non-aryl carbons, a result consistent with significant solvent intervention. Indeed, deuterium exchange experiments showed that methyl hydrogens of thioethers **1a, b, i, j** each exchanged with half-lives of ca. 25 s at –10 ºC, whereas benzyl hydrogen exchange was faster, completing in <25 s at the same temperature.

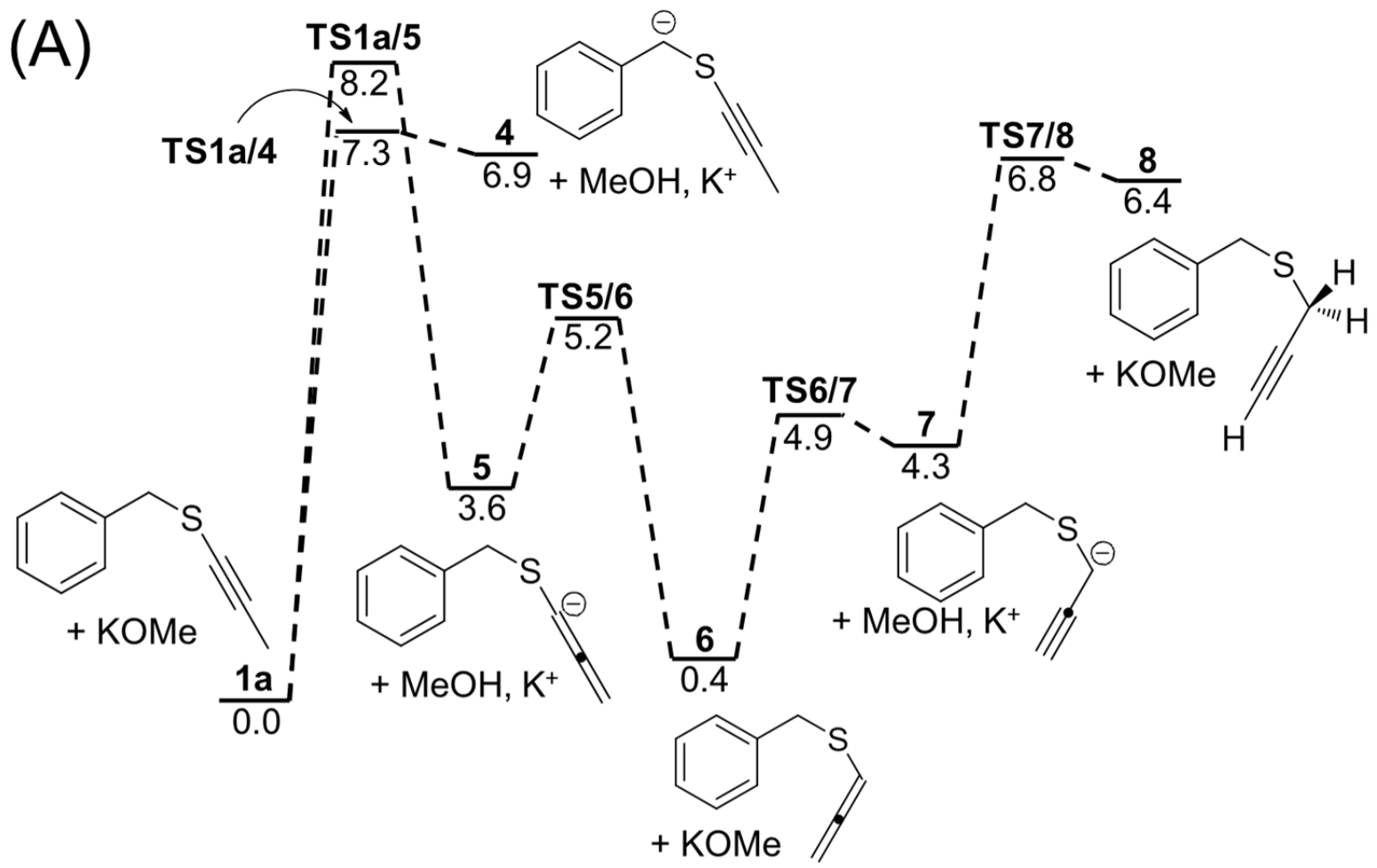

Figure 3-2A. CPCM-CAM-B3LYP/6-311+G(d,p) optimized potential energy surface in kcal/mol including thermal corrections for enthalpy (273.15 K). KOMe, K^+, and MeOH molecules were modeled explicitly. Transition states were confirmed by intrinsic reaction coordinate (IRC) calculations.

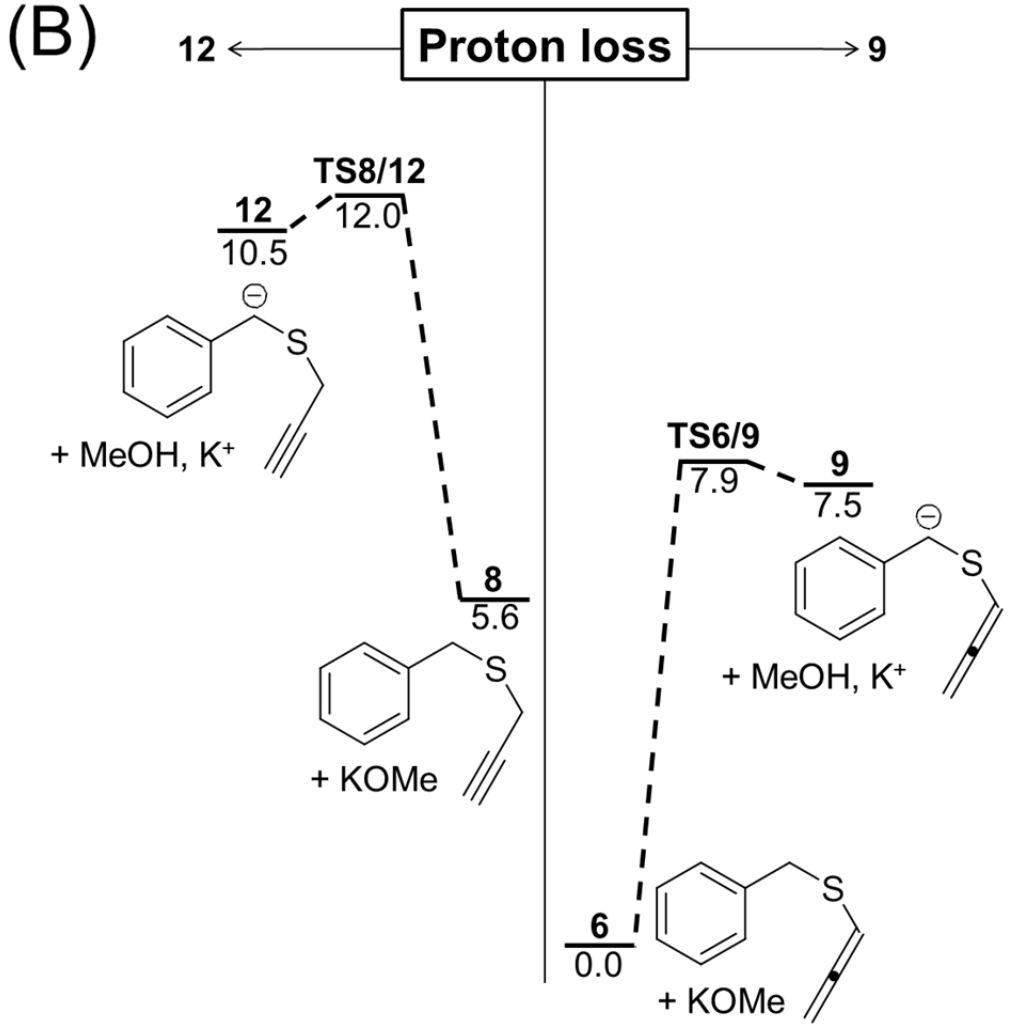

Figure 3-2B. CPCM-CAM-B3LYP/6-311+G(d,p) optimized potential energy surface in kcal/mol including thermal corrections for enthalpy (273.15 K). KOMe, K^+, and MeOH molecules were modeled explicitly. Transition states were confirmed by intrinsic reaction coordinate (IRC) calculations.

Related experiments reaffirmed that the preferred tautomeric state of the 3-carbon unit was the 1-propynyl form as propargyl or allenyl tautomers were never observed by ^{1}H NMR of the cyclization mixture contents. Such an observation is fully consistent with past literature that indicates the conjugated form is the more thermodynamically stable.[27b-e] Similarly, the computed protonation-deprotonation equilibria which involve **1a**, **4-8** show relatively low activation energies of 0.4-8.2

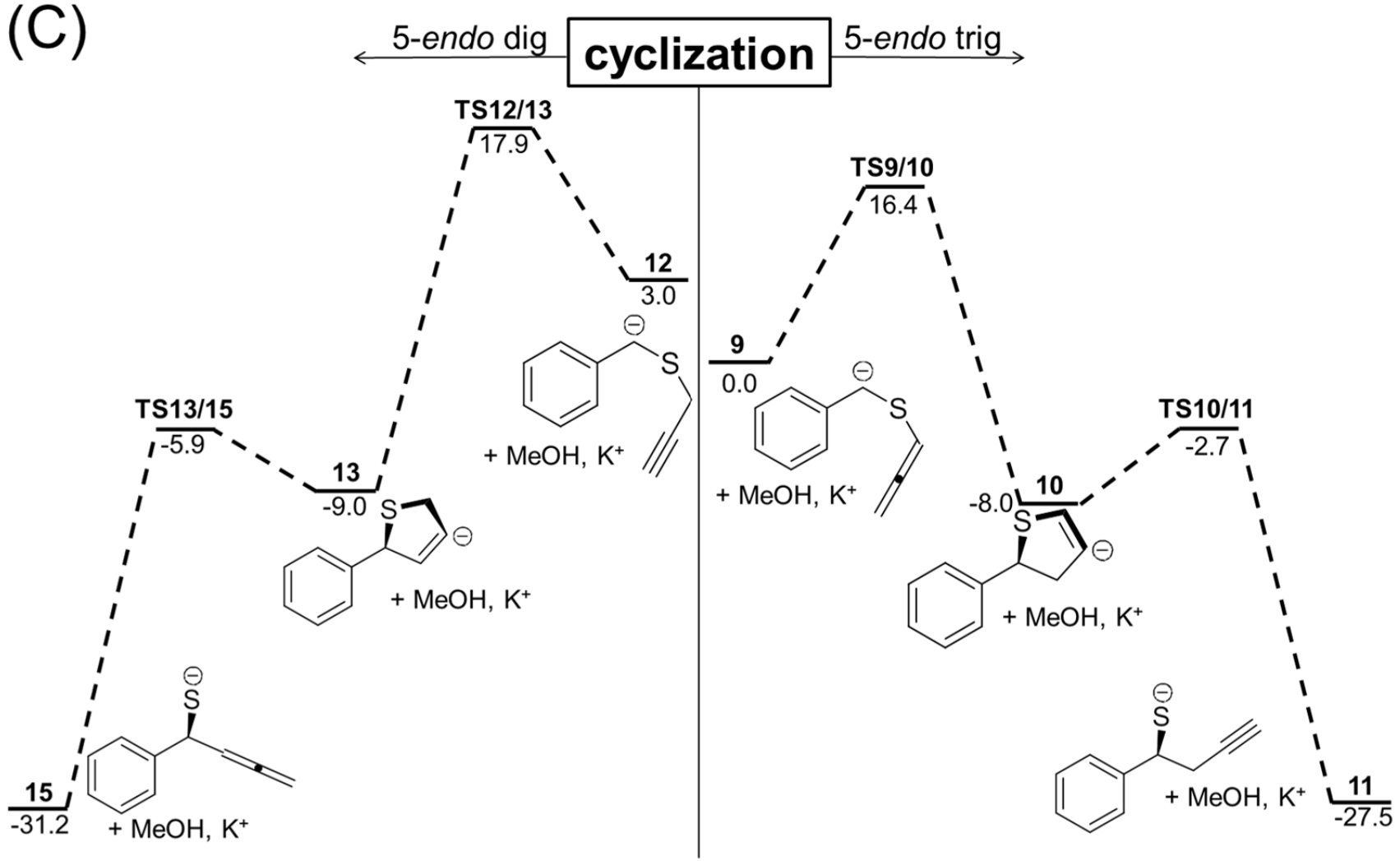

Figure 3-2C. CPCM-CAM-B3LYP/6-311+G(d,p) optimized potential energy surface in kcal/mol including thermal corrections for enthalpy (273.15 K). KOMe, K^+, and MeOH molecules were modeled explicitly. Transition states were confirmed by intrinsic reaction coordinate (IRC) calculations.

kcal/mol and provide an explanation of how proton or deuterium can be incorporated in all C-H sites except on the phenyl ring.

In the condensed phase, our computations did not find a transition state(s) for the isomerization of **2a** to **14**. Additional control experiments on **2b** in CD_3CN revealed minimal incorporation of D into the material. The 2,3-dihydro isomer (**2b**) is not amenable to migration of the double bond because its exchange is quite slow. The equilibrium between **2b** and **14b** was not proven due to this slow exchange. The rate of H/D exchange of the starting material is substantially more rapid. Our collaborators noted that re-exposure of **14u** (2,5-dihydro isomer of **2u**) to the reaction conditions causes the **2u**/**14u** isomer ratio to be re-established. However, **2u** does not exchange when re-exposed to the reaction conditions in CD_3CN. The reaction is most certainly a base mediated cyclization onto the terminus of the three carbon unit. The experimental exchange and computational data suggests that the propynyl/allenyl/propargyl equilibrium is dynamic, with the propynyl as the most populated entity.

From Figure 3-2A, it is evident that formation of allenyl species is favored to the propargyl species and accounts for the path to 2,3-dihydrothiophene product in acetonitrile. 2,3-Dihydrothiophene **2a** and 2,5-dihydrothiophene **14** are essentially isoenergetic. The relative energies of these two dihydrothiophene products were calculated to be within 2.8 kcal/mol of each other. A change in the solvent or benzyl alkynyl sulfide structure may shift the reaction to propargyl species and the path to 2,5-dihydrothiophene product. The more rapid exchange at the benzylic site suggests that benzylic anions are available to attack the terminus of the 3-carbon unit when unsaturation is available (see Figure 3-2C).

While there is ongoing interest in assessing *endo* vs *exo* cyclization preferences for single species,[28] we were not able to locate literature analyses of competitive *endo* cyclizations of equilibrating species. Given our findings, the chemistry at hand does not present a true competition; nevertheless our determination of transition state energies and parameters permits a comparison of two different but closely related entities. The simplicity of the system may serve as a model for other fundamental cyclizations affording five-membered rings. Baldwin's rules suggest the 5-*endo*-dig cyclization should be allowed, and the 5-*endo*-trig should not.[29] However, the 5-*endo*-trig example in the current paper is allene-based with a geometry very close to the alkyne tautomer and was not specifically addressed by Baldwin.[30] As such, the cyclization tendencies of this comparison are difficult to distinguish without the assistance of computational chemistry.

The transitions states **TS9/10** and **TS12/13** differ only by a few kcal/mol. Furthermore, many of the calculated parameters are quite similar in the two transition states. For instance, the degrees of rehybridization of the benzylic carbon in the transitions states, as measured by changing dihedral angles, are essentially indistinguishable. However, the transition state differences worth noting relate to C-C bond formation, C3-S bond lengthening and the bending of the three carbon unit (Table 3-3).

Transition state **TS9/10** exhibits C-C bond forming at 2.37 Å, C3-S bond *lengthening* of 0.13 Å and a bend of the allene unit to 134º. As a comparison, **TS12/13** has closer C-C contacts at 2.33 Å, extra lengthening of C3-S (0.21 Å) and a lesser degree of bending at the sp hybridized carbon (137º). Clearly, **TS12/13** calls upon and benefits from the extra lengthening of the C3-S bond and there is less inclination to bend at the allenyl/propynyl central carbon. Both of these features permit advanced C-C bond formation in the transition state. The **TS9/10** transition state is achieved with

more bending at the allenyl carbon but with less developed C-C bond formation and does not require as much C3-S bond lengthening.

Table 3-3. Selected Geometrical Parameters for the Crucial Species Involved in the Cyclization.[a]

	9		**12**	
Bond lengths of key bonds	C2-C1	1.30	C2-C1	1.20
	C3-C2	1.30	C3-C2	1.45
	S4-C3	1.80	S4-C3	1.86
Indication of planarity of anion	C7-C6-C5-H17	-164.7	C7-C6-C5-H18	-171.3
	C8-C6-C5-H17	20.00	C8-C6-C5-H18	14.3
3-C bond angle	C1-C2-C3	178.6	C1-C2-C3	179.6
	TS9/10		**TS12/13**	
Bond lengths of key bonds	C2-C1	1.36	C2-C1	1.24
	C3-C2	1.29	C3-C2	1.42
	S4-C3	1.94	S4-C3	2.04
Bond forming distance	C5-C1	2.37	C5-C1	2.33
3-C bond angle	C1-C2-C3	133.8	C1-C2-C3	137.0
Rehybridization dihedral angles	C7-C6-C5-H17	173.5	C7-C6-C5-H18	173.0
	C8-C6-C5-H17	-8.33	C8-C6-C5-H18	-8.2
	10		**13**	
Bond lengths of key atoms	C1-C2	1.52	C2-C1	1.34
	C2-C3	1.33	C3-C2	1.49
	C3-S4	1.86	S4-C3	1.90
3-C bond angle	C3-C2-C1	109.5	C3-C2-C1	112.4

[a] The numbering scheme is shown in Figure 3-1A-B. Bond distances in Å. Bond angles and dihedral angles in degrees.

The data suggest the allene is more receptive to cyclization than the propynyl unit, as it demonstrates a greater propensity to bend during the cyclization. It is possible that such behavior

would also come into play with other 5-*endo*-dig/trig cyclizations such as with systems absent of sulfur or any other atom that could accommodate electron density.

3.4. Conclusions

A simple base-induced transition metal free 5-*endo* cyclization of benzyl 1-alkynyl sulfides **1** proceeds without the need for activation by electron withdrawing substituents directly attached to skeletal carbons. The 2,3-dihydrothiophene products **2** can be readily forwarded to 2-aryl thiophenes. Computation chemistry was performed to assist in the understanding the mechanism of cyclization and to establish which allenyl/propargyl tautomer is likely involved in the cyclization.

It is significant that the allenyl species **6**, formed in a stepwise path via **5**, is more stable than the propargyl species **8**. The weaker benzylic proton affinity of **6** than **8** favors the base induced reaction of **6**. From allenyl species **6**, 2,3-dihydrothiophene **2a** can be formed in three steps, including base **9**, which undergoes a 5-*endo*-trig cyclization to **10**.

Chapter 4. Quinones, Monoradicals and Diradicals from 3- and 4-mercaptocatechol and 3,4-bismercaptocatechol: A Computational Study

4.1. Introduction

A number of studies have focused on the antioxidant properties of phenols, catechols, and thiols.[1] However; the literature appears to be devoid of studies that address antioxidant compounds that contain *both* aromatic alcohol and thiol groups, to compare the radical-forming properties with compounds that contain either aromatic alcohol or thiol groups. Phenols can form the corresponding phenoxyl radical. Catechols can form O-centered radicals ($HOC_6H_4O^{\bullet}$ or $^{\bullet}OC_6H_4O^{\bullet}$), *o*-quinones, or triplet diradicals. Thiols can form an S-centered thiylradical. An earlier study on phenols and aromatic thiols noted differences on the polymerization of methyl methacrylate.[2] More recently, as part of a biomimetic study, sulfur-containing catechols have been observed.

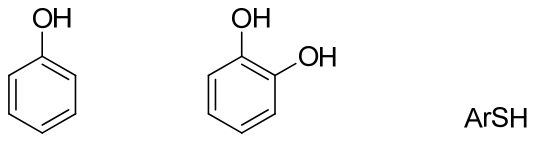

phenol **catechol** **thiol**

It was previously reported the formation of 3-mercaptocatechol (**1**), 4-mercaptocatechol (**2**), and 3,4-bismercaptocatechol (**3**) among other products (*e.g.*, **4**–**6**) from the reaction of *o*-benzoquinone and reduced elemental sulfur (hydrogen polysulfides), H_2Sx.[3] Characterization of **1**–**3**

can be found in the literature.[3-5] However, no spectroscopic evidence or otherwise exists for semiquinone and quinone structures corresponding to **1–3**. As reports neither for the oxidation of mercapto- and bismercaptocatechols **1**-**3** or of other sulfur-containing catechols do not seem to exist, we wished to study possible radical and diradical intermediates that may arise from oxidations of **1–3**. Little is known about the relative energetics of forming a thiocarbonyl group ($R_2C=S$)[6] versus a carbonyl group ($R_2C=O$) from such precursors.

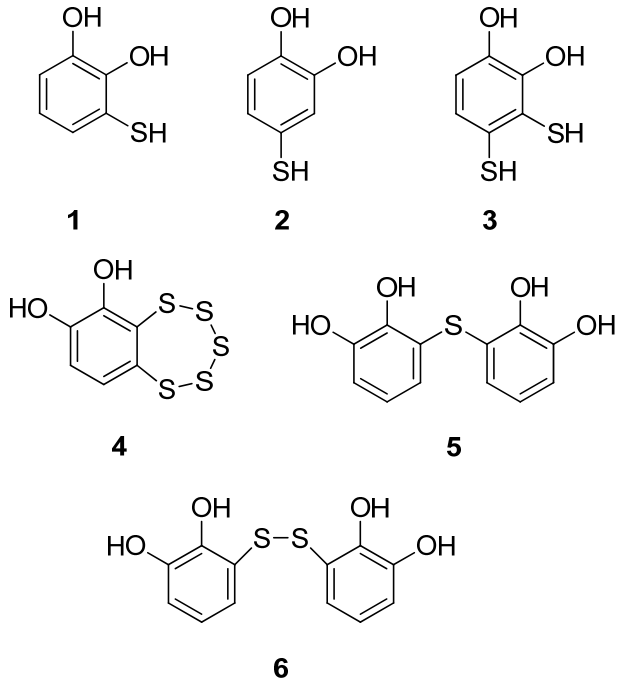

It would be a challenging task to determine the assignment of intermediates in one and two electron oxidations of **1–3**. Thus, computational theory was applied here, in which the objective of the study was to compare stabilities of free radical, quinone, and thioquinone compounds and to predict the preferred structures. Spin distributions were also assessed theoretically to aid in determining relative stabilities of open-shell diradicals. The stabilities of singlet and triplet diradicals

from the loss of two hydrogen atoms from **3** have been predicted. Information on the loss of hydrogen atoms from **1–3** may also reveal factors related to antioxidant activity.

4.2. Computational Methods

Standard computational protocols were used.[7] Gas-phase density functional theory (DFT) calculations were determined with B3LYP[8,9] and Pople's 6-31G(d) and 6-311+G(d,p) basis sets employing the Gaussian03 suite of programs.[10] Geometry optimizations were carried out at the B3LYP/6-31G(d) level. Closed-shell calculations gave the lowest energies for **1–3**, quinones, and dithiete **3k**, whereas open-shell calculations gave the lowest energies for radicals and diradicals. Triplet UB3LYP/6-311+G(d,p) energies were obtained using the singlet-diradical optimized geometry.[11,12] Spin corrected values are reported for UB3LYP/6-311+G(d,p) energies when the open-shell singlet was contaminated with the triplet by means of the spin correction procedure of Yamaguchi and co-workers,[13,14] in which the energy of the lower spin state is corrected by the following formula:

$$ {}^{l}E_{SC} \approx {}^{l}E_{BS} + \frac{{}^{l}\langle S^2 \rangle}{{}^{h}\langle S^2 \rangle - {}^{l}\langle S^2 \rangle} ({}^{l}E_{BS} - {}^{h}E) $$

where l and the h refer to low and high spin states, respectively, which provides the energy of the corrected singlet state. Computations of radical and diradicals derived from **1–3** using the more rigorous G3 or G4 methods would be desirable,[15] but were not possible due to limitations on computational resources. Nevertheless, B3LYP/6-311+G(d,p)//B3LYP/6-31G(d) calculations yielded hydrogenation energies of *ortho*-, *meta*-, and *para*-benzoquinone to form the corresponding benzenediol that are correlated reasonably well with G3 theory and with experimental values[16] (cf.

entries 1–3, Table 4-1). Getting the heat of formation of phenols and catechols has proven to be difficult, the experimental error bars are large (3–4 kcal/mol) (entry 1, Table 4-1).[17] The energetics obtained were corrected for ZPE and for enthalpies (298. 15K and 1 atm).[18]

Table 4-1. Hydrogenation Energies [ΔH_{hyd} (kcal/mol)] of a Series of Benzoquinones to Form the Corresponding Benzenediols.

Entry	Method	*o*-benzoquinone[a]		*m*-benzoquinone[a]		*p*-benzoquinone[a]	
1	Experiment[b]	42.8	± 4.1	74.8	± 4.1	38.5	± 3.0
2	G3[b]	44.6		72.2		34.1	
3	B3LYP/a//B3LYP/b[c]	42.0		64.6		32.8	

[a] Computed values obtained from reactions (a)-(c), which include the sum of electronic and thermal enthalpies. [b] Ref 17. [c] a = 6-311+G(d,p); b = 6-31G(d).

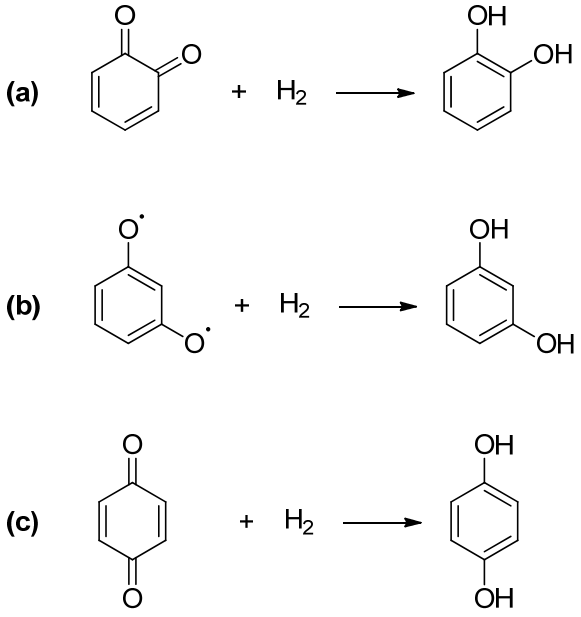

The success of DFT methods can be asserted on previous B3LYP/6-31+G(d,p) studies that have been successful in predicting redox potentials of quinones.[19] We[20] and others[21–25] have used B3LYP/6-31G(d) or B3LYP/6-31+G(d) computations, which performed well in predicting the relative energetics of 1,2-dithiacyclobutene (dithiete, *o*-$C_2H_2S_2$) and dithioethanedial (S=CHCH=S).

Similarly, Contini *et al.* conducted B3LYP/TZVP//B3LYP/6-31G(d) calculations and showed that *o*-thioquinones react with electron rich-alkenes by forming benzoxathiin cycloadducts, which were consistent with the product outcome observed in experimental studies.[26,27] Additional evidence for the suitability of DFT methods is due to Cramer *et al.*[28,29] and Houk *et al.*,[30] as they have reported that the energetics of diradicals calculated with unrestricted DFT are in reasonable agreement with methods such as CCSD(T), which account for long-range correlation effects.

4.3. Results and Discussion

We report the results of a DFT study on sulfur-substituted catechols **1–3**, their corresponding quinones, monoradicals, diradicals, and a dithiete. We start by describing the computed structural features of **1–3**. Second, we describe the computed heats of formation (ΔH_f^0) of quinone, monoradical, diradical, and dithiete structures, which could theoretically arise from oxidations of **1–3**.

4.3.1. Computed Structures

Compounds **1–3** were optimized to minima at the B3LYP/6-31G(d) level of theory (Table 4-2). Phenol and catechol have C_S symmetry. Compounds **1–3** have C_1 symmetry. Bismercaptocatechol **3** favors three intramolecular hydrogen bonds, an OHO hydrogen bond, an OHS hydrogen bond, and an SHS hydrogen bond. Low-energy conformers of catechol and **1–3** show H–O bonds [*e.g.*, the H–O bond distances of 2.12 Å (Ha–O2 catechol), 2.12 Å (Ha–O2 **1**), 2.12 Å (Hb–O1 **2**), 2.09 Å (Hb–O2 **3**)] and H–S bond distances somewhat similar to each other [2.45 Å (Hb–S1 **1**) and 2.95 Å (Hd–S1 **3**)]. The calculated structures predict that the O−H–O bonds possess a planar structure. The

dihedral angles of catechol (Ha−O1−C1−C2), **1** (Ha−01−C1−C2), and **3** (Hb−O2−C2−C1) are equal to 0.0º. On the other hand, the S−H–O and S−H–S bonds are out of plane. The dihedral angle of **1** (Hc−S1−C3−C4) is equal to 91.7º, that of **2** (Hd−S3−C4−C3) is equal to 47.6º, and that of **3** (Hd−S2−C4−C3) is equal to 55.5º. The suitability of the B3LYP/6-31G(d) computations are based on their adequate reproduction of the experimental X-ray data of phenol[31] and thiophenol.[32] The computed heats of formation of the mono- and diradicals, and quinones are the subject of the following sections.

Table 4-2. Calculated Bond Lengths of Phenol, Catechol, and **1**-**3** (in Å)

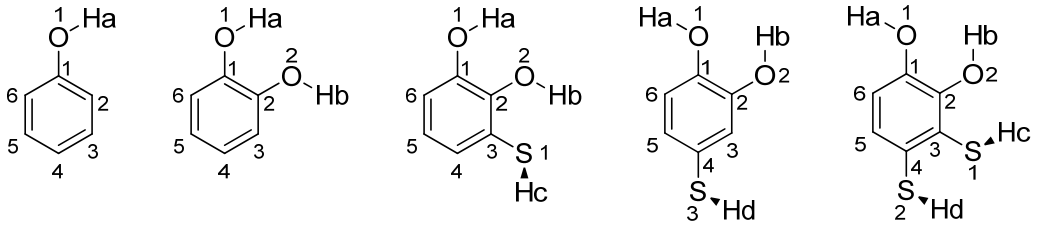

phenol **catechol** **1** **2** **3**

Compound	C1-O1	C2-O2	C3-S1	C4-S2	O2-S1
phenol	1.37	1.38	-	-	-
catechol	-	1.36	-	-	-
1	1.36	1.37	1.80	-	3.06
2	1.38	1.36	-	1.80	-
3	1.38	1.37	1.78	1.79	3.01

Compound	Ha--O2	Hb--S1	Hb--O1	Hc--O2	Hd--S2
phenol	-	-	-	-	-
catechol	2.12	-	3.64	-	-
1	2.12	2.45	-	-	-
2	-	-	2.12	-	-
3	-	-	2.09	2.23	2.95

Structures optimized at the B3LYP/6-31G(d) level.

4.3.2. Heats of Formation, ΔH_f°

The experimental heats of formation for phenol and catechol have been reported.[33,34] In our calculations phenol is predicted to have a value of $\Delta H_{f(gas)}^\circ$ = -22.8 kcal/mol obtained by ring conserving isodesmic reactions from reaction (i), and a value of -23.1 kcal/mol from reaction (ii), which compare well with the experimental value (-23.0 ± 0.1 kcal/mol)[35] (Table 4-3). Catechol is predicted to have a value of $\Delta H_{f(gas)}^\circ$ = -67.6 kcal/mol from reaction (iii), a value of -66.5 from reaction (iv), which compare well with the experimental value of about -65.7 ± 0.3 kcal/mol.[36,37] Compound **1** is predicted to have a value of $\Delta H_{f(gas)}^\circ$ = -61.8 kcal/mol obtained isodesmically from reaction (v). Compound **2** is predicted to have a value of $\Delta H_{f(gas)}^\circ$ = -58.7 kcal/mol from reaction (vi). Compound **3** is predicted to have a value of $\Delta H_{f(gas)}^\circ$ = -51.9 kcal/mol from reaction (vii).

Table 4-3. Calculated $\Delta H_{f(gas)}^\circ$ of Phenol, Catechol, and **1**-**3** (kcal/mol)

Compound	Calculated $\Delta H_{f(gas)}^\circ$	Experimental $\Delta H_{f(gas)}^\circ$
Phenol	-23.2±0.4[a]	-23.0±0.2[f]
Catechol	-67.1±0.8[b]	-65.7±0.3[g]
1	-61.8[c]	-
2	-58.7[d]	-
3	-51.9[e]	-

[a] Reactions i and ii. [b] Reactions iii and iv. [c] Reaction v. [d] Reaction vi. [e] Reaction vii. [f] Ref. 34. [g] Ref. 35 and 36. Computed values obtained with B3LYP/6-311+G(d,p)//B3LYP/6-31G(d).

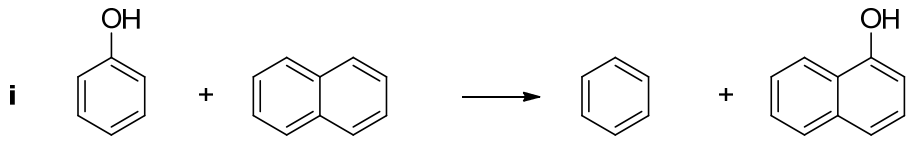

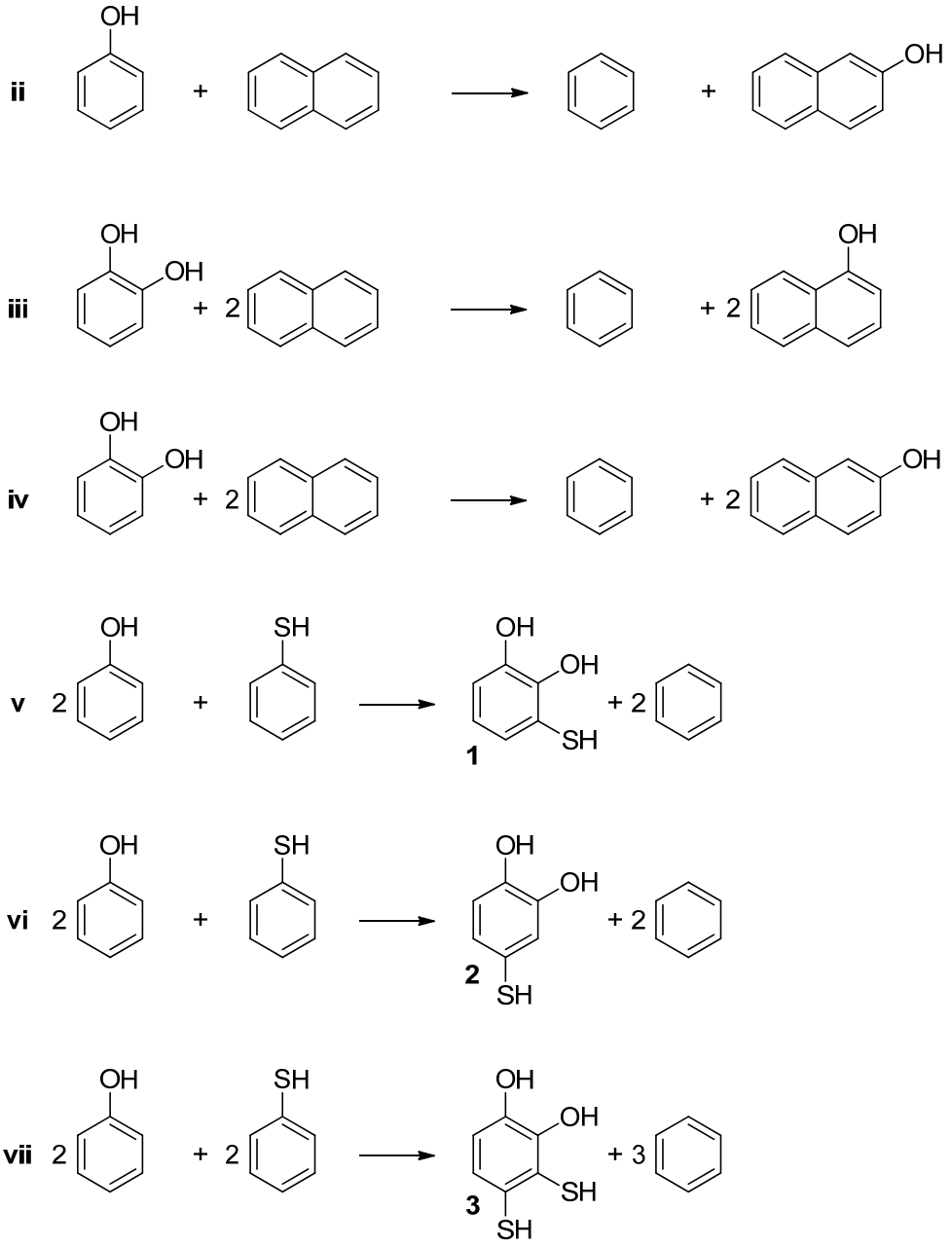

The above analysis suggests that our computed gas-phase heats of formation are in good agreement with the experiment data. Few experimental heats of formation of aryl oxygen- or sulfur-radicals are described in the literature.[33] DiLabio and Mulder reported an experimental $\Delta H^{\circ}_{f(\text{gas})}$ value for hydroxyphenoxy radical of 79.7 kcal/mol.[38] Described next are computations of monoradicals from hydrogen atom loss of **1**–**3**.

4.3.3. Monoradicals

We report computed $\Delta H^{\circ}_{f(gas)}$ for monoradicals **1a–1c**,**2a–2c**,**3a–3d** (Tables 4-4 to 4-6). Calculations were performed at the B3LYP/6-311+G(d,p)//B3LYP/6-31G(d) level, and the isogyric reactions used to arrive at the relative energetics are described in the footnotes of Tables 4-3 to 4-5. For example, hydroxymercaptophenoxy radical **1a** and two benzene molecules were compared

Table 4-4. B3LYP/6-311+G(d,p)//B3LYP/6-31G(d) Calculated $\Delta H^{\circ}_{f(gas)}$ for **1a**-**c**[a]

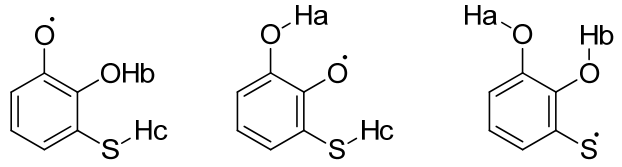

1a **1b** **1c**

Compound	Calculated $\Delta H^{\circ}_{f(gas)}$ (kcal/mol)	Relative $\Delta H^{\circ}_{f(gas)}$ (kcal/mol)	$<S^2>$
1a	-55.0	8.5	0.75
1b	-59.6	3.9	0.75
1c	-63.5	(0.0)	0.75

[a] Values obtained from isogyric reactions viii-x. Values include the sum of electronic and thermal enthalpies. The calculated $\Delta H^{\circ}_{f(gas)}$ for 3-mercaptocatechol **1** is -61.8 kcal/mol (Table 4-3).

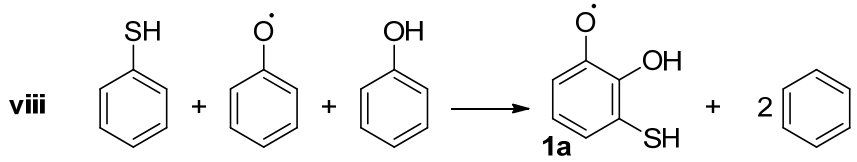

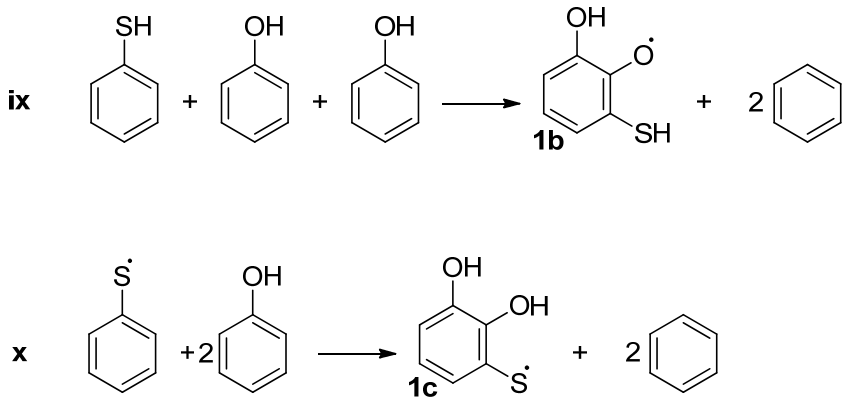

isogyrically with benzenethiol, phenoxy radical, and phenol (reaction (viii), Table 4-4). Compounds **1a**–**1c**,**2a**–**2c**, and **3a**–**3d** all possess computed $<S^2>$ values of 0.75.

Table 4-5. B3LYP/6-311+G(d,p)//B3LYP/6-31G(d) Calculated $\Delta H^{\circ}_{f(gas)}$ for **2a**-**c**[a]

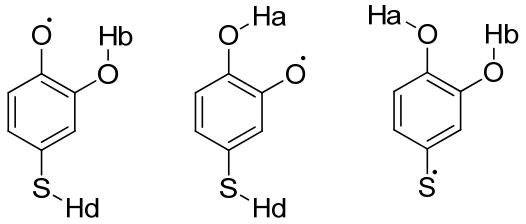

2a **2b** **2c**

Compound	Calculated $\Delta H^{\circ}_{f(gas)}$ (kcal/mol)	Relative $\Delta H^{\circ}_{f(gas)}$ (kcal/mol)	$<S^2>$
2a	-59.8	(0.0)	0.75
2b	-55.7	4.1	0.75
2c	-57.8	2.0	0.75

[a] Values obtained from isogyric reactions xi-xiii. Values include the sum of electronic and thermal enthalpies. The calculated $\Delta H^{\circ}_{f(gas)}$ for 4-mercaptocatechol **2** is -58.7 kcal/mol (Table 4-3).

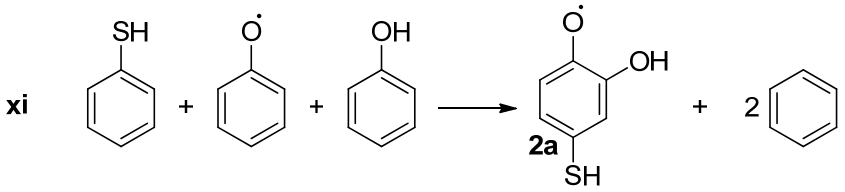

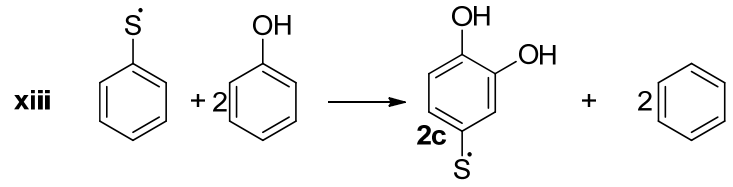

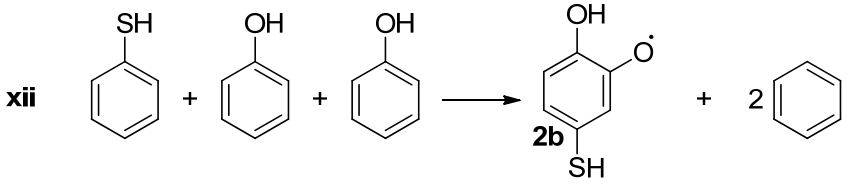

The S-centered radical **1c** is predicted to be of greater stability compared with the O-centered radicals **1a** and **1b** (Table 4-4). However, the monoradicals **2a**–**2c** reveal a different stability pattern, in which the O-centered radical **2a** is of greater stability compared with S-centered radical **2c** and O-centered radicals **2b** (Table 4-5). Compound **2b** is destabilized by 4.1 kcal/mol compared with **2a**. Our computed data show that monoradicals derived from the hydrogen atom abstraction of **3** can yield four different radical structures, **3a**–**3d** (Table 4-6). S-centered radicals **3c** and **3d** are slightly lower in energy compared with the O-centered radicals **3a** and **3b**. The energetics of **3a**–**3d** are similar and thus appear to be isoenergetic. This suggests that the stability of the monoradicals **1a**–**1c**,**2a**–**2c**,**3a**–**3d** is not limited to the single variable of radical localization on sulfur versus oxygen.

Calculations predict that monoradicals **1a–1c**, **2a–2c**, and **3a–3d** can form by a one-electron process; namely, hydrogen atom loss from the corresponding neutral compounds, **1–3**. There is a fairly small energy difference between the radicals within each series. How neutral **1–3** may lose two electrons, namely, the loss of two hydrogen atoms from **1–3** to access diradicals, quinones, thioquinones, dithioquinones, and a benzodithiete is the focus of the next section.

Table 4-6. B3LYP/6-311+G(d,p)//B3LYP/6-31G(d) Calculated $\Delta H^{\circ}_{f(\mathrm{gas})}$ for **3a**-**d**[a]

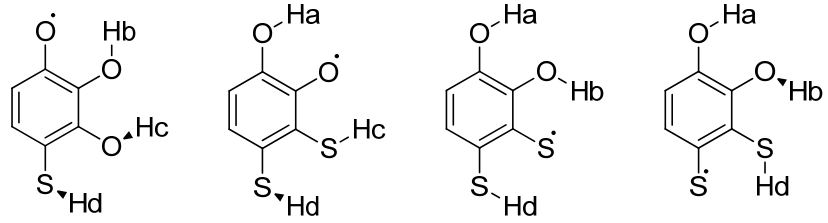

3a **3b** **3c** **3d**

Compound	Calculated $\Delta H^{\circ}_{f(\mathrm{gas})}$ (kcal/mol)	Relative $\Delta H^{\circ}_{f(\mathrm{gas})}$ (kcal/mol)	$<S^2>$
3a	-50.2	1.5	0.75
3b	-50.6	1.1	0.75
3c	-51.7	(0.0)	0.75
3d	-51.1	0.6	0.75

[a] Values obtained from isogyric reactions xiv-xvii. Values include the sum of electronic and thermal enthalpies. The calculated $\Delta H^{\circ}_{f(\mathrm{gas})}$ for 3,4-bismercaptocatechol **3** is -51.9 kcal/mol (Table 4-3).

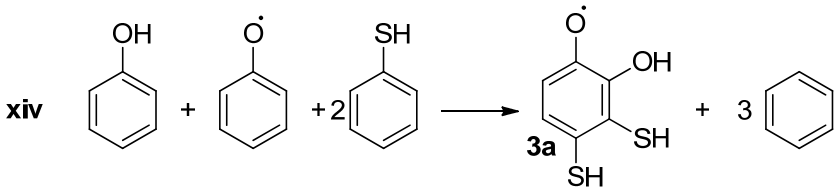

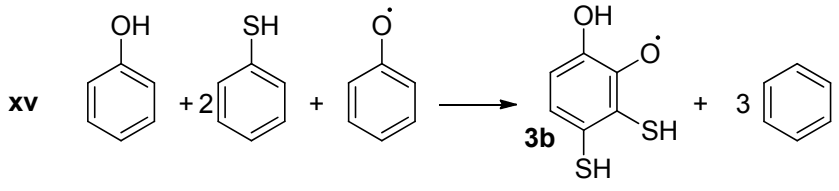

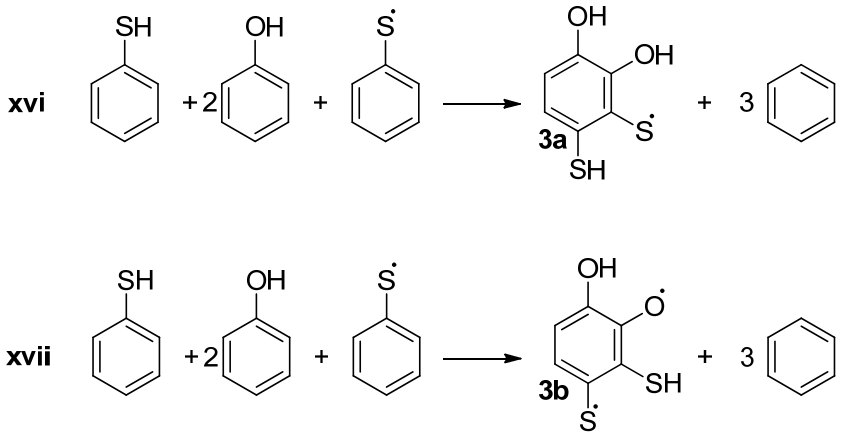

4.3.4. Diradicals

Calculated $\Delta H^{\circ}_{f(gas)}$ of quinones and diradicals **1d–1f**, **2d–2f**, **3a–3j**, and a dithiete **3k** are reported (Tables 4-7 to 4-9). The isogyric reactions used to arrive at the predicted energetics are described in the footnotes of Tables 4-7 to 4-9. For example, 3-mercapto-*o*-benzoquinone **1d** and benzene are compared isogyrically with benzenethiol and *o*-benzoquinone (reaction (xviii), Table 4-7). The $<S^2>$ values of **1d**, **1e**, **2d**, **2e**, **3e**, **3h**, **3j**, and **3k** are about equal to zero. Compounds **1f**, **2f**, **3f**, **3g**, and **3i** possess $<S^2>$ values of about 2.0. Triplet energies were obtained using the singlet–diradical optimized geometries of **1f**, **2c**, **3f**, and **3i** to determine whether the ground states were singlet or triplet. The singlet–triplet gap (ΔE_{ST}) of **2f** was estimated using the triplet-diradical optimized geometry since the singlet-state geometry did not converge under default convergence criteria.

o-Benzoquinone **1d** is more stable than the *o*-thiobenzoquinone **1e** and the non-Kekulé diradical **1f**. Triplet **1f** is lower in energy than singlet **1f**. The energy of triplet **1f** is nonetheless quite high (endothermic by 21.1 kcal/mol) compared to **1d**. A triplet diradical is also observed in **2f** when considering the series **2d–2f** (Table 4-8). The *p*-thioquinone **2e** is more stable than the *o*-thioquinone

2d and the O- and S-centered triplet diradical **2f**. Compound **2d** lies 5.0 kcal/mol above **2e**. A greater number of possible radical and quinone intermediates arise from the abstraction of two hydrogen atoms from **3**, namely **3e–3k** (Table 4-9). The energetics favor the formation of dithiete **3k**, which is pronounced, compared with **3e–3i**, although the formation of **3j** may be competitive since it is only destabilized by 4.9 kcal/mol. Dithietes are known in a number of experimental systems.[39,40] Dithiobenzoquinone **3e** is destabilized by 15.5 kcal/mol compared with the most stable isomer dithiete **3k**. The equivalent 4-membered ring peroxide, benzo[c][1,2]dioxete (**3l**) is a high-energy isomer, endothermic by 81.5 kcal/mol relative to the corresponding dithiete **3k** (Equation 4-1, page 71).

Table 4-7. B3LYP/6-311+G(d,p)//B3LYP/6-31G(d) Calculated $\Delta H^{\circ}_{f(gas)}$ for **1d**-**f**[a]

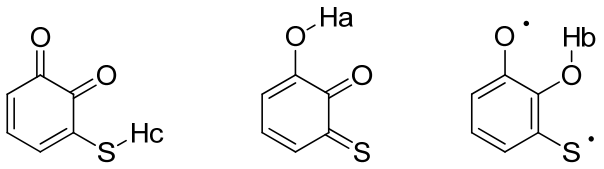

1d **1e** **1f**

Compound	Calculated $\Delta H^{\circ}_{f(gas)}$ (kcal/mol)	Relative $\Delta H^{\circ}_{f(gas)}$ (kcal/mol)	$<S^2>$
1d	-14.0	(0.0)	0.00
1e	-10.2	3.8	0.00
1f	7.1	21.1[b]	2.04[c]

[a] Values obtained from isogyric reactions xviii-xx, which include the sum of electronic and thermal enthalpies. [b] Triplet ground state. [c] ΔE_{ST} = 9.8 kcal/mol. The $<S^2>$ value of singlet **1f** singlet is 0.10.

xviii

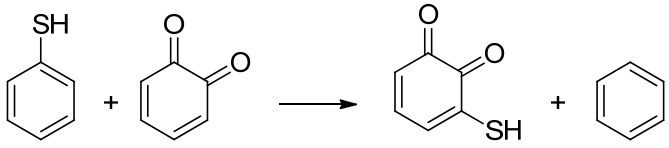

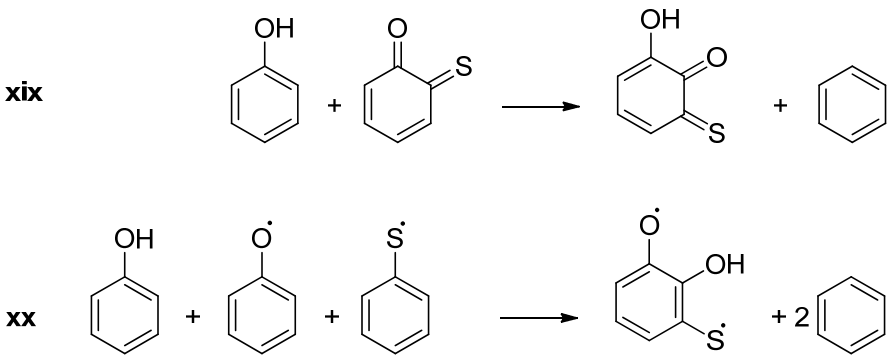

In all cases, the non-Kekulé diradicals are high-energy species compared with the closed shell species. It is not surprise to see the diradicals are much higher in energy; for example, *m*-quinones are known to be far less stable than *o*- and *p*-quinones.[41,42] The above singlet–triplet energy gaps appear to be reasonably predicted even though a relatively low level of theory was used. For comparison, the ΔE_{ST} of *m*-xylylene diradical (**7**) is predicted to be 13.4 kcal/mol [B3LYP/6-311+G(d,p)//B3LYP/6-31G(d) with spin projection], 13.2 kcal/mol [B3LYP/6-31G(d) with spin projection],[43,44] 7.1 kcal/mol [UCCSD(T)/4-31G],[45] ~10 kcal/mol (π-CI),[46,47] and 11.0 kcal/mol [CASPT2N/6-31G(d)],[48] which compares well with the experimental value of 9.6 kcal/mol measured by photoelectron spectroscopy.[49] The isogyric B3LYP/6-311+G(d,p)//B3LYP/6-31G(d) $\Delta H^{\circ}_{f(gas)}$ of triplet ground state diradical **7** is 77.2 kcal/mol, which is similar to the experimental value of 80 ± 3 kcal/mol [Equation (4-2)].[50]

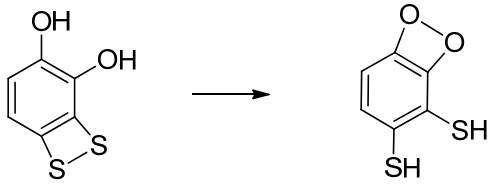

3k **3l**

0 kcal/mol 81.5 kcal/mol

(4-1)

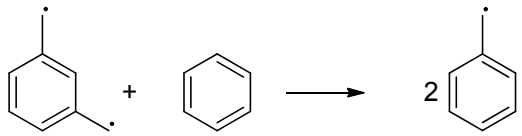

7 (4-2)

Table 4-8. B3LYP/6-311+G(d,p)//B3LYP/6-31G(d) Calculated $\Delta H^{\circ}_{f(gas)}$ for **2d-f**[a]

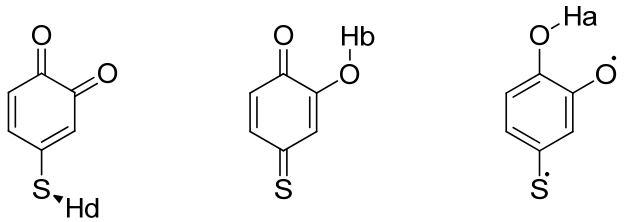

2d **2e** **2f**

Compound	Calculated $\Delta H^{\circ}_{f(gas)}$ (kcal/mol)	Relative $\Delta H^{\circ}_{f(gas)}$ (kcal/mol)	$<S^2>$
2d	-14.0	5.0	0.00
2e	-19.0	(0.0)	0.00
2f	7.1	26.1 [b]	2.04 [c]

[a] Values obtained from isogyric reactions xxi-xxiii, which include the sum of electronic and thermal enthalpies. [b] Triplet ground state. [c] ΔE_{ST} = 7.1 kcal/mol. It was determined using a single point calculation of the singlet compound on the triplet-diradical optimized geometry.

xxi

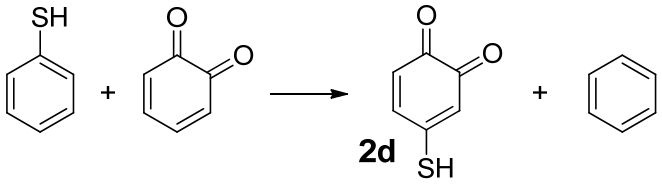

xxii

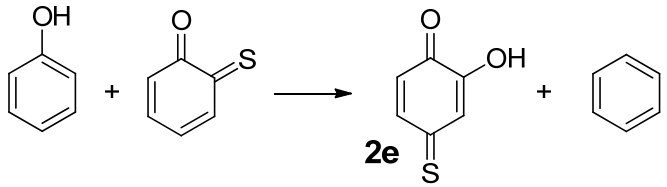

xxiii

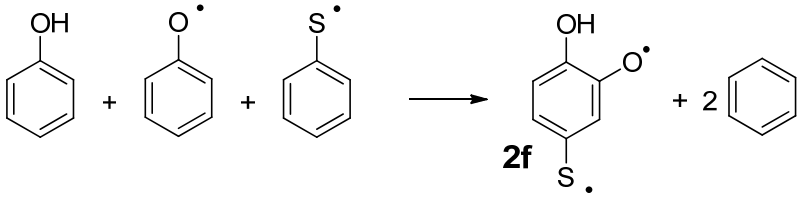

Table 4-9. B3LYP/6-311+G(d,p)//B3LYP/6-31G(d) Calculated $\Delta H^{\circ}_{f(gas)}$ for **3e**-**k**[a]

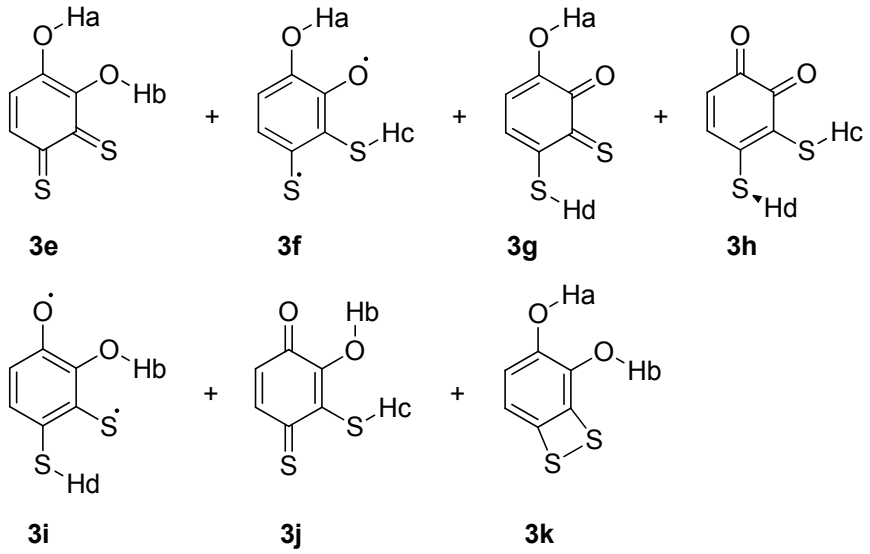

Compound	Calculated $\Delta H^{\circ}_{f(gas)}$ (kcal/mol)	Relative $\Delta H^{\circ}_{f(gas)}$ (kcal/mol)	$<S^2>$
3e	-9.1	15.5	0.00
3f	-2.7	21.9[b,c]	2.02
3g	-2.0	22.6[d,f]	0.04
3h	-12.8	11.8	0.00
3i	-0.9	23.7[b,g]	2.03
3j	-19.7	4.9	0.00
3k	-24.6	(0.0)	0.00

[a] Values obtained from isogyric reactions xxiv-xxx, which include the sum of electronic and thermal enthalpies. [b] Triplet ground state. [c] ΔE_{ST} gap is equal to 7.1 kcal/mol. The $<S^2>$ value of singlet **3f** is 0.09. [d] Singlet ground state. [f] ΔE_{ST} gap is equal to about 1 kcal/mol. The $<S^2>$ value of singlet **3g** is 0.05. [g] ΔE_{ST} gap is equal to 3.9 kcal/mol. The $<S^2>$ value singlet **3g** is 0.14. The calculated $\Delta H^{\circ}_{f(gas)}$ for **3** is -51.9 kcal/mol (Table 4-3).

xxiv

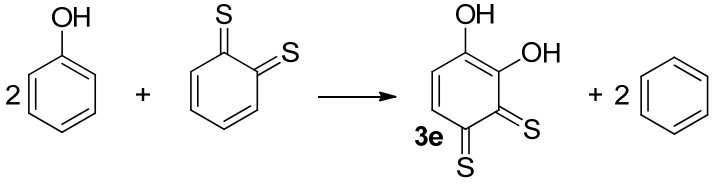

xxv

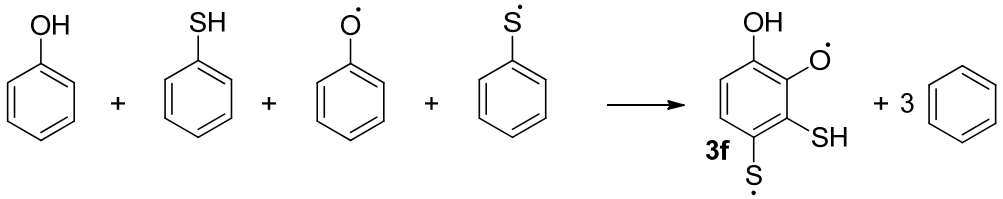

xxvi

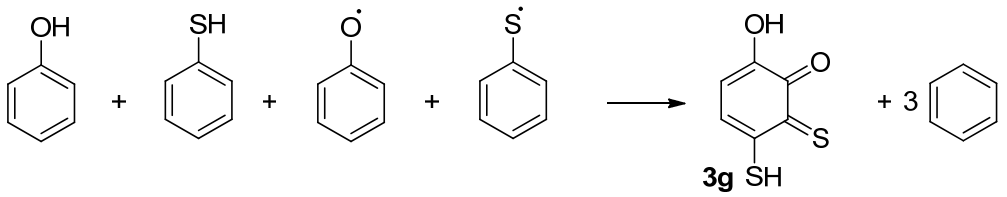

xxvii

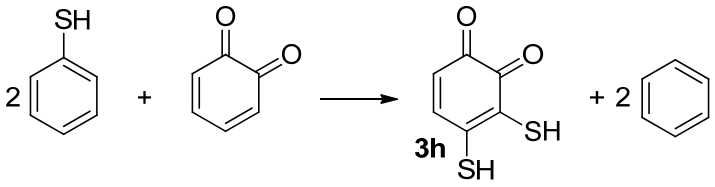

xxviii

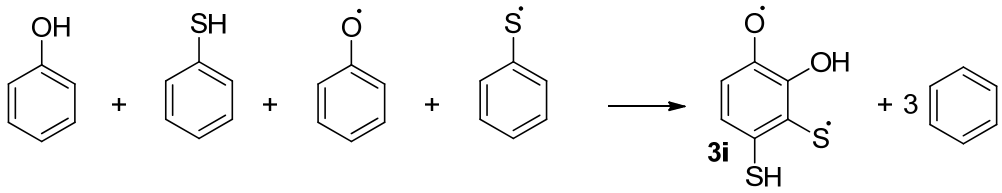

xxix

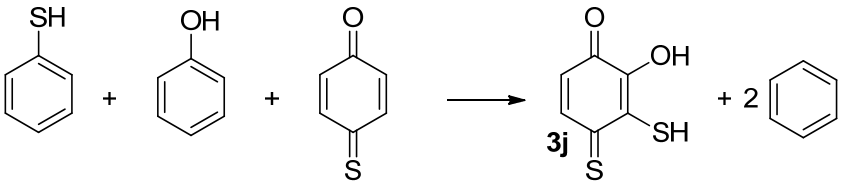

xxx

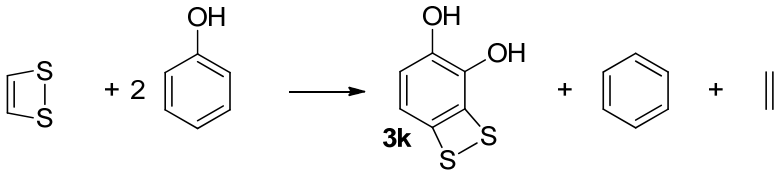

4.4. Conclusion

This study has uncovered a new aspect to 3,4-bismercaptocatechol chemistry. The calculations predict the formation of dithiete **3k** from the loss of two hydrogen atoms in **3** instead of the formation of quinone or diradical intermediates. Non-Kekulé diradicals are destabilized compared with their *o*- or *p*-quinone counterparts, which may be intuitively obvious, but allowed us

to predict the structures likely to emerge when two H atoms are removed from **1–3**. Our theoretical study also provides evidence that monoradical stability is not determined solely by whether the radical is centered on the sulfur or oxygen center (cf., **1a** with **2c**, and **3b** with **3d**). We do not ascribe a trend in radical stability due to intramolecular hydrogen bonding or loss thereof, in which one could imagine stronger OHO type hydrogen bonds compared with SHO and SHS hydrogen bonds (cf., **1c** with **1a**, and **3d** with **3a**). For **1–3**, the SHO and SHS hydrogen bonds are twisted out-of-plane, but the OHO hydrogen bonds are in-plane. Our study cannot discriminate whether a pathway is favored in a simultaneous two-electron process or by two sequential one-electron processes from **1–3**. Aside from the interest in products formed from the loss of hydrogen atoms from **1–3**, it is of special significance that the factors related to hydrogen atom loss are coupled with chain termination in dimer or oligomer structures.

BIBLIOGRAPHY

CHAPTER 1

(1) (a) Thorwirth, S.; McCarthy, M. C.; Gottlieb, C. A.; Thaddeus, P.; Gupta, H., Stanton, J. F. *J. Chem. Phys.* **2005**, *123*, 1. (b) Burrow, P. L.; Birks, J. W. *Anal. Chem.* **1997**, *69*, 1299. (c) Hassanzadeh, P.; Andrews, L. *J. Phys. Chem.* **1992**, *96*, 6579. (d) Brabson, G. D.; Mielke, Z.; Andrews, L. *J. Phys. Chem.* **1991**, *95*, 79. (e) Meyer, B.; Oommen, T. V.; Stroyerh. T *J. Mol. Spectrosc.* **1972**, *42*, 335.

(2) (a) Lyons, J. R. *J. Sulfur Chem.* **2008**, *29*, 269. (b) Moses, J. I.; Zolotov, M. Y.; Fegley, B. *Icarus* **2002**, *156*, 76. (c) Spencer, J. R.; Jessup, K. L.; McGrath, M. A.; Ballester, G. E.; Yelle, R. *Science* **2000**, *288*, 1208. (d) Lewis, J. S.; Kreimendahl, F. A. *Icarus* **1980**, *42*, 330.

(3) Nakayama, J. *J. Sulfur Chem.* **2009**, *30*, 393.

(4) (a) Denk, M. K. *Eur. J. Inorg. Chem.* **2009**, 1358. (b) Rene-Boisneuf, L.; Scaiano, J. C. *Chem. Mater.* **2008**, *20*, 6638. (c) Steudel, R. in *Chemistry of the Non-Metals*, W. de Gruyter: New York, NY., 1977; pp 204. (d) Casal, H. L.; Scaiano, J. C. *J. Photochem.* **1985**, *30*, 253. (e) Tebbe, F. N.; Wasserman, E.; Peet, W. G.; Vatvars, A.; Hayman, A. C. *J. Am. Chem. Soc.* **1982**, *104*, 4971.

(5) Ishii, A.; Nakabayashi, M.; Nakayama, J. *J. Am. Chem. Soc.* **1999**, *121*, 7959.

(6) (a) Mahendran, A.; Vuong, A.; Aebisher, D.; Gong, Y.; Bittman, R.; Arthur, G.; Kawamura, A.; Greer, A. *J. Org. Chem.* **2010**, *75*, 5549. (b) Brzostowska, E. M.; Paulynice, M.; Bentley, R.; Greer, A. *Chem. Res. Toxicol.* **2007**, *20*, 1046. (c) Brzostowska, E. M.; Greer, A. *J. Am. Chem. Soc.* **2003**, *125*, 396. (d) Greer, A. *J. Am. Chem. Soc.* **2001**, *123*, 10379.

(7) (a) Kataura, H.; Maniwa, Y.; Kodama, T.; Kikuchi, K.; Hirahara, K.; Suenaga, K.; Iijima, S.; Suzuki, S.; Achiba, Y.; Krätschmer, W. *Synth. Met.* **2001**, *121*, 1195. (b) Li, L. J.; Khlobystov, A. N.; Wiltshire, J. G.; Briggs, G. A. D.; Nicholas, R. J. *Nat. Mater.* **2005**, *4*, 481. (c) Smith, B. W.; Monthioux, M.; Luzzi, D. E. *Nature* **1998**, *396*, 323. (d) Takenobu, T.; Takano, T.; Shiraishi, M.; Murakami, Y.; Ata, M.; Kataura, H.; Achiba, Y.; Iwasa, Y. *Nat. Mater.* **2003**, *2*, 683. (e) Simon, F.; Kuzmany, H.; Rauf, H.; Pichler, T.; Bernardi, J.; Peterlik, H.; Korecz, L.; Fülöp, F.; Jánossy, A. *Chem. Phys. Lett.* **2004**, *383*, 362. (f) Yanagi, K.; Miyata, Y.; Kataura, H. *Adv. Mater.* **2006**, *18*, 437. (g) Alvarez, L.; Almadori, Y.; Arenal, R.; Babaa, R.; Michel, T.; Le Parc, R.; Bantignies, J. L.; Jousselme, B.; Palacin, S.; Hermet, P.; Sauvajol, J. L. *J. Phys. Chem. C* **2011**, *115*, 11898. (h) Smeu, M.; Zahid, F.; Ji, W.; Guo, H.; Jaidann, M.; Abou-Rachid, H. *J. Phys. Chem. C* **2011**, *115*, 10985. (i) Kaczmarek-Kedziera, A. *J. Phys. Chem. A* **2011**, *115*, 5210. (i) Costa, P. M. F. J.; Gautam, U. K.; Bando, Y.; Golberg, D. *Carbon* **2010**, *49*, 342. (j) Kobayashi, K.; Suenaga, K.; Saito, T.; Shinohara, H.; Iijima, S. *Adv. Materials* **2010**, *22*, 3156. (k) Wang, Y.; Huang, Y.; Yang, B.; Liu, R. *Carbon* **2008**, *46*, 276. (m) Nishide, D.; Dohi, H.; Wakabayashi, T.; Nishibori, E.; Aoyagi, S.; Ishida, M.; Kikuchi, S.; Kitaura, R.; Sugai, T.; Sakata, M. *Chem. Phys. Lett.* **2006**, *428*, 356.

(8) (a) Yim, W.-L.; Johnson, J. K. *J. Phys. Chem. C* **2009**, *113*, 17636. (b) Maranzana, A.; Serra, G.; Giordana, A.; Tonachini, G.; Barco, G.; Causa, M. *J. Phys. Chem. A* **2005**, *109*, 10929. (c) Chen, Z.; Ziegler, K. J.; Shaver, J.; Hauge, R. H.; Smalley, R. E. *J. Phys. Chem. B* **2006**, *110*, 11624. (d) Kar, T.; Akdim, B.; Duan, X.; Pachter, R. *Chem. Phys. Lett.* **2004**, *392*, 176.

(9) (a) Osuna, S.; Houk, K. N. *Chem. Eur. J.* **2009**, *15*, 13219. (b) Sabirov, D.; Khursan, S.; Bulgakov, R. *Russ. Chem. Bull.* **2008**, *57*, 2520. (c) Ogrin, D.; Chattopadhyay, J.; Sadana, A. K.; Billups, W. E.; Barron, A. R. *J. Am. Chem. Soc.* **2006**, *128*, 11322. (d) Park, S.; Srivastava, D.; Cho, K. *Nano Lett.* **2003**, *3*, 1273. (e) Astakhova, T. Y.; Vinogradov, G. A.; Gurin, O. D.; Menon, M. *Russ. Chem. Bull.* **2002**, *51*, 764.

(10) (a) Zhang, Y.-F.; Liu, Z.-F. *J. Phys. Chem. B* **2004**, *108*, 11435. (b) Chan, S.-P.; Chen, G.; Gong, X. G.; Liu, Z.-F. *Phys. Rev. Lett.* **2003**, *90*, 086403.

(11) Lin, T.; Zhang, W.-D.; Huang, J.; He, C. *J. Phys. Chem. B* **2005**, *109*, 13755.

(12) Doyle, C. D.; Rocha, J.-D. R.; Weisman, R. B.; Tour, J. M. *J. Am. Chem. Soc.* **2008**, *130*, 6795.

(13) (a) Dresselhaus, M. S.; Dresselhaus, G.; Saito, R. *Solid State Commun.* **1992**, *84*, 201. (b) Dillon, A. C. *Chem. Rev.* **2010**, *110*, 6856.

(14) Harpp, D. N.; Smith, R. A. *J. Am. Chem. Soc.* **1982**, *104*, 6045.

(15) Fort, E. H.; Donovan, P. M.; Scott, L. T. *J. Am. Chem. Soc.* **2009**, *131*, 16006.

(16) (a) Del Canto, E.; Flavin, K.; Movia, D.; Navois, C.; Bittencourt, C.; Giordani, S. *Chem. Mater.* **2011**, *23*, 67. (b) Denis, P. A. *J. Phys. Chem. C* **2009**, *113*, 5612. (c) Denis, P. A. *Int. J. Quantum Chem.* **2009**, *109*, 772. (d) Denis, P. A.; Faccio, R. *Chem. Phys. Lett.* **2008**, *460*, 486. (e) Liu, J.; Rinzler, A. G.; Dai, H.; Hafner, J. H.; Bradley, R. K.; Boul, P. J.; Lu, A.; Iverson, T.; Shelimov, K.; Huffman, C. B.; Rodriguez-Macias, F.; Shon, Y. S.; Lee, T. R.; Colbert, D. T.; Smalley, R. E. *Science* **1998**, *280*, 1253.

(17) Frisch, M. J. T., Trucks, G. W.; Schlegel, H. B.; Scuseria, G. E.; Robb, M. A.; Cheeseman, J. R.; Scalmani, G.; Barone, V.; Mennucci, B.; Petersson, G. A.; Nakatsuji, H.; Caricato, M.; Li, X.; Hratchian, H. P.; Izmaylov, A. F.; Bloino, J.; Zheng, G.; Sonnenberg, J. L.; Hada, M.; Ehara, M.; Toyota, K.; Fukuda, R.; Hasegawa, J.; Ishida, M.; Nakajima, T.; Honda, Y.; Kitao, O.; Nakai, H.; Vreven, T.; Montgomery, Jr., J. A.; Peralta, J. E.; Ogliaro, F.; Bearpark, M.; Heyd, J. J.; Brothers, E.; Kudin, K. N.; Staroverov, V. N.; Kobayashi, R.; Normand, J.; Raghavachari, K.; Rendell, A.; Burant, J. C.; Iyengar, S. S.; Tomasi, J.; Cossi, M.; Rega, N.; Millam, N. J.; Klene, M.; Knox, J. E.; Cross, J. B.; Bakken, V.; Adamo, C.; Jaramillo, J.; Gomperts, R.; Stratmann, R. E.; Yazyev, O.; Austin, A. J.; Cammi, R.; Pomelli, C.; Ochterski, J. W.; Martin, R. L.; Morokuma, K.; Zakrzewski, V. G.; Voth, G. A.; Salvador, P.; Dannenberg, J. J.; Dapprich, S.; Daniels, A. D.; Farkas, Ö.; Foresman, J. B.; Ortiz, J. V.; Cioslowski, J.; Fox, D. J.; Gaussian, Inc.: Wallingford CT,, 2009.

(18) Jensen, F. in *Introduction to Computational Chemistry*, 2nd ed.; Wiley: Chichester, U.K., 2007, pp 177-203.

(19) Cramer, C. J. in *Essentials of Computational Chemistry,* 2nd ed.; Wiley: Chichester, U.K., 2004; pp 249-300.

(20) Zhao, Y.; Truhlar, D. G. *J. Chem. Theory Comput.* **2008**, *4*, 1849.

(21) (a) Becke, A. D. *Phys. Rev. A* **1988**, *38*, 3098. (b) Perdew, J. P. *Phys. Rev. B: Condens. Matter* **1986**, *33*, 8822. (c) Becke, A. D. *J. Chem. Phys.* **1993**, *98*, 5648.

(22) (a) Slater, J. C. in *The Self-Consistent Field for Molecular and Solids*, *Quantum Theory of Molecular and Solids,* Vol. 4 (McGraw-Hill, New York, 1974) pp 16. (b) Vosko, S. H.; Wilk, L.; Nusair, M. *Can. J. Phys.* **1980**, *58*, 1200.

(23) (a) Matsubara, T.; Maseras, F.; Koga, N.; Morokuma, K. *J. Phys. Chem.* **1996**, *100*, 2573. (b) Svensson, M.; Humbel, S.; Froese, R. D. J.; Matsubara, T.; Sieber, S.; Morokuma, K. *J. Phys. Chem.* **1996**, *100*, 19357.

(24) (a) McCarthy, M. C.; Thorwirth, S.; Gottlieb, C. A.; Thaddeus, P. *J. Am. Chem. Soc.* **2004**, *126*, 4096. (b) Rice, J. E.; Amos, R. D.; Handy, N. C.; Lee, T. J.; Schaefer, H. F. *J. Chem. Phys.* **1986**, *85*, 963. (c) Millefiori, S.; Alparone, A. *J. Phys. Chem. A* **2001**, *105*, 9489. (d) Goddard, J. D.; Chen, X.; Orlova, G. *J. Phys. Chem. A* **1999**, *103*, 4078. (e) Koch, W.; Natterer, J.;

Heinemann, C. *J. Chem. Phys.* **1995**, *102*, 6159. (f) Francisco, J. S.; Lyons, J. R.; Williams, I. H. *J. Chem. Phys.* **2005**, *123*, 054302. (g) Azizi, Z.; Roos, B. O.; Veryazov, V. *Phys. Chem. Chem. Phys* **2006**, *8*, 2727. (h) Oyedepo, G. A.; Wilson A. K. *J. Phys. Chem. A* **2010**, *114*, 8806. (i) Peterson, K. A.; Lyons, J. R.; Francisco, J. S. *J. Chem. Phys.* **2006,** *125*, 084314.
(25) Flemmig, B.; Wolczanski, P. T.; Hoffmann, R. *J. Am. Chem. Soc.* **2005**, *127*, 1278.
(26) (a) Ivanic, J.; Atchity, G. J.; Ruedenberg, K. *J. Chem. Phys.* **1997**, *107*, 4307. (b) Glezakou, V.-A.; Elbert, S. T.; Xantheas, S. S.; Ruedenberg, K. *J. Phys. Chem. A* **2010**, *114*, 8923.
(27) Halls, M. D.; Schlegel, H. B. *J. Phys. Chem. B* **2002**, *106*, 1921.
(28) Bondi, A. *J. Phys. Chem.* **1964**, *68*, 441.
(29) Lawler, H. M.; Areshkin, D.; Mintmire, J. W.; White, C. T. *Phys. Rev. B: Condens. Matter* **2005**, *72*, 233403.
(30) Yumura, T. *Phys. Chem. Chem. Phys.* **2011**, *13*, 337.
(31) (a) Denk, M. K. *Eur. J. Inorg. Chem.* **2009**, 1358. (b) Otto, A. H.; Steudel R. *Eur. J. Inorg. Chem.* **1999**, 2057.
(32) (a) Jones, R. O.; Ballone, P. *J. Chem. Phys.* **2004**, *121*, 7535. (b) Jones, R. O.; Ballone, P. *J. Chem. Phys.* **2003**, *118*, 9257. (c) Hunsicker, S.; Jones, R. O.; Ganteför, G. *J. Chem. Phys.* **1995**, *102*, 5917. (d) Jones, R. O. *J. Chem. Phys.* **1986**, *84*, 318.
(33) Lei, X.; Doubleday, C. E.; Zimmt, M. B.; Turro, N. J. *J. Am. Chem. Soc.* **1986**, *108*, 2444.
(34) Eliseev, A. A.; Chernysheva, M. V.; Verbitskii, N. I.; Kiseleva, E. A.; Lukashin, A. V.; Tretyakov, Y. D.; Kiselev, N. A.; Zhigalina, O. M.; Zakalyukin, R. M.; Vasiliev, A. L.; Krestinin, A. V.; Hutchison, J. L.; Freitag, B. *Chem. Mater.* **2009**, *21*, 5001.
(35) Steudel, Y.; Steudel, R.; Wong, M. W. *Chem. Eur. J.* **2002**, *8*, 217.
(36) Denis, P. A.; Iribarne, F. *Int. J. Quantum Chem.* **2010**, *110*, 1764.
(37) Houk, K. N. *Helv. Chim. Acta* **2010**, *93*, 1241.
(38) Heymann, D.; Bachilo, S. M.; Weisman, R. B.; Marriott, T.; Cataldo, F. *Fullerenes, Nanotubes and Carbon Nanostructures* **2002**, *10*, 37.
(39) (a) Sabirov, D. Sh.; Khursan, S. L.; Bulgakov, R. G. *J. Molec. Graph. Model.* **2008**, *27*, 124. (b) Heymann, D. *Fullerenes, Nanotubes and Carbon Nanostructures* **2004**, *12*, 715.
(40) (a) Sugihara, Y.; Abe, K.; Nakayama, J. *Heteroatom Chem.* **1999**, *10*, 638. (b) Yomoji, N.; Takahashi, S.; Chida, S.-I.; Ogawa, S.; Sato, R. *J. Chem. Soc., Perkin Trans 1.* **1993**, *1995*, 306. (c) Kimura, T.; Hanzawa, M.; Tsujimura, K.; Takahashi, T.; Kawai, Y.; Horn, E.; Fujii, T.; Ogawa, S.; Sato, R. *Bull. Chem. Soc. Jpn.* **2002**, *75*, 817.
(41) Bil, A.; Latajka, Z.; Morrison, C. A. *J. Phys. Chem. A* **2009**, *113*, 9891.
(42) Criegee, R. *Angew. Chem., Int. Ed. Engl.* **1975**, *87*, 745.

CHAPTER 2

(1) Wasserman, H. H.; Larsen, D. L. *J. Chem. Soc., Chem. Commun.* **1972**, 253.
(2) Aubry, J.-M.; Pierlot, C.; Rigaudy, J.; Schmidt, R. *Acc. Chem. Res.* **2003**, *36*, 668.
(3) Saito, I.; Matsuura, T. In *Singlet oxygen*; Wasserman, H. H., Murray, R. W., Eds.; Academic Press: New York :, 1979; Vol. 40, p 511.
(4) Balci, M. *Chem. Rev.* **1981**, *81*, 91.
(5) Clennan, E. L.; Foote, C. S.; Wiley: 1992, p 255.
(6) Turro, N. J.; Chow, M. F. *J. Am. Chem. Soc.* **1981**, *103*, 7218.

(7) Ben-Shabat, S.; Itagaki, Y.; Jockusch, S.; Sparrow, J. R.; Turro, N. J.; Nakanishi, K. *Angew. Chem., Int. Ed.* **2002**, *41*, 814.
(8) Aubry, J.-M.; Mandard-Cazin, B.; Rougee, M.; Bensasson, R. V. *J. Am. Chem. Soc.* **1995**, *117*, 9159.
(9) Pierlot, C.; Poprawski, J.; Marko, J.; Aubry, J. M. *Tetrahedron Lett.* **2000**, *41*, 5063.
(10) Liang, Z.; Zhao, W.; Wang, S.; Tang, Q.; Lam, S.-C.; Miao, Q. *Org. Lett.* **2008**, *10*, 2007.
(11) Pierlot, C.; Aubry, J.-M. *Chem. Commun.* **1997**, 2289.
(12) Saito, I.; Nagata, R.; Matsuura, T. *Tetrahedron Lett.* **1981**, *22*, 4231.
(13) Wixom, M. R. *J. Phys. Chem.* **1990**, *94*, 4926.
(14) Fudickar, W.; Linker, T. *Chem. Eur. J.* **2006**, *12*, 9276.
(15) Zehm, D.; Fudickar, W.; Linker, T. *Angew. Chem., Int. Ed.* **2007**, *46*, 7689.
(16) Sheats, J. R. *Trends Phys. Chem.* **1992**, *3*, 191.
(17) Mondal, R.; Shah, B. K.; Neckers, D. C. *J. Photochem. Photobiol., A* **2007**, *192*, 36.
(18) Twarowski, A. J. *J. Phys. Chem.* **1988**, *92*, 6580.
(19) Twarowski, A.; Dao, P. *J. Phys. Chem.* **1988**, *92*, 5292.
(20) Garavelli, M.; Bernardi, F.; Olivucci, M.; Robb, M. A. *J. Am. Chem. Soc.* **1998**, *120*, 10210.
(21) Bobrowski, M.; Liwo, A.; Oldziej, S.; Jeziorek, D.; Ossowski, T. *J. Am. Chem. Soc.* **2000**, *122*, 8112.
(22) Sevin, F.; McKee, M. L. *J. Am. Chem. Soc.* **2001**, *123*, 4591.
(23) Langeland, J. L.; Werstiuk, N. H. *Can. J. Chem.* **2003**, *81*, 525.
(24) Singleton, D. A.; Hang, C.; Szymanski, M. J.; Meyer, M. P.; Leach, A. G.; Kuwata, K. T.; Chen, J. S.; Greer, A.; Foote, C. S.; Houk, K. N. *J. Am. Chem. Soc.* **2003**, *125*, 1319.
(25) Ricca, A.; Bauschlicher, C. W., Jr.; Maiti, A. *Phys. Rev. B: Condens. Matter Mater. Phys.* **2003**, *68*, 035433/1.
(26) Zhang, Y. F.; Liu, Z. F. *J. Phys. Chem. B* **2004**, *108*, 11435.
(27) Yim, W. L.; Liu, Z. F. *Chem. Phys. Lett.* **2004**, *398*, 297.
(28) Paterson, M. J.; Christiansen, O.; Jensen, F.; Ogilby, P. R. *Photochem. Photobiol.* **2006**, *82*, 1136.
(29) Burgert, R.; Schnoeckel, H.; Grubisic, A.; Li, X.; Stokes, S. T.; Bowen, K. H.; Gantefoer, G. F.; Kiran, B.; Jena, P. *Science* **2008**, *319*, 438.
(30) Leach, A. G.; Houk, K. N.; Foote, C. S. *J. Org. Chem.* **2008**, *73*, 8511.
(31) Wasserman, H. H.; Wiberg, K. B.; Larsen, D. L.; Parr, J. *J. Org. Chem.* **2005**, *70*, 105.
(32) Inoue, Y.; Ueoka, T.; Kuroda, T.; Hakushi, T. *J. Chem. Soc., Perkin Trans. 2* **1983**, 983.
(33) Ueda, T.; Kanomata, N.; Machida, H. *Org. Lett.* **2005**, *7*, 2365.
(34) Marshall, J. A.; Audia, V. H.; Jenson, T. M.; Guida, W. C. *Tetrahedron* **1986**, *42*, 1703.
(35) Paquette, L. A.; Trova, M. P. *J. Am. Chem. Soc.* **1988**, *110*, 8197.
(36) Whitlock, B. J.; Whitlock, H. W., Jr. *J. Am. Chem. Soc.* **1983**, *105*, 838.
(37) Kanomata, N.; Ochiai, Y. *Tetrahedron Lett.* **2001**, *42*, 1045.
(38) Dale, J. *Top. Stereochem.* **1976**, *9*, 199.
(39) Winnik, M. A. *Chem. Rev.* **1981**, *81*, 491.
(40) Marshall, J. A. *Acc. Chem. Res.* **1980**, *13*, 213.
(41) Marshall, J. A. *Chem. Rev.* **1989**, *89*, 1503.
(42) Busch, D. H.; Alcock, N. W. *Chem. Rev.* **1994**, *94*, 585.
(43) Fraser, S. J.; Winnik, M. A. *J. Chem. Phys.* **1981**, *75*, 4683.
(44) Stevens, J. C.; Busch, D. H. *J. Am. Chem. Soc.* **1980**, *102*, 3285.
(45) Lin, W. K.; Alcock, N. W.; Busch, D. H. *J. Am. Chem. Soc.* **1991**, *113*, 7603.
(46) Eaton, P. E.; Leipzig, B. D. *J. Am. Chem. Soc.* **1983**, *105*, 1656.
(47) Li, Y.; Thiemann, T.; Mimura, K.; Sawada, T.; Mataka, S.; Tashiro, M. *Eur. J. Org. Chem.* **1998**, *1998*, 1841.

(48) Paquette, L. A.; Fabris, F.; Tae, J.; Gallucci, J. C.; Hofferberth, J. E. *J. Am. Chem. Soc.* **2000**, *122*, 3391.
(49) Paquette, L. A.; Mendez-Andino, J. *Tetrahedron Lett.* **2001**, *42*, 967.
(50) Tobe, Y.; Fujita, H.; Wakaki, I.; Terashima, K.; Kobiro, K.; Kakiuchi, K.; Odaira, Y. *J. Chem. Soc., Perkin Trans. 1* **1984**, 2681.
(51) Newkome, G. R.; Theriot, K. J.; Gupta, V. K.; Balz, R. N.; Fronczek, F. R. *Inorg. Chim. Acta* **1986**, *114*, 21.
(52) Wada, Y.; Ishimura, T.; Nishimura, J. *Chem. Ber.* **1992**, *125*, 2155.
(53) Schwartz, M. H.; Rosenfeld, S. M.; Lee, C. I.; Jasinski, J. P.; Dardon, E. H. *Tetrahedron Lett.* **1992**, *33*, 6275.
(54) Inokuma, S.; Gao, S.-R.; Nishimura, J. *Chem. Lett.* **1995**, 689.
(55) Nakamura, Y.; Hayashida, Y.; Wada, Y.; Nishimura, J. *Tetrahedron* **1997**, *53*, 4593.
(56) Elk, S. B. *J. Chem. Inf. Comput. Sci.* **1987**, *27*, 70.
(57) Davis, W. M.; Zask, A.; Nakanishi, K.; Lippard, S. J. *Inorg. Chem.* **1985**, *24*, 3737.
(58) Chang, M. H.; Masek, B. B.; Dougherty, D. A. *J. Am. Chem. Soc.* **1985**, *107*, 1124.
(59) Masek, B. B.; Santarsiero, B. D.; Dougherty, D. A. *J. Am. Chem. Soc.* **1987**, *109*, 4373.
(60) Dalla, C. A.; Mandolini, L.; Pasquini, C.; Schiaffino, L. *J. Org. Chem.* **2005**, *70*, 9814.
(61) Brown, A. B.; Whitlock, H. W., Jr. *J. Am. Chem. Soc.* **1989**, *111*, 3640.
(62) Dodzuik, H.; Leszczynski, J.; Nowinski, K. S. *J. Mol. Struct.: THEOCHEM* **1997**, *391*, 201.
(63) Würthwein, E.-U.; Chandrasekhar, J.; Jenmis, E. D.; von Ragué Schleyer, P. *Tetrahedron Lett.* **1981**, *22*, 843.
(64) Wiberg, K. B. *Tetrahedron Lett.* **1985**, *26*, 5967.
(65) Frisch, M. J.; Trucks, G. W.; Schlegel, H. B.; Scuseria, G. E.; Robb, M. A.; Cheeseman, J. R.; Montgomery, J. A.; Vreven, T.; Kudin, K. N.; Burant, J. C.; Millam, J. M.; Iyengar, S. S.; Tomasi, J.; Barone, V.; Mennucci, B.; Cossi, M.; Scalmani, G.; Rega, N.; Petersson, G. A.; Nakatsuji, H.; Hada, M.; Ehara, M.; Toyota, K.; Fukuda, R.; Hasegawa, J.; Ishida, M.; Nakajima, T.; Honda, Y.; Kitao, O.; Nakai, H.; Klene, M.; Li, X.; Knox, J. E.; Hratchian, H. P.; Cross, J. B.; Bakken, V.; Adamo, C.; Jaramillo, J.; Gomperts, R.; Stratmann, R. E.; Yazyev, O.; Austin, A. J.; Cammi, R.; Pomelli, C.; Ochterski, J. W.; Ayala, P. Y.; Morokuma, K.; Voth, G. A.; Salvador, P.; Dannenberg, J. J.; Zakrzewski, V. G.; Dapprich, S.; Daniels, A. D.; Strain, M. C.; Farkas, O.; Malick, D. K.; Rabuck, A. D.; Raghavachari, K.; Foresman, J. B.; Ortiz, J. V.; Cui, Q.; Baboul, A. G.; Clifford, S.; Cioslowski, J.; Stefanov, B. B.; Liu, G.; Liashenko, A.; Piskorz, P.; Komaromi, I.; Martin, R. L.; Fox, D. J.; Keith, T.; Laham, A.; Peng, C. Y.; Nanayakkara, A.; Challacombe, M.; Gill, P. M. W.; Johnson, B.; Chen, W.; Wong, M. W.; Gonzalez, C.; Pople, J. A. *Gaussian 03,* Revision D.01, Gaussian, Inc., Gaussian, Inc.: Pittsburgh, PA, 2003.
(66) Hypercube, Inc.: 1115 NW 4th Street, Gainesville, Florida 32601, USA.
(67) Jensen, F. *Introduction to Computational Chemistry*; 2nd Ed. ed.; John Wiley & Sons: Chichister, UK, **2007**.
(68) Dennington II, R.; Keith, T.; Millam, J. **2007**.
(69) Dinadayalane, T. C.; Sastry, G. N. *J. Chem. Soc., Perkin Trans. 2* **2002**, 1902.
(70) Punnagai, M.; Dinadayalane, T. C.; Sastry, G. N. *J. Phys. Org. Chem.* **2004**, *17*, 152.
(71) Dinadayalane, T. C.; Punnagai, M.; Sastry, G. N. *J. Mol. Struct.: THEOCHEM* **2003**, *626*, 247.
(72) Geetha, K.; Dinadayalane, T. C.; Sastry, G. N. *J. Phys. Org. Chem.* **2003**, *16*, 298.
(73) Tantillo, D. J.; Lee, J. K. *Annu. Rep. Prog. Chem., Sect. B: Org. Chem.* **2007**, *103*, 272.
(74) Beno, B. R.; Wilsey, S.; Houk, K. N. *J. Am. Chem. Soc.* **1999**, *121*, 4816
(75) Leach, A. G.; Houk, K. N.; Reymond, J.-L. *J. Org. Chem.* **2004**, *69*, 3683-3692.

(76) Wodrich, M. D.; Corminboeuf, C.; Schreiner, P. R.; Fokin, A. A.; Von, S. P. *Org. Lett.* **2007**, *9*, 1851.
(77) Zhao, Y.; Truhlar, D. G. *Acc. Chem. Res.* **2008**, *41*, 157.
(78) Zhang, X.; Du, H.; Wang, Z.; Wu, Y.-D.; Ding, K. *J. Org. Chem.* **2006**, *71*, 2862.
(79) Izquierdo, M.; Osuna, S.; Filippone, S.; Martin-Domenech, A.; Sola, M.; Martin, N. *J. Org. Chem.* **2009**, *74*, 1480.
(80) Wieczorek, R.; Dannenberg, J. J. *J. Phys. Chem. B* **2008**, *112*, 1320.
(81) Wieczorek, R.; Dannenberg, J. J. *J. Am. Chem. Soc.* **2005**, *127*, 14534.
(82) Koblenz, T. S.; Wassenaar, J.; Reek, J. N. H. *Chem. Soc. Rev.* **2008**, *37*, 247.
(83) Clennan, E. L.; Pace, A. *Tetrahedron* **2005**, *61*, 6665.
(84) Natarajan, A.; Kaanumalle, L. S.; Jockusch, S.; Gibb, C. L. D.; Gibb, B. C.; Turro, N. J.; Ramamurthy, V. *J. Am. Chem. Soc.* **2007**, *129*, 4132.
(85) Greer, A. *Nature* **2007**, *447*, 273.
(86) Chin, K. K.; Trevithick-Sutton, C. C.; McCallum, J.; Jockusch, S.; Turro, N. J.; Scaiano, J. C.; Foote, C. S.; Garcia-Garibay, M. A. *J. Am. Chem. Soc.* **2008**, *130*, 6912.
(87) Cojocaru, B.; Laferriere, M.; Carbonell, E.; Parvulescu, V.; Garcia, H.; Scaiano, J. C. *Langmuir* **2008**, *24*, 4478.
(88) Jockusch, S.; Sivaguru, J.; Turro, N. J.; Ramamurthy, V. *Photochem. Photobiol. Sci.* **2005**, *4*, 403.

CHAPTER 3

(1) Loire, G.; Prim, D.; Andrioletti, B.; Rose, E.; Persoons, A.; Sioncke, S.; Vaissermann, J. *Tetrahedron Lett.* **2002**, *43*, 6541. (b) Tilak, B. D.; Desai, H. S.; Gupte, S. S. *Tetrahedron Lett.* **1964**, *24*, 1609. (c) Yang, S. M.; Shie, J. J.; Fang, J. M.; Nandy, S. K.; Chang, H. Y.; Lu, S. H.; Wang, G. *J. Org. Chem.* **2002**, *67*, 5208. (d) Conley, R. A.; Heindel, N. D. *J. Org. Chem.* **1976**, *41*, 3743. (e) Ye, X. S.; Wong, H. N. C. *J. Org. Chem.* **1997**, *62*, 1940. (f) Sun, J.; Xia, E.-Y.; Zhang, L.-L.; Yan, C.-G. *Eur. J. Org. Chem.* **2009**, 5247. (g) Rossy, P. A.; Hoffmann, W.; Mueller, N. *J. Org. Chem.* **1980**, *45*, 617.
(2) (a) Dong, S.; Paquette, L. A. *J. Org. Chem.* **2005**, *70*, 1580. (b) Al-Masoudi, N. A.; Al-Soud, Y. A.; Khodair, A. I. *Phosphorus, Sulfur Silicon Relat. Elem.* **2003**, *178*, 1199. (c) Chong, Y.; Choo, H.; Choi, Y.; Mathew, J.; Schinazi, R. F.; Chu, C. K. *J. Med. Chem.* **2002**, *45*, 4888. (d) Corsaro, A.; Pistara, V.; Chiacchio, M. A.; Vittorino, E.; Romeo, R. *Tetrahedron Lett.* **2007**, *48*, 4915. (e) Haraguchi, K.; Nishikawa, A.; Sasakura, E.; Tanaka, H.; Nakamura, K. T.; Miyasaka, T. *Tetrahedron Lett.* **1998**, *39*, 3713. (f) Kumamoto, H.; Nakai, T.; Haraguchi, K.; Nakamura, K. T.; Tanaka, H.; Baba, M.; Cheng, Y.-C. *J. Med. Chem.* **2006**, *49*, 7861. (g) Miller, J. A.; Pugh, A. W.; Ullah, G. M. *Tetrahedron Lett.* **2000**, *41*, 3265. (h) Paquette, L. A.; Fabris, F.; Gallou, F.; Dong, S. *J. Org. Chem.* **2003**, *68*, 8625.
(3) (a) Ferguson, A. C.; Adlington, R. M.; Martyres, D. H.; Rutledge, P. J.; Cowley, A.; Baldwin, J. E. *Tetrahedron* **2003**, *59*, 8233. (b) Martyres, D. H.; Baldwin, J. E.; Adlington, R. M.; Lee, V.; Probert, M. R.; Watkin, D. J. *Tetrahedron* **2001**, *57*, 4999. (c) Johnson, J. W.; Evanoff, D. P.; Savard, M. E.; Lange, G.; Ramadhar, T. R.; Assoud, A.; Taylor, N. J.; Dmitrienko, G. I. *J. Org. Chem.* **2008**, *73*, 6970.

(4) (a) Block, E. *Sci. Synth.* **2007**, *33*, 203. (b) Brichacek, M.; Njardarson, J. T. *Org. Biomol. Chem.* **2009**, *7*, 1761. (c) Samet, A. V.; Shestopalov, A. M.; Nesterov, V. N.; Semenov, V. V. *Synthesis* **1997**, 623.

(5) (a) Dawood, K. M. *Synth. Commun.* **2001**, *31*, 1647. (b) Shestopalov, A. M.; Bogomolova, O. P.; Litvinov, V. P. *Synthesis* **1991**, 277. (c) Kalai, T.; Saska, P.; Szabo, Z.; Jeko, J.; Hankovszky, O. H.; Hideg, K. *Synth. Comm.* **1997**, *27*, 2041. (d) Baharfar, R.; Hosseinnia, R.; Baghbanian, S. M. *Letters in Organic Chemistry* **2008**, *5*, 128. (e) Lei, M.-Y.; Xiao, Y.-J.; Liu, W.-M.; Fukamizu, K.; Chiba, S.; Ando, K.; Narasaka, K. *Tetrahedron* **2009**, *65*, 6888. (f) Lei, M.-Y.; Fukamizu, K.; Xiao, Y.-J.; Liu, W.-M.; Twiddy, S.; Chiba, S.; Ando, K.; Narasaka, K. *Tetrahedron Lett.* **2008**, *49*, 4125. (g) Watanabe, N.; Kikuchi, M.; Maniwa, Y.; Ijuin, H. K.; Matsumoto, M. *J. Org. Chem.* **2010**, *75*, 879. (h) Baraldi, P. G.; Cacciari, B.; Manfredini, S.; Pollini, G. P.; Simoni, D.; Spalluto, G.; Zanirato, V. *J. Org. Chem.* **1995**, *60*, 1461. (i) Chatterjee, P.; Murphy, P. J.; Pepe, R.; Shaw, M. *J. Chem. Soc., Perkin Trans. 1* **1994**, 2403. (j) Nagase, R.; Gotoh, H.; Katayama, M.; Manta, N.; Tanabe, Y. *Heterocycles* **2007**, *72*, 697.

(6) (a) McDonald, F. E.; Burova, S. A.; Huffman, L. G., Jr. *Synthesis* **2000**, 970. (b) Rahim, M. A.; Fujiwara, T.; Takeda, T. *Synlett* **1999**, 1029.

(7) (a) Crich, D.; Krishnamurthy, V. *Tetrahedron* **2006**, *62*, 6830. (b) Crich, D.; Patel, M. *Org. Lett.* **2005**, *7*, 3625.

(8) McConachie, L. K.; Schwan, A. L. *Tetrahedron Lett.* **2000**, *41*, 5637.

(9) Motto, J. M.; Castillo, Á.; Greer, A.; Montemayer, L. K.; Sheepwash, E. E.; Schwan, A. L. *Tetrahedron* **2011**, *67*, 1002-1010

(10) (a) McCairn, M. C.; Kreouzis, T.; Turner, M. L. *J. Mater. Chem.* **2010**, *20*, 1999. (b) Shoji, Y.; Yoshio, M.; Yasuda, T.; Funahashi, M.; Kato, T. *J. Mater. Chem.* **2010**, *20*, 173. (c) Yoon, M.-H.; Facchetti, A.; Stern, C. E.; Marks, T. J. *J. Am. Chem. Soc.* **2006**, *128*, 5792.

(11) Gaussian 09, Revision A.1, Frisch, M. J.; Trucks, G. W.; Schlegel, H. B.; Scuseria, G. E.; Robb, M. A.; Cheeseman, J. R.; Scalmani, G.; Barone, V.; Mennucci, B.; Petersson, G. A.; Nakatsuji, H.; Caricato, M.; Li, X.; Hratchian, H. P.; Izmaylov, A. F.; Bloino, J.; Zheng, G.; Sonnenberg, J. L.; Hada, M.; Ehara, M.; Toyota, K.; Fukuda, R.; Hasegawa, J.; Ishida, M.; Nakajima, T.; Honda, Y.; Kitao, O.; Nakai, H.; Vreven, T.; Montgomery, Jr., J. A.; Peralta, J. E.; Ogliaro, F.; Bearpark, M.; Heyd, J. J.; Brothers, E.; Kudin, K. N.; Staroverov, V. N.; Kobayashi, R.; Normand, J.; Raghavachari, K.; Rendell, A.; Burant, J. C.; Iyengar, S. S.; Tomasi, J.; Cossi, M.; Rega, N.; Millam, N. J.; Klene, M.; Knox, J. E.; Cross, J. B.; Bakken, V.; Adamo, C.; Jaramillo, J.; Gomperts, R.; Stratmann, R. E.; Yazyev, O.; Austin, A. J.; Cammi, R.; Pomelli, C.; Ochterski, J. W.; Martin, R. L.; Morokuma, K.; Zakrzewski, V. G.; Voth, G. A.; Salvador, P.; Dannenberg, J. J.; Dapprich, S.; Daniels, A. D.; Farkas, Ö.; Foresman, J. B.; Ortiz, J. V.; Cioslowski, J.; Fox, D. J. Gaussian, Inc., Wallingford CT, 2009.

(12) Cossi, M.; Rega, N.; Scalmani, G.; Barone, V. *J. Comput. Chem.* **2003**, *24*, 669.

(13) Limacher, P. A.; Mikkelsen, K. V.; Luthi, H. P. *J. Chem. Phys.* **2009**, *130*, 194114/1.

(14) York, D. M.; Karplus, M. *J. Phys. Chem. A* **1999**, *103*, 11060

(15) (a) Bondi, A. *J. Phys. Chem.* **1964**, *68*, 441-451. (b) Li, J.-N.; Fu, Y.; Liu, L.; Guo, Q.-X. *Tetrahedron* **2006**, *62*, 11801.

(16) GaussView, Version 5, Dennington, R.; Keith, T.; Millam, J. *Semichem Inc.*, Shawnee Mission KS, 2009.

(17) (a) Lingwood, M.; Hammond, J. R.; Hrovat, D. A.; Mayer, J. M.; Borden, W. T., *J. Chem. Theory Comput.* **2006,** *2*, 740 ; (b) Schreiner, P. R.; Fokin, A. A.; Pascal, R. A.; Meijere, A. de *Org. Lett.* **2006**, *8*, 3635; (c) Wodrich, M. D.; Corminboeuf, C.; Schreiner, P. R.; Fokin, A. A.; Schleyer, P. V. *Org. Lett.* **2007**, *9*, 1851; (d) Zhao, Y.; Truhlar, D. G. *Org. Lett.* **2006**, *8*, 5753;

(e) Zhao, Y.; Gonzalez-Garcia, N.; Truhlar, D. G. *J. Phys. Chem. A* **2005**, *109*, 2012; (f) Check, C. E.; Gilbert, T. M., *J. Org. Chem.* **2005,** *70*, 9828.
(18) (a) Grimme, S. *Angew. Chem., Int. Ed.* **2006,** *45*, 4460; (b) Wodrich, M. D.; Corminboeuf, C.; Schleyer, P. v. R., *Org. Lett.* **2006,** *8*, 3631.
(19) (a) Tawada, Y.; Tsuneda, T.; Yanagisawa, S.; Yanai, T.; Hirao, K. *J. Chem. Phys.* **2004,** *120*, 8425; (b) Yanai, T.; Tew, D. P.; Handy, N. C. *Chem. Phys. Lett.* **2004,** *393*, 51; (c) Limacher, P. A.; Mikkelsen, K. V.; Luthi, H. P. *J. Chem. Phys.* **2009,** *130*, 194114.
(20) Zhao, Y.; Truhlar, D. G. *Acc. Chem. Res.* **2008**, *41*, 157.
(21) Pedley, J. B. in *Thermodynamic Data and Structures of Organic Compounds;* Thermodynamic Research Center: College Station, TX, 1994; Vol. 1.
(22) Woodcock, H. L.; Schaefer, H. F.; Schreiner, P. R. *J. Phys. Chem. A* **2002**, *106*, 11923.
(23) Zhao, Y.; Truhlar, D. G. *J. Phys. Chem. A* **2006**, *110*, 10478.
(24) Kobychev, V. B.; Vitkovskaya, N. M.; Klyba, N. S.; Trofimov, B. A. *Russ. Chem. Bull.* **2002**, *51*, 774.
(25) (a) Becke, A. D. *Phys. Rev. A: Gen. Phys.* **1988**, *38*, 3098. (b) Lee, C.; Yang, W.; Parr, R. G. *Phys. Rev. B: Condens. Matter* **1988**, *37*, 785. (c) Becke, A. D. *J. Chem. Phys.* **1993**, *98*, 5648. (d) Yanai, T.; Tew, D. P.; Handy, N. C. *Chem. Phys. Lett.* **2004**, *393*, 51.
(26) Wheeler, S. E.; Houk, K. N. *J. Am. Chem. Soc.* **2009,** *131*, 3126.
(27) (a) Simon, S.; Duran, M.; Dannenberg, J. J. *J. Chem. Phys.* **1996,** *105*, 11024. (b) Block, E.; Zhao, S. H. *J. Org. Chem.* **1992**, *57*, 5815. (c) Guillerm, G.; Guillerm, D.; Vandenplas-Witkowki, C.; Rogniaux, H.; Carte, N.; Leize, E.; Van, D. A.; De, C. E.; Lambert, C. *J. Med. Chem.* **2001**, *44*, 2743. (d) Kende, A. S.; Smith, C. A. *J. Org. Chem.* **1988**, *53*, 2655. (e) Biellmann, J.-F.; Ducep, J.-B. *Org. React.* **1982**, *27*, pp. 245. (e) Stirling, C. J. M. *J. Chem. Soc., Suppl.* **1964**, *No. 1*, 5856.
(28) (a) Alabugin, I. V.; Manoharan, M. *J. Am. Chem. Soc.* **2005**, *127*, 12583. (b) Nevado, C.; Cardenas, D. J.; Echavarren, A. M. *Chem.--Eur. J.* **2003**, *9*, 2627. (c) Chung, L. W.; Wiest, O.; Wu, Y.-D. *J. Org. Chem.* **2008**, *73*, 2649. (d) Friedrich, J.; Walczak, K.; Dolg, M.; Piestert, F.; Lauterbach, T.; Worgull, D.; Gansaeuer, A. *J. Am. Chem. Soc.* **2008**, *130*, 1788. (e) Liu, F.; Liu, K.; Yuan, X.; Li, C. *J. Org. Chem.* **2007**, *72*, 10231. (f) Tsubusaki, T.; Nishino, H. *Tetrahedron* **2009**, *65*, 9448. (g) Vasilevsky, S. F.; Mikhailovskaya, T. y. F.; Mamatyuk, V. I.; Salnikov, G. E.; Bogdanchikov, G. A.; Manoharan, M.; Alabugin, I. V. *J. Org. Chem.* **2009**, *74*, 8106.
(29) (a) Baldwin, J. E. *J. Chem. Soc., Chem. Commun* **1976**, *18*, 734 (b) Baldwin, J. E.; Cutting, J.; Dupont, W.; Kruse, L.; Silberman, L.; Thomas, R. C. *J. Chem. Soc., Chem. Commun.* **1976**, 736.
(30) Our collaborators are gratefull to Prof. H.-U. Reissig of the Institut für Chemie und Biochemie - Organische Chemie at the Freie Universität Berlin for pointing this out.

CHAPTER 4

(1) Valentine, J. S.; Foote, C. S.; Greenberg, A.; Liebman, J. F. Eds.; in *Active Oxygen in Biochemistry*; Blackie Academic & Professional: NewYork, NY, 1995.
(2) Barton, S. C.; Bird, R. A.; Russell, K. E. *Can. J. Chem.* **1963**, *41,* 2737.
(3) 3-Mercaptocatechol **1** and 3,4-bismercaptocatechol **3**: See Aebisher, D.; Brzostowska, E. M.; Mahendran, A.; Greer, A. *J. Org. Chem.* **2007**, *72,* 2951.

(4) 3-Mercaptocatechol **1**: See Sumitomo Chemical Co. Ltd. , Jpn. Kokai Tokkyo Koho **1983**, JP 19820114.
(5) 4-Mercaptocatechol **2**: D'Ischia, M.; Testa, G.; Mascagna, Do.; Napolitano,A. *Gazz. Chim. Ital.* **1995**, *125,* 315; Mascagna, D.; d'Ischia, M.; Costantini, C.; Prota, G. *Synth. Commun.* **1994**, *24,* 35; Patent: Whalley, W. G. US 19760420 1976; Daneke, J.; Jahnke, U.; Pankow, B.; Wanzlick, H. W. *Tetrahedron Lett.* **1970**, *15,* 1271.
(6) Molina, M. T.; Yáñez, M.; Mó, O.; Notario, R.; Abboud, J. -L. M. in *Supplement A3 the Chemistry of Double-bonded Functional Groups Part 2*; Patai, S., Ed.; John Wiley & Sons: New York, 1997; pp. 1355.
(7) Jensen, F. in *Introduction to Computational Chemistry*, 2nd ed.; John Wiley & Sons: Chichester, U. K., 2007.
(8) Becke, A. D. *J. Chem. Phys.* **1993**, *98,* 5648.
(9) Lee, C.;Yang, W.; Parr, R. G. G. *Phys. Rev. B* **1988**, *37,* 785.
(10) Frisch, M. J.; Trucks, G. W.; Schlegel, H. B.; Scuseria, G. E.; Robb, M. A.; Cheeseman, J. R.; Montgomery, J. A.; Vreven, T.; Kudin, K. N.; Burant, J. C.; Millam, J. M.; Iyengar, S. S.; Tomasi, J.; Barone, V.; Mennucci, B.; Cossi, M.; Scalmani, G.; Rega, N.; Petersson, G. A.; Nakatsuji, H.; Hada, M.; Ehara, M.; Toyota, K.; Fukuda, R.; Hasegawa, J.; Ishida, M.; Nakajima, T.; Honda, Y.; Kitao, O.; Nakai, H.; Klene, M.; Li, X.; Knox, J. E.; Hratchian, H. P.; Cross, J. B.; Bakken, V.; Adamo, C.; Jaramillo, J.; Gomperts, R.; Stratmann, R. E.; Yazyev, O.; Austin, A. J.; Cammi, R.; Pomelli, C.; Ochterski, J. W.; Ayala, P. Y.; Morokuma, K.; Voth, G. A.; Salvador, P.; Dannenberg, J. J.; Zakrzewski, V. G.; Dapprich, S.; Daniels, A. D.; Strain, M. C.; Farkas, O.; Malick, D. K.; Rabuck, A. D.; Raghavachari, K.; Foresman, J. B.; Ortiz, J. V.; Cui, Q.; Baboul, A. G.; Clifford, S.; Cioslowski, J.; Stefanov, B. B.; Liu, G.; Liashenko, A.; Piskorz, P.; Komaromi, I.; Martin, R. L.; Fox, D. J.; Keith, T.; Laham, A.; Peng, C. Y.; Nanayakkara, A.; Challacombe, M.; Gill, P. M. W.; Johnson, B.; Chen, W.; Wong, M. W.; Gonzalez, C.; Pople, J. A. *Gaussian 03,* Revision D.01, Gaussian, Inc., Gaussian, Inc.: Pittsburgh, PA, 2003.
(11) Fort, R. C. Jr.; Getty, S. J.; Hrovat, D. A.; Lahti, P. M.; Borden, W. T. *J. Am. Chem. Soc.* **1992**, *114,* 7549.
(12) Gräfenstein, J.; Hjerpe, A. M.; Kraka, E.; Cremer, D. *J. Phys. Chem. A* **2000**, *104,* 1748.
(13) Yamaguchi, K.; Jensen, F.; Dorigo, A,; Houk, K. N. *Chem. Phys. Lett.* **1998**, *149,* 537.
(14) Yamaguchi, K.; Kawakami, T.; Nagao, H.; Yamaguchi, K. *Chem. Phys. Lett.* **1994**, *231,* 25.
(15) Denis, P. A. *J. Chem. Theory Comput.* **2005**, *1,* 900.
(16) Zysman-Colman, E.; Harpp, D. N. *J. Sulfur Chem.* **2004**, *25,* 291.
(17) Fattahi, A.; Kass, S. R.; Liebman, J. F.; Matos, M. A. R.; Miranda, M. S.; Morais, V. M. F. *J. Chem. Soc.* **2005**, *127,* 6116.
(18) Wiest, O.; Montiel, D. C.; Houk, K. N. *J. Phys. Chem. A* **1997**, *101,* 8378.
(19) Namazian, M.; Almodarresieh, H. A.; Noorbala, M. R.; Zare, H. R. *Chem. Phys. Lett.* **2004**, *396,* 424; VandeVondele, J.; Sulpizi, M.; Sprik, M. *Angew. Chem. Int. Ed.* **2006**, *45,* 1936.
(20) Greer, E. M.; Aebisher, D.; Greer, A.; Bentley, R. *J. Org. Chem.* **2008**, *73,* 280.
(21) Timoshkin, A.; Frenking, G. *J. Chem. Phys.* **2000**, *113,* 8430.
(22) Orlova, G.; Goddard, J. D. *J. Chem. Phys.* **2000**, *112,* 10085.
(23) Mann, M.; Fabian, J. *Int. J. Quantum Chem.* **1996**, *60,* 859.
(24) Breitenstein, M.; Schutz, R.; Schweig, A. *J. Org. Chem.* **1982**, *47,* 1979.
(25) González, L.; Mó O.;Yáñez, M. *Chem. Phys. Lett.* **1996**, *263,* 407.
(26) Contini, A.; Leone, S.; Menichetti, S.; Viglianisi, C.; Trimarco, P. *J. Org. Chem.* **2006**, *71,* 5507.
(27) Menichetti, S.; Viglianisi, C. *Tetrahedron* **2003**, *59,* 5523.

(28) Cramer, C. J. in *Essentials of Computational Chemistry,* 2nd ed.;Wiley: Chichester, England, 2004; pp 487.
(29) Cramer, C. J. *J. Am. Chem. Soc.* **1998**, *120,* 6261.
(30) Goldstein, E.; Beno, B.; Houk, K. N. *J. Am. Chem. Soc.* **1996**, *118,* 6036.
(31) Lampert, H.; Mikenda, W.; Karpfen, A. *J. Phys. Chem. A* **1997**, *101,* 2254.
(32) Voronkov, M. G.; Deryagina, E. N. *Russ. Chem. Rev.* **1990**, *59,* 778.
(33) Afeefy, H. Y.; Liebman, J. F.; Stein, S. E. in *NIST ChemistryWebbook, NIST Standard Reference Database Number 69*; Linstrom, P. J.; Mallard, W. G. Eds.; National Institute of Standards and Technology: Gaithersburg, MD, 2005. http://webbook. nist. gov.
(34) Andon, R. J. L.; Biddiscombe, D. P.; Cox, J. D.; Handley, R.; Harrop, D.; Herington, E. F. G.; Martin, J. F. *J. Chem. Soc.* **1960**, 5246.
(35) Slayden, S. W.; Liebman, J. F. in *The Chemistry of Phenols*; Rappoport, Z. Ed.;Wiley, Chichester, 2003, pp. 223.
(36) Sabbah, R.; Buluku, E. N. L. E. *Can. J. Chem.* **1991**, *69,* 481.; Ribeiro Da Silva, M. D. M. C.; Ribeiro Da Silva, M. A. V. *J. Chem. Thermo.* **1984**, *16,* 1149.
(37) Finch, A.; Gardner, P. J.;Wu, D. *Thermochim. Acta*, **1983**, *66,* 333.
(38) DiLabio, G. A.; Mulder, P. *Chem. Phys. Lett.* **2006**, *417,* 566.
(39) Nakayama, J.; Ishii, A. *Adv. Heterocyclic Chem.* **2000**, *77,* 221.
(40) Ishii, A.; Nakayama, J. *Rev. Heteroatom Chem.* **1998**, *19,* 1.
(41) Berson, J. A. in *The Chemistry of the Quinonoid Compounds*, Vol. 2, Part 1. Patai, S. , Rappaport, Z. eds., Wiley: NewYork, 1988; pp 455.
(42) Platz, M. S.; in *Diradicals*; Borden, W. T. Ed.; Academic Press: NewYork, 1982, pp 195.
(43) Neuhaus, P.; Grote, D.; Sander, W. *J. Am. Chem. Soc.* **2008**, *130,* 2993.
(44) Zhang, G.; Li, S. *Tetrahedron* **2003**, *59,* 3499.
(45) Datta, S. N.; Mukherjee, P.; Jha, P. P. *J. Phys. Chem. A* **2003**, *107,* 5049.
(46) Kato, S.; Morokuma, K.; Feller, D.; Davidson, E. R.; Borden, W. T. *J. Am. Chem. Soc.* **1983**, *105,* 1791.
(47) Fort, R. C.; Getty, S. J.; Hrovat, D. A.; Lahti, P. M.; Borden, W. T. *J. Am. Soc. Chem.* **1992**, *114,* 7549.
(48) Hrovat, D. A.; Murcko, M. A.; Lahti, P. M.; Borden, W. T. *J. Chem. Soc. , Perkin Trans.* **1998**, *2,* 1037.
(49) Wenthold, P. G.; Kim, J. B.; Lineberger, W. C. *J. Am. Chem. Soc.* **1997**, *119,* 1354.
(50) Hammad, L. A.; Wenthold, P. G. *J. Am. Chem. Soc.* **2000**, *122,* 11203.